

**TERMINAL OXIDASES, FLAVODIIRON PROTEINS AND NITRIC OXIDE:  
INSIGHTS INTO REACTION MECHANISMS AND BIOLOGICAL ROLES**

**ELENA FORTE**

**Dottorato di Ricerca in BIOCHIMICA XVII Ciclo 2001-2004**

**Dipartimento di Scienze Biochimiche “Rossi Fanelli”  
Università degli Studi di Roma “La Sapienza”**

**Docente guida e coordinatore della Scuola di Dottorato**

**PROF. PAOLO SARTI**

Dipartimento di Scienze Biochimiche, Università degli Studi di Roma “La Sapienza”

**Docenti esaminatori**

**Prof. Maurizio Paci**

Dipartimento di Scienze e Tecnologie Chimiche, Università di Roma "Tor Vergata"

**Prof. Giovanni Antonini**

Dipartimento di Biologia, Università di Roma "Roma Tre"

**Prof. Nazareno Capitanio**

Dipartimento di Scienze Biomediche, Università di Foggia

## ABSTRACT

Terminal oxidases catalyse the oxygen reduction to water and a synchronous  $H^+$  translocation. Proton and electron transfer must be carefully regulated for this fundamental molecular machine to work efficiently. Terminal oxidases have been shown to interact with nitric oxide (NO), a key molecule in many patho-physiological processes, cell signalling and host pathogen responses; several studies have reported the mitochondrial cytochrome *c* oxidase inhibition by NO and its emerging physiological relevance, as well as the ability of some bacterial terminal oxidases to reduce NO to  $N_2O$ . NO may be a poison for cells and microorganisms; thus, enzymes actively oxidising or reducing it could play a role in NO detoxification. *Escherichia coli* flavodiiron protein has been recently proposed to catalyse nitric oxide reduction.

In this thesis kinetic studies were used to investigate i) the electron-proton coupling upon of cytochrome *c* oxidase reduction, ii) the role of the K and D channel in this process and iii) the nitric oxide inhibition mechanism of cytochrome *c* oxidase. Functional amperometric studies elucidated some aspects of the interaction of nitric oxide with i) bacterial cytochrome *bd* and *bo<sub>3</sub>* oxidase and ii) flavodiiron proteins from *E.coli* and the pathogenic protist *Trichomonas vaginalis*.

## ABBREVIATIONS

**CcOX**: mitochondrial cytochrome *c* oxidase

**Mb**: myoglobin

**MbO<sub>2</sub>**: oxymyoglobin

**FIRd**: flavorubredoxin

**ROO**: rubredoxin–oxygen oxidoreductase

**FDP**: flavodiiron protein

**NO**: nitric oxide (IUPAC: nitrogen monoxide)

**NAD(P)H**: reduced nicotinamide adenine dinucleotide (phosphate)

**FMN**: flavin mononucleotide

**FAD**: flavin adenine dinucleotide

*Catalytic intermediates of CcOX active site:*

**O**: fully reduced intermediate

**E**: single electron reduced intermediate

**R**: fully reduced intermediate

**P**: peroxy intermediate

**F**: ferryl intermediate

*Mutant enzyme nomenclature:*

**D124N** denotes the substitution of aspartate 124 in subunit I for asparagine

**K354M** denotes the substitution of lysine 354 in subunit I for methionine

## TABLE OF CONTENTS

### 1. INTRODUCTION

#### 1.1. Terminal oxidases

1.1.1 Overview.....	1
1.1.2 Structures.....	2
1.1.3 Catalysis and oxygen reduction.....	3
1.1.4 Proton pathways.....	4
1.1.5 Proton pumping.....	5
1.1.6 Conformations.....	6

#### 1.2. Flavodiiron proteins

1.2.1 Overview.....	7
1.2.2 Structure of <i>Desulfovibrio Gigas</i> rubredoxin oxygen- oxidoreductase(ROO).....	8

#### 1.3. Nitric oxide in biology

1.3.1 Nitric oxide and prokaryotes.....	8
1.3.2 Nitric oxide and eukaryotes.....	9
1.3.3 Nitric oxide biochemistry.....	10
1.3.4 Interaction with iron- proteins.....	11
1.3.5 Nitric oxide and cytochrome c oxidase.....	12
1.3.6 Nitric oxide and inhibition of mitochondrial respiration .....	13

### 2. AIMS OF THE THESIS .....15

### 3.METHODS

3.1 Isolation and purification of cytochrome c oxidase .....	18
3.2 UV-visible absorption spectroscopy .....	18
3.3 Time-resolved absorption spectroscopy.....	19
3.3.1 Apparatus.....	19
3.3.2 Data analysis.....	20
3.3.3 The use of the pH sensitive dye phenol red.....	21
3.4 Preparation and titration of aqueous solutions of NO.....	22
3.5 Amperometric measurement of [O <sub>2</sub> ] and [NO].....	22
3.5.1 General principles and experimental set-ups.....	22
3.5.2 Stoichiometry of NO/CcOX reactions.....	22
3.5.3 NO reductase activity.....	23
3.5.4 NO inhibition measurement.....	23

### 3.6 Immunoblotting.....23

### 4. RESULTS AND DISCUSSION

4.1 The redox-linked protonation of cytochrome c oxidase during the reductive phase of the catalytic cycle .....	24
4.1.1 Effect on chloride bound to the active site on beef heart cytochrome oxidase (CcOX) .....	24
4.1.2 Implications for the proton uptake coupled to	

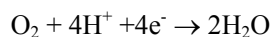
CcOX reduction.....	26
<b>4.2 The role of the K and D proton conducting pathways during the reductive phase of cytochrome oxidase catalytic cycle. ....</b>	<b>28</b>
4.2.1 Effect of the K354M and D124M mutations on proton-electron transfer coupled to <i>Paracoccus denitrificans</i> cytochrome c oxidase reduction.....	28
4.2.2 Role of the K and D proton pathways during enzyme reduction .....	30
<b>4.3. The reaction of nitrosylated cytochrome c oxidase with oxygen and the competition between MbO<sub>2</sub> and cytochrome c oxidase.....</b>	<b>31</b>
4.3.1 The reaction of reduced nitrosylated cytochrome c oxidase with oxygen.....	31
4.3.2 NO dissociation from nitrosylated COX in anaerobiosis.....	33
4.3.3 On the competition between MbO <sub>2</sub> and CcOX in turnover.....	33
4.3.4 Physiological relevance of NO dissociation from nitrosylated CcOX and the competition between oxyMb and CcOX in turnover.....	34
<b>4.4 Nitric oxide and the bacterial bo<sub>3</sub> oxidase.....</b>	<b>35</b>
4.4.1. The reaction of NO with fast oxidized and reduced cytochrome bo <sub>3</sub> purified from <i>Escherichia coli</i> .....	35
4.4.2 Implications for the interaction of NO with cytochrome bo <sub>3</sub> .....	37
<b>4.5 NO and the bacterial bd-type quinol oxidases.....</b>	<b>38</b>
4.5.1 The reaction of NO with bd oxidases purified from the bacteria <i>Escherichia coli</i> and <i>Azotobacter vinelandii</i> .....	38
4.5.2 Considerations on the interaction of NO with the bd-type quinol oxidases.....	40
<b>4.6 Nitric oxide and <i>Escherichia coli</i> flavorubredoxin .....</b>	<b>41</b>
4.6.1 NO reductase activity of <i>Escherichia coli</i> flavorubredoxin .....	41
4.6.2 Implications for the NO reductase activity of <i>Escherichia coli</i> flavorubredoxin.....	42
<b>4.7 NO and <i>Trichomonas vaginalis</i>.....</b>	<b>43</b>
4.7.1 <i>Trichomonas vaginalis</i> degrades NO.....	43
4.7.2 Relevance of the NO reductase activity detected in <i>Trichomonas vaginalis</i> .....	45
<b>CONCLUSIONS .....</b>	<b>47</b>
<b>REFERENCES .....</b>	<b>50</b>

# 1. INTRODUCTION

## 1.1 Terminal oxidases.

### 1.1.1 Overview

Terminal oxidases are fundamental enzymes ubiquitous among aerobic organisms and represent the last component of the respiratory chain located within the inner mitochondrial membrane of eukaryotes and the cytoplasmic membrane of prokaryotes and archaea. They catalyse the reduction of molecular oxygen to water:



The protons required in the water formation (scalar  $\text{H}^+$ ) are taken up from the negative side of the membrane (N-side), whereas the electrons come from the positive side (P-side) of the membrane, contributing to generation of a transmembrane electrochemical potential gradient. In most oxidases this reaction is coupled to the proton pumping of additional four protons (vectorial  $\text{H}^+$ ) across the membrane from the N side. The transmembrane proton and voltage gradient, generated by the oxidase and the other components of the respiratory chain, is directly converted to useful energy forms *via* energy conserving ATP synthase.

Most respiratory oxidases belong to the haem-copper oxidase superfamily which is defined by two criteria: i) a high sequence similarity within the largest subunit (subunit I) and ii) a bimetallic active site consisting of a haem and copper ion in terminal oxidases. Within the superfamily there are differences in the electron-donating substrates and in the redox components of the enzyme. The two main branches of the oxidases family are the cytochrome *c* oxidases (among the most studied are the cytochrome *aa*<sub>3</sub> from bovine heart and from the bacterium *Paracoccus denitrificans*) and the quinol oxidases (for example cytochrome *bo*<sub>3</sub> from the bacterium *Escherichia coli*) which use respectively the water soluble, haem containing cytochrome *c* and a lipid soluble quinol molecule (ubiquinol or menaquinol) as electron donors. Haem-copper oxidases are multi-subunit complexes. The redox chemistry is mediated by metal cofactors embedded in the subunits I and II which constitute the minimal functional unit (oxygen reduction and proton pumping). The enzyme, however, is not correctly assembled without subunit III. Subunit I is the largest and contains a low spin protohaem (heme *a* or haem *b* and *o*) acting as the electron donor to a binuclear centre that is composed of haem (heme *a*<sub>3</sub> or *o*<sub>3</sub>) and a copper ion ( $\text{Cu}_\text{B}$ ). Subunit II in cytochrome *c* oxidase contains the dinuclear  $\text{Cu}_\text{A}$  centre that transfer electrons from cytochrome *c* to the low spin haem. The ubiquinol oxidases do not contain  $\text{Cu}_\text{A}$  site, but the ubiquinol binding-site. Subunit III does not contain redox centres and it has been suggested to be important in channelling oxygen to and structurally stabilising the active site. Other subunits (up to 13) may be present in eukaryotic oxidases with, probably, regulatory functions. In the mammalian enzyme subunits I, II and III are mitochondrial encoded, while subunits IV to XIII are nuclear encoded. NO reductase, the enzyme that catalyses the reduction of NO to  $\text{N}_2\text{O}$  in denitrifying bacteria, is part of the haem-copper oxidase superfamily (Saraste and Castresana 1994) and contains a haem and iron in the binuclear site. The somewhat similar diatomic structure of the active site of both oxygen and NO reductases suggested that the haem-copper oxidases might bind and reduce NO, hypothesis demonstrated in some bacterial oxidases (Giuffr  et al. 1999) (Forte et al. 2001) but not in the in terminal mammalian enzyme (Stubauer et al. 1998).

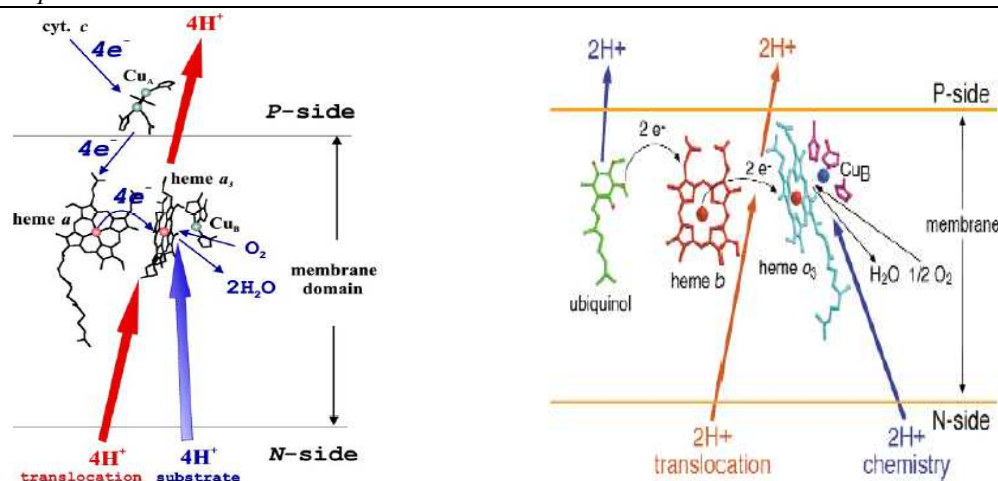


**Fig.1.1 Orientation of the metal cofactors and electron pathways in terminal oxidases.** Right: cytochrome *c* oxidase [Verkhovsky et al. Nature 1999]. Left: quinol *bo*<sub>3</sub> oxidase [Abramson Nat. Struct. Biol. 2000].

The bacterial quinol cytochrome *bd* is the only well characterised bacterial terminal oxidase unrelated to the haem-copper superfamily (see for a review Junemann 1997). This protein, although the three-dimensional structure is not yet available, does not reveal apparent sequence homology to oxidases of the haem-copper family and, interestingly, does not contain copper or non-haem iron in the active site. The purified *bd* oxidases are composed of two different membrane subunits with three redox sites: the haem *b*<sub>558</sub> involved in quinol oxidation, the high spin haem *b*<sub>595</sub> which might play a role analogous to Cu<sub>B</sub> in haem-copper oxidases, probably forming with haem *d* the active site where the oxygen chemistry occurs. This enzyme does not pump protons. It has been suggested that cytochrome *bd* serves as a high affinity oxidase to support respiration under microaerobic conditions and protect anaerobic processes from inhibition by oxygen.

### 1.1.2 Structure.

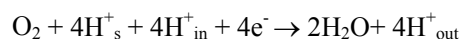
Protein crystallography has revealed the similar structural framework of different terminal oxidases. The crystal structure of three cytochrome *c* oxidases, the mammalian (from beef heart Tsukihara et al. 1995, Tsukihara et al. 1996, Yoshikawa et al. 1998), the *Paracoccus denitrificans* (Iwata et al. 1995, Ostermeier et al. 1997) and the *Rhodobacter sphaeroides* (Svensson-Ek et al. 2002) enzymes, were solved with the resolution of 2.3-2.8 Å and in different redox and ligand states of the active site (oxidised, azide-bound for the *Paracoccus* enzyme and oxidised, azide bound, reduced, reduced bound to CO for the mammalian one). The structure of the quinol *bo*<sub>3</sub> oxidase from *Escherichia coli* (Abramson et al. 2000) determined at 3.5 Å shows that the overall architecture of this enzyme is comparable to that of cytochrome *c* oxidase displaying a high degree of similarity within the core subunits (I, II, III). The structure of the 12 transmembrane barrels (helices I–XII) in subunit I, almost identical in all enzymes, contains three metal cofactors, the low spin haem, the high spin and Cu<sub>B</sub> the active site. The membrane-spanning region of quinol *bo*<sub>3</sub> oxidase subunit I contains a cluster of polar residues exposed to the interior of the lipid bilayer that is not present in the cytochrome *c* oxidases. Mutagenesis studies on these residues strongly suggest that this region forms a quinone binding site that is located in a cleft formed by trans-membrane helices I, II and III, allowing direct exposure to the membrane bilayer. Subunit II is in contact with subunit I and has two helices and a hydrophilic β-barrel domain protruding in the cytosol (or extracellular side) of the membrane; this globular water-soluble domain, covering part of subunit I, holds in cytochrome *c* oxidases the fourth metal centre, Cu<sub>A</sub> with two copper atoms that acts as the primary electron acceptor from cytochrome *c*. The quinol oxidase has no Cu<sub>A</sub> centre and lacks some of the metal ligating residues. Subunit III has seven helices in cytochrome *c* oxidases and five in the quinol oxidase whose position is, however, the same of helices III–VII in cytochrome *c* oxidase. Phospholipid molecules were observed between subunit IV and the other subunits in the cytochrome *c* oxidases, but not in ubiquinol oxidase.

The X-ray data confirmed the structure of the metal centres and the electron pathways predicted on the basis of spectroscopic studies and site directed mutagenesis. The two copper atoms of the Cu<sub>A</sub> site in cytochrome *c* oxidases can accept one electron at the time from cytochrome *c* forming a

mixed valence complex. They are bridged by the sulphur atoms of two cysteines in a tetrahedral geometry that recalls the structure of [2Fe-2S] centres; the additional ligands of this centre are two histidine residues (H161 and H204), a methionine (M207) and a glutamate (E198). Cu<sub>A</sub> is roughly equidistant from the two haems, both located at the same depth in the membrane (~1/3 from the P side of the membrane), perpendicularly to the membrane plane and to each other (the angle between the two haem planes is about 100°). Electrons from Cu<sub>A</sub> may reach haem *a* through the haem propionates, two arginine residues (R439 and R438) and one histidine ligand (H204). Heme *a* is low-spin (hexacoordinate) with two axial histidine ligands, His 61 and His 378 and it is a very short distance (edge to edge is 4.7 Å) from haem *a*<sub>3</sub>, which is high spin, (pentacoordinate) with one axial histidine ligand (H376). This latter residue may be involved in the electron transfer between the haems in addition to F377 and another histidine (H378). The modelling of the binuclear centre in the oxidized enzyme shows a continuous electron density between Fea<sub>3</sub> and Cu<sub>B</sub> that has been associated to either a peroxide (beef heart CcOX) or a water molecule bound to haem iron and a hydroxyl anion bound to the copper (*Paracoccus denitrificans* and *Rhodobacter sphaeroides* enzymes). Interestingly, this electron density is absent in the structure of the reduced enzymes. The Cu<sub>B</sub> atom, only few Å apart from haem *a*<sub>3</sub> (4-5 Å depending on the enzyme source and on the redox/ligand state of the two metals), is coordinated by two and three histidines residues in the bovine and in the *Paracoccus* enzyme, respectively. Another relevant structural finding emerged from the high resolution cytochrome *c* structures is a cross-linkage between the aromatic rings of the histidine ligand of Cu<sub>B</sub> and a tyrosine residue closed to the active site (H240 and Y244 in the bovine enzyme). This tyrosine may act as H atom donor towards oxygen during its reduction; the radical formed may be stabilized by delocalisation on both tyrosine and histidine. However, it is not clear if the formation of the bond is necessary for appropriate function or is a side reaction, a consequence of the formation of a tyrosyl radical during catalysis. Chemical evidences (Buse et al. 1999) from four distantly related cytochrome *c* oxidases (the mammalian, *Paracoccus denitrificans* and two from *Thermus thermophilus*) confirmed this peculiar structural feature.

### 1.1.3 Catalysis and oxygen reduction.

The overall reaction catalysed by most terminal oxidases is



where the subscript “s” denotes substrate protons and “in” and “out” the pumped protons from the N to the P-side. The catalytic function of terminal oxidases involves oxygen reduction chemistry, sequential electron and proton transfer reactions and, usually, proton pumping linked to the exoergonic events of oxygen reduction. The pathways of electron transfer from the electron donating substrate to oxygen have been identified by spectroscopic, mutagenesis and crystallographic studies. The catalytic cycle can be divided into a reductive part (electron input to the enzyme) an oxidative part (electron output from the enzyme to oxygen).

In the reductive phase of the cytochrome *c* oxidase catalytic cycle, the first step is Cu<sub>A</sub> reduction by cytochrome *c* after formation of an electrostatic complex between the two proteins; thus this interaction is dependent on pH and ionic strength. After cytochrome *c* binding, there is a very rapid electron transfer to Cu<sub>A</sub> (>10<sup>5</sup> Hill 1994) and from Cu<sub>A</sub> to haem *a* (K<sub>eq</sub>=2, k<sub>f</sub>= 7x10<sup>3</sup>-4x10<sup>4</sup> s<sup>-1</sup>, k<sub>r</sub>= 3x10<sup>3</sup>-1x10<sup>4</sup> s<sup>-1</sup> Einarsson et al. 1995), whose reduction is thermodynamically favoured. The subsequent electron transfer to the haem *a*<sub>3</sub>-Cu<sub>B</sub> centre has been proposed to be the rate-limiting step of the catalytic cycle. This intramolecular electron transfer occurs on the millisecond time scale when reducing the oxidized enzyme and on the microsecond scale when studying the oxidation process; to rationalise this difference it has been hypothesized that the rate of reduction of haem *a*<sub>3</sub>-Cu<sub>B</sub> may be limited by either a conformational change (kinetic control Brunori et al. 1997) or by the transfer of protons, required to compensate the negative charge, to the active site



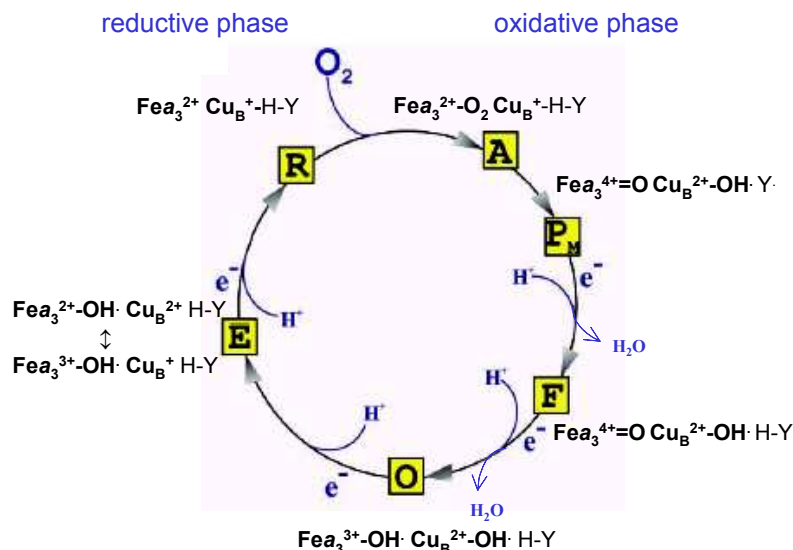


**Fig.1.2. Proposed mechanism of oxygen reduction to water at the active site of cytochrome oxidase.**

which raises its redox potential (thermodynamic control Verkhovsky et al. 1995). The sequential electron transfer from haem *a* to the oxidized active site (“O”  $\text{Fe}^{3+}\text{-Cu}_B^{2+}$ ) through formation of the single electron reduced species (E:  $\text{Fe}^{2+}\text{-Cu}_B^{2+} \leftrightarrow \text{Fe}^{3+}\text{-Cu}_B^{+}$ ) forms the complete reduced species “R” ( $\text{Fe}^{2+}\text{-Cu}_B^{+}$ ).

The oxidative phase starts with the binding of oxygen to this last intermediate to form the instable “A” ( $[\text{Fe}_a^{2+}\text{-Cu}_B^{+}]\text{-O}_2$ ) species, rapidly decaying into the peroxy state (“P”). This species, initially proposed to be a peroxide adduct ( $\text{Fe}^{3+}\text{-O-O-Cu}_B^{2+}$ ) as a result of a two-electrons reduction process, was shown by Raman spectroscopy to be actually a ferryl intermediate ( $\text{Fe}^{\text{IV}}=\text{O}$ ), evidencing that the splitting of the  $\text{O}=\text{O}$  bond has already occurred as well the formal transfer of the four electrons required to reduce oxygen to water (Proshlyakov et al. 1998) (Fabian and Palmer 1998). Three of these electrons may be transferred to oxygen from the metals of the binuclear site ( $\text{Fe}^{2+}\text{-Cu}_B^{+} \leftrightarrow \text{Fe}^{\text{IV}}\text{-Cu}_B^{2+}$ ) and the fourth by the nearby tyrosine which, releasing a proton, forms the tyrosyl radical, assumed to be stabilized by the delocalisation of the unpaired electron on the aromatics ring of both tyrosine and histidine. Electron transfer from haem *a* to P produces the F intermediate, which has the same ferryl structure of P but without the radical ( $\text{Fe}^{\text{IV}}=\text{O}\text{-Cu}_B^{2+}\text{-OH}^{\cdot}$ , Tyr H). Further electron transfer from haem *a* complete the cycle regenerating the O species.

#### 1.1.4 Proton pathways

Terminal oxidases should bear proton conducting transmembrane channels for substrate protons (used in water formation) to the binuclear centre and for pumped protons through the enzyme. Proton transfer pathways commonly consist of protein-spanning networks of protonable residues and/or bound water molecules connected via hydrogen bonds (proton “wires”). The X-ray structure evidenced at least two putative proton-conducting pathways, the K and D channel, connecting the N-side of the membrane with the active site. The K-channel contains an essential lysine in the middle of the pathway, K354 (according to *Paracoccus denitrificans* numbering) as predicted and proven by mutagenesis studies. It starts from the Glu78 and continues through Ser 291, the Lys354 and Thr351 residues, the hydroxyl group of the hydroxyethyl farnesyl group of the haem *a*<sub>3</sub> to a Tyr280 and Hys376 residue, close to the oxygen-binding centre (corresponding to the Glu 62, Ser255, Lys 319, Thr316, Tyr244 and Hys240 of the bovine enzyme).

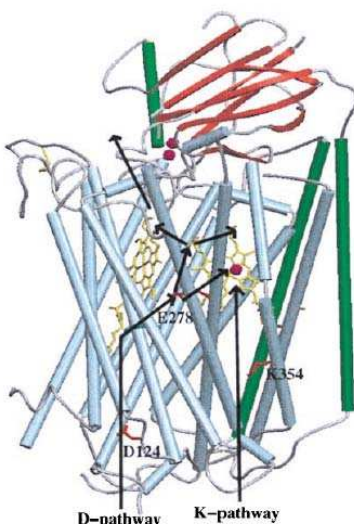


**Fig.1.3 Subunit one (green and red) and subunit II (blu) structure and proposed proton pathways of *P.denitrificans* oxidase [Michel *Proc.Natl.Acad. Sci. USA* 1998].**

The D channel starts with an important aspartate residue at the proton input side, Asp124 (91 in the bovine enzyme). This residue is connected to Glu278 (Glu242), close to the active site, through Tyr203, Ser134, Ser192, Ser193, Tyr35, Asn199, Asn131 and water molecules. A third putative proton pathway, the H-channel, was identified in the structure of the mammalian cytochrome *c* oxidase (Tsukihara et al. 1996) (Yoshikawa et al. 1998) and later in the *P. denitrificans* one (Ostermeier et al. 1997). Contrary to the K and D pathways, the H-channel comes in contact with haem *a* and ensures the connectivity of this centre with the P-side of the membrane. It starts from Asn 451 and through Tyr 371, the propionate of haem *a* and Tyr 54 arrives to the Asp51 located near the interface with subunit II and Cu<sub>A</sub> site.

The sequence of electron transfer events from cytochrome *c* or quinol to oxygen through the different metal cofactors is well defined, however the correlated mechanism and routes by which the protons required for the redox chemistry (scalar protons) and the generation of the electrochemical gradient (vectorial protons) are transferred to the active site or translocated across the membrane are not completely clear at molecular level. Site-specific mutagenesis studies confirmed the presence of the proton conducting pathways, but the involvement of each channel during the catalytic cycle is still under debate. The K channel appear to be involved mainly in the electron transfer associated to the E formation but its role in other redox linked protonations is not completely ruled out: the proton associated the E→R transition was proposed to occur either through the D-channel (Verkhovsky, 1999) or K-pathway with an additional proton being pumped through the D pathway (Ruitenberget al. 2002). The D channel participates in the H<sup>+</sup> transfer coupled to the oxidation of the enzyme and in the proton pumping. The H-channel is most clearly delineated in the bovine heart oxidase (Yoshikawa et al. 1998) and has been proposed to be functionally important for the translocation of pumped protons in the mammalian oxidase since the conformational modification of the bovine enzyme upon oxidation and reduction results in changes in the access of Asp51 to the bulk solvent. However mutagenesis studies showed that this channel is not functionally important for proton pumping in the prokaryotic oxidases (*Paracoccus denitrificans* (Pfitzner et al. 1998) and *Rhodobacter spaeroides* (Lee et al. 2000)).

### 1.1.5 Proton pumping

To understand how cytochrome *c* oxidase pumps protons the following questions have to be answered: 1) which step(s) of the catalytic cycle are coupled to the translocation of proton through the membrane and 2) what is the mechanism of H<sup>+</sup> transfer against the electrochemical gradient. Initially (Wikstrom 1989) proton translocation was proposed to occur during the exoergonic oxidative phase of the catalytic cycle (P→F and F→O). Later on, the steps of the reductive phase (O→R) have been also proposed to be part of the proton pumping mechanism (Kannt et al. 1998) (Verkhovsky et al. 1999). The translocation of two protons during the reductive phase was further confirmed in electrometric studies (Bloch et al. 2004) showing that it occurs only when the metastable state O<sub>H</sub>, formed in the

oxidative phase, is reduced. In this hypothesis, however,  $O_H$  may alternatively relax to stable form,  $O$ , bearing the haem  $a_3$ - $Cu_B$  site in the enzyme as isolated, which follows a different reaction pathway no longer coupled to proton pumping. Interestingly, switching between the two catalytic pathways might regulate the efficiency of ATP synthesis.

Electron transfer from cytochrome  $c$  to haem  $a$  (via  $Cu_A$ ) was initially proposed to be linked to the uptake of a proton from the N-side into an undefined “pumping site” within the membrane domain. Subsequent transfer of the electron to the binuclear haem  $a_3$ - $Cu_B$  site is linked to release of the proton from the pumping site to the P-side of the membrane, followed by uptake of the substrate proton from the N-side into the binuclear site to produce water. In this view, the uptake of the substrate proton into the binuclear site is an essential component of the proton-pumping mechanism since it may electrostatically facilitate the release of protons to be pumped. On this basis, it was proposed the histidine cycle model (Morgan et al. 1994). According to this hypothesis, the conformational changes required by the proton pump could be triggered by the dissociation of a histidine ligand of  $Cu_B$ . A histidine shuttle mechanism found support in the original *P.denitrificans* crystal structure where electron density for one of the histidine ligand was missing; however at higher resolution structures this histidine had an ordered structure. Furthermore, the different redox and ligand states of the mammalian structures showed a conformational change at the level of aspartate 51. This residue, changing its accessibility to the solvent during the transition from reduced to oxidized CcOX, may be involved in a pump mechanism, although only in mammals (Okuno et al. 2003) since it is not conserved in plant and bacterial oxidases. A recent and more general model for the mechanism of proton pumping (Wikstrom et al. 2003) proposes a key role for a conserved glutamate residue (E286 of *Rhodobacter sphaeroides*), considered the branching point for substrate and pumped proton. This aminoacid is connected through the polar residues of the D channel and a close-by pool of water molecules to the haem  $a_3$ - $Cu_B$  site (where oxygen is reduced) and the  $\Delta$ -propionate of haem  $a_3$  which are part of the exit path for pump protons (Iwata et al. 1995, Puustinen and Wikstrom 1999, Hofacker et al. 1998). The proton-linked electron transfer between haem  $a$  and haem  $a_3$  produces changes in the electric field sensed by the water molecules and orientates them to form a water molecule array for either proton transfer from the E286 to the exit pathway (proton pumped) or to the binuclear site (scalar protons). The hydrophobic environment makes the water molecules very sensitive to the electric forces generated by metal and polar groups. Based on electrostatic and molecular dynamics, this proton pumping model provides a simple and attractive solution to some key problems: i) it explains the unique arrangement of the cofactors in the structure, ii) it suggests how the same proton pathway (D channel) may be used both for the transfer of scalar and vectorial protons and, iii) it proposes a specific role of the water molecules produced at the active site, finally, iv) it correlates the generation of the transmembrane proton gradient to the rate limiting step of the catalytic cycle (reduction of the binuclear site).

#### 1.1.6 Conformations.

The purified enzyme possesses different kinetic behaviour towards oxygen and other ligands (such as cyanide), depending on the experimental conditions used during the purification procedures and kinetic assays. These properties have been associated to different protein conformations.

*Resting and pulsed.* The *resting* form is characterized by a turnover rate two to ten times slower compared to the *pulsed* form (Antonini et al. 1977, Antonini et al. 1985) and by a polyphasic kinetics of cyanide binding (Nicholls et al. 1972) which is monophasic in the *pulsed* enzyme (Sarti et al. 1983). The enzyme in the *resting* state is usually obtained following purification procedure set up by Yonetani (Yonetani 1961), while the *pulsed* one is commonly obtained by exposing CcOX to a reduction and reoxygenation cycle. These two conformations can be interconverted in a reversible process (Sarti et al. 1983).

*Slow and fast.* The purification procedure of Hartzell and Beinert allows the isolation of a form that binds cyanide with monophasic kinetics. Incubation of this enzyme either with anions such as formate or at  $pH < 7$  leads to a less reactive conformation towards cyanide. The two forms have been defined as *slow* and *fast*, depending on their reactivity towards the ligands and have been distinguished from the resting and pulsed conformation.

The kinetic and optical properties of the more reactive *fast* and *pulsed* forms, however, suggest that these conformations could be the same, as the *slow* and *resting* one; despite similarities, it should be mentioned that while the *pulsed* form slowly converts into the *resting* one, the *fast* that does not decay into the *slow*.

Relevant to the reactivity of the binuclear centre, another form of the cytochrome oxidase is the chloride-ligated enzyme obtained by purifying the enzyme in buffers containing this anion. The Soret spectrum of this form is very similar to that of the *fast* form, but the cyanide binding properties are intermediate between the *slow* and the *fast* conformation. Moreover bound chloride prevents the fast reaction of the oxidized enzyme with NO (Giuffr  et al. 1998). EXAFS data confirmed the presence of a heavy atom bridging haem  $a_3$  and Cu<sub>B</sub>, likely a chloride, at the active site of the oxidized CcOX (Scott et al. 1988).

## 1.2 Flavodiironproteins.

### 1.2.1 Overview

The flavodiiron proteins, first named as A-type flavoproteins (Wasserfallen et al. 1998), constitute a large super family of enzymes widespread among strict or facultative anaerobic Bacteria and Archea. Interestingly, recent genomic analyses have proven the existence of genes encoding for homologous proteins in some pathogenic and anaerobic amitochondriate protozoa (Andersson et al. 2003). These enzymes are characterized by the conservation of a two-domain structural core: the N-terminal domain with a metallo  $\beta$ -lactamase like fold, harbouring a diiron catalytic centre, and a second domain, having a short chain flavodoxin-like fold containing a flavin mononucleotide (FMN) moiety. Members of this family may have additional domains fused at the C-terminal and according to these domain composition can be divided in three classes: the predominant A class having only the two domain core, the B class containing an additional rubredoxin-like domain with a mononuclear iron (FeCys<sub>4</sub> binding motifs), and the C class with an additional module of  $\sim 170$  residues with similarities with the NAD(P)H flavin oxidoreductase and detected only in cyanobacteria. The different domain composition reflects the different types of electron transfer chains, each one terminating with the reduction of the diiron centre by FMN. In the *Desulfovibrio gigas* (expressing a class A enzyme) a reductase transfer electrons from NADH to the rubredoxin, which in turn reduces the bidomain rubredoxin–oxygen oxidoreductase (ROO). In *Moorella thermoacetica* the rubredoxin and the NADH-reductase are fused together in a single high molecular weight polypeptidic chain (Das et al. 2001) that efficiently reduces the flavodiiron protein at expense of NADH. *E.coli* flavorubredoxin (FIRd) belongs to the class B enzymes and was shown (Gomes et al. 2000) to directly reacts with its NADH-dependent reductase (FIRd-reductase) containing a FAD cofactor. As in the other enterobacteria, the genes encoding for both FIRd and the reductase are in the same operon. The fusion with the rubredoxin observed in class B enzymes may have enhanced the electron transfer efficiency. An extreme module fusion is present in *Synechocystis* (Vicente et al. 2002) and in other cyanobacteria where the multi-component electron transfer chain is abolished. In this case, the fusion of NAD(P)H-flavin reductase to the flavodiiron core allows the protein to receive electrons directly from NAD(P)H and perform intramolecular electron transfer to the active site.

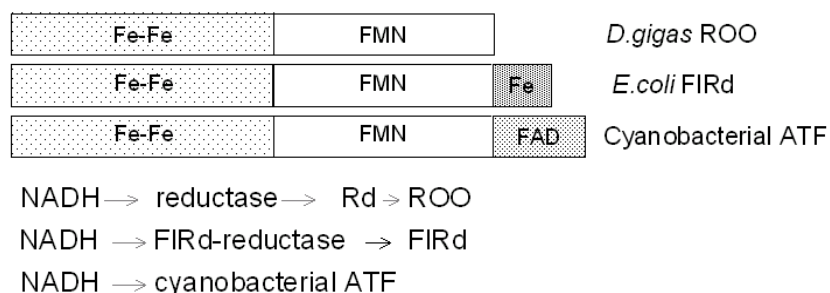


**Fig.1.4 Flavodiiron proteins structural modules and electron transfer chain.**

The first function assigned to the flavodiiron protein purified from *D. gigas* was the reduction of oxygen to water and the same function was later reported for the *E. coli* and *Synechocystis* enzymes. Since the exact turnover value for this reaction is still unclear, the physiological relevance of the oxidase activity is still undefined. Interestingly, molecular genetic studies (Gardner et al. 2002) revealed that *E. coli* grown anaerobically possess a nitric oxide reductase activity insensitive to cyanide and lost upon deletion of the gene encoding for the FIRd. The presence of NO seems to be required for the FIRd expression since no significant anaerobic NO consumption was observed in its absence.

The level of FIRd transcription has been shown to increase in the presence of nitrite and high NO concentration ( $> 50\mu\text{M}$  da Costa et al. 2003). Oxygen exposure was shown to inhibit the expression and the NO reductase activity in *E.coli* (Gardner et al. 2002; Gardner et al. 2003, da Costa et al. 2003). Altogether these data suggest an important involvement of the FIRd in the metabolism of NO.

### 1.2.2 Structure of *Desulfovibrio Gigas rubredoxin–oxygen oxidoreductase (ROO)*.

The structure of *Desulfovibrio Gigas* ROO (Frazao et al. 2000) is the only one available for this family of proteins. The X-ray structure, solved at the resolution of  $2.5\text{ \AA}$ , shows a quaternary structure as a functional head to tail homodimer (Fig.1.5). Each dimer is composed by two structurally distinct domain: the N-terminal domain with a  $\alpha\beta/\beta\alpha$  arrangement, similar to the Zn- $\beta$ -lactamases domain but with a diiron centre instead of zinc, and the C-terminal domain with a typical  $\alpha\beta\alpha$  flavodoxin-fold containing one FMN domain. The dimeric head to tail arrangement has a functional importance. In fact, the  $35\text{ \AA}$  distance between the two redox centres within each monomer, too long for an efficient electron transfer between them, is shortened in the dimer: the FMN cofactor of one monomer is in contact to the diiron centre of the other monomer. The FMN methyl group C8M

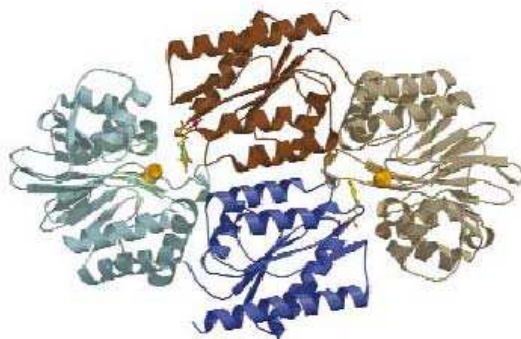


**Fig.1.5 Structure of the flavodiiron protein of *Desulfovibrio gigas*** (Frazao Nat. Struct Biol. 2000). The ROO dimer (monomers in blue and brown), showing the  $\beta$ -lactamase-like (light) domain with iron (orange spheres) and the flavodoxin-like (dark) one containing FMN (stick model).

is in van der Waals contact with the carboxylate from glutamate 81, one of the ligand of Fe1 and form a a very short electron pathway between the centres. In addition the dimeric conformation avoid FMN exposure to the bulk solvent, since in the monomer the FMN iso-alloxazine ring point to the surface of the flavodoxin module. The diiron distance ( $3.4\text{ \AA}$ ) is compatible with those determined for the di-ferroc centre. This centre is coordinated by histidine, glutamates and aspartates (His79-X-Glu82-X-Asp83-X-His146-X-His226) and bridged by a hydroxo species and the carboxylate of Asp165. The analysis of the nature of the metal ligands suggested that minor substitutions are necessary to change a di-zinc into a diiron site. This variation in the same structural fold explains the different activity of the enzymes, a Lewis-acid catalysis in  $\beta$ -lactamase and redox active centre in flavodiiron proteins, able to reduce oxygen and nitric oxide.

## 1.3 Nitric oxide in biology

### 1.3.1 Nitric oxide and prokaryotes

In prokaryotes NO is mainly produced by soil bacteria as key intermediate in the nitrogen cycle. Denitrifying bacteria play a pivotal role in this biogeochemical cycle being the only biological source of nitrogen; in these microorganisms NO is synthesized during the reduction of nitrate to nitrogen in a reaction catalysed by nitrite reductase (NIR)(Cutruzzola 1999). This electrogenic process evolved to provide energy conversion under anaerobic and microaerophilic conditions. It has also recently proposed that NO may also be formed during ammonification by the action of the pentahaem nitrite reductase (Corker and Poole 2003). Interestingly bacterial NO synthase has been found in *Nocardia species* (Chen and Rosazza 1994), *Bacillus subtilis* (Adak et al. 2002) and *Staphylococcus aureus* (Hong et al. 2003). The biological relevance of bacterial NOS-like proteins is still uncertain, but the puzzling surprising similarity of these enzymes to mammalian NOSs broaden the perspective of NO biochemistry and function. The bacteria may be exposed in their natural environment to nitric oxide produced abiotically (decomposition of nitrite for instance) or biotically, mainly by denitrifying/ammonifiers bacteria or macrophages, therefore it is likely that many species of microorganisms have not only evolved the ability to recognise NO in their environment, but also the

ability to elicit a defensive mechanisms to remove NO. This molecule, at high concentration, may have in fact deleterious effects on the cell, being able itself or associated to reactive oxygen species to react with proteins, lipids and nucleic acids. The prokaryotic responses to NO toxicity are not completely established and seems to include: i) enzymes that directly degrade NO; ii) enzymes that detoxify reactive oxygen species avoiding the formation of reactive nitrogen species, such as peroxynitrite; iii) DNA repairing enzymes, iv) iron homeostasis regulators, that decrease the formation of iron-adducts and v) enzymes that counteract the oxidative and nitrosative stress generating the pyridine nucleotides.

### 1.3.2 Nitric oxide and eukaryotes

The relevance of the NO synthesis in bacterial bioenergetics has been known for a long time (Renner and Becker 1970) while the potential relevance of the action of this molecule in eukaryotes became apparent after the discovery in the 1980s that NO is a biological mediator (Palmer et al. 1987). A very intense research of the function of NO in living organisms followed. In mammals, NO has been proposed to be involved in several processes, such as the blood vessel dilation, the regulation of the immune function, the neurotransmission in the brain and in the peripheral nervous system, the modulation of mitochondrial respiration (Ignarro et al. 2002, Bogdan 2001, Moncada et al 2002, Brown 1999, Sarti et al. 2003). Similar findings in vertebrates and invertebrates suggested a high conservation of the main NO signalling pathways during evolution (Torreilles 2001). The involvement of NO and NO synthesis in plant disease resistance to infection and the discovery of NO synthesis activity in protozoa and yeast have also been documented. Comparative investigations on the NO functions in different organisms have provided insights into the early evolutionary roles of this molecule. An involvement of NO in the cellular defence of *Limulus polyphemus*, an arthropod which has not evolved in 500 million years, and in the feeding response of *Hydra*, the most primitive organism possessing a nervous system, have been evidenced, suggesting that NO could be one of the most earliest signalling molecules.

In eukaryotic cells NO is mostly synthesized from the aminoacid L-arginine by a family of NO synthases (NOS). Three main NOSs are expressed in mammals (Alderton et al. 2001) and differ in their functions, aminoacid sequence and posttranslational modification. Two of these, the “endothelial” (eNOS) and “neuronal” (nNOS) isoforms, which are named after the tissue in which they were first identified, are expressed constitutively and generate NO for signalling purposes. Both are acutely activated by calcium/ calmodulin, alternatively they may be activated or inhibited by phosphorylation via various protein kinases. There is an inducible isoform (iNOS), which releases large quantity of NO during inflammatory or immunological defence reactions, and is involved in tissue damage. Once induced by cytokines, endotoxins or oxidative stress, this enzyme not dependent on calcium, produces higher concentration of NO and for longer period than the other NOSs. Another difference between the inducible and the constitutive forms may be the intracellular localization, since eNOS and nNOS are provided with membrane anchor moieties, which are lacking in the iNOS. Interestingly, immunohistochemical and later biochemical studies have provided evidence for a localization of a NOS at the inner membrane of mitochondria (mitochondrial NOS or mtNOS), recently identified as the alpha isoform of neuronal or NOS-1, (Haynes et al. 2004). Although, its actual existence is not consensual due to the lack of mitochondrial targeting sequence or the use, in most immunochemical studies, of aspecific antibodies towards the different isoforms, the hypothesis of a mitochondrial isoform is of great interest because of the critical role that this molecule has on mitochondrial respiration (Brown and Borutaite 2001). All these NOSs are homodimers of subunits with a bidomain structure: an oxygenase domain within the aminoterminal half and a reductase domain within the carboxy terminal half. They use oxygen as oxidant, NADPH as reducing substrate and five cofactors (FAD, FMN, calmodulin, tetrahydrobiopterin and haem 560) in a two step reaction: in the first step L-arginine incorporates an oxygen atom in its guanidinic group, producing the unstable intermediate N<sup>o</sup>-hydroxy-L-arginine which, in the second step, is oxidised to L-citrulline releasing NO. It has been hypothesized that in the functional dimeric enzyme the flavin cofactors of the reductase domain transfer electrons from NADPH to the oxygenase domain of the second monomer containing the oxygen binding haem and the L-arginine active site. The involvement of NO synthase has been evidenced also in other vertebrates, invertebrates and in some protozoa and yeast. While NOS had been generally considered to be the primary NO source in cellular systems, there have also been reports that enzyme-independent NO generation also occurs. NO can be generated in tissues by either



direct disproportionation or reduction of nitrite to NO under the acidic and highly reduced conditions encountered in the stomach, skin surface or in disease states, such as ischemia (Zweier et al. 1999).

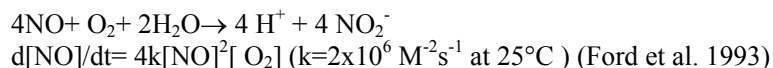
### 1.3.3 NO biochemistry.

NO has been defined a Janus molecule since, depending on its intracellular concentration and localization, may act as physiological signalling molecule or as a toxic agent. The two-faced NO actions may be explained by both the extensive and complex NO chemistry and the variety of potential reactive biological targets. This chemical variability can be simplified by the distinction between direct and indirect effects (Wink et al. 1996): the first are due to those reactions fast enough to occur directly between this gas and specific biological target, the second are mediated by reactive nitrogen oxide species (RNOS) formed from the reaction of NO with either oxygen or superoxide which are indicated as reactive nitrogen species (RNS: ONOO<sup>-</sup>, NO<sub>2</sub>, N<sub>2</sub>O<sub>3</sub>, N<sub>2</sub>O<sub>4</sub>, etc).

The reactions in which NO has direct effect are based upon the presence of an unpaired electron (NO<sup>•</sup>). As a free radical, NO promptly reacts with other radicals and metal complexes. Examples of the effect mediated by NO are its antiproliferative action through its combination with the catalytically competent tyrosyl radical in ribonucleotide reductase, a key enzyme in DNA synthesis (Lepoivre et al. 1991), its protection against lipid peroxidation chain reactions mediated by the trapping propagatory peroxy or alkoxy radicals at near diffusion rate (Wink et al. 1994), its effect on vascular tone, platelet function, neurotransmission due to the activation of soluble guanylate cyclase upon a iron-nitrosyl complex formation. Nitric oxide can bind to most metal transition and interaction with iron (Cooper 1999), copper (Torres and Wilson 1999) and cobalt (Rochelle et al. 1995) has been reported in biological systems. The most relevant reactions in which NO participates, however, are those with iron and can involve i) mere binding or ii) binding and metabolism. NO binds reversibly to ferrous iron (Fe<sup>2+</sup>) as O<sub>2</sub> and CO. These gases have similar dimension, hydrophobicity and uncharged character and can access the same cellular iron pool, no matter if it is protein or no protein bound. Thus, competition for the same sites may occur between NO and oxygen, present at higher concentration in most physiological conditions. The combination rate of O<sub>2</sub> and NO with several iron proteins is in the order 10<sup>7</sup>-10<sup>8</sup> M<sup>-1</sup>s<sup>-1</sup>, whereas that of CO is lower (usually <10<sup>7</sup>M<sup>-1</sup>s<sup>-1</sup>), probably due to the fact that Fe<sup>2+</sup>-CO complex prefers linear geometry (in model haem) but is often forced to bind with a bent angle because of the steric hindrance in proteins. Fe<sup>2+</sup>-O<sub>2</sub> and Fe<sup>2+</sup>-NO complexes in contrast are characterized by a bent geometry. Interestingly, NO binding to Fe<sup>2+</sup> decreases the affinity of the haem proximal ligand and its displacement can induce conformational changes that may affect the catalysis as in guanylate cyclase. On the other hand, protein conformational changes, forcing a ligand to bind to a nitrosyl complex, could make the Fe-NO bond weak and induce NO de-binding. The modification of the Fe<sup>2+</sup> microenvironment may explain the high NO dissociation rate measured in guanylate cyclase (0.05 s<sup>-1</sup> Kharitonov et al. 1997) and cytochrome *c* oxidase (0.004 s<sup>-1</sup> Sarti et al. 2000) compared to the value of 10<sup>-4</sup> 10<sup>-5</sup> s<sup>-1</sup> of myoglobin and hemoglobin (Sharma and Ranney 1978). The decreased NO affinity for the haem makes NO an efficient signalling molecule; fast recovery from activation or inhibition is in fact required for a fine regulation of enzymes activities and signal transduction. Besides formation of reversible complexes, the interaction haem/ NO includes redox reaction leading to NO metabolism of nitrite and nitrate. Examples are the reactions of Fe<sup>2+</sup>-NO complex with oxygen and of Fe<sup>2+</sup>-O<sub>2</sub> with NO forming nitrate and ferric iron. These reactions has been proposed to be involved in the NO scavenging *in vivo* by haemoglobin and myoglobin due to the high rate of the irreversible nitrate formation. Differently from CO and O<sub>2</sub>, NO is able to bind also to the iron in its oxidized state. Although the affinity of NO for Fe<sup>3+</sup> is lower than for Fe<sup>2+</sup> and its binding is less reversible, catalase inhibition occurs upon NO binding to the ferric form. Additionally, in Fe<sup>3+</sup>-NO complexes the transfer of electrons from NO to the iron, which is reduced to Fe<sup>2+</sup>, can occur. Although these reactions are slow on the biological time scale (minutes), they are important with the stable haem-NO adducts because, given the very slow off rates, would avoid the accumulation of such complexes *in vivo*. Reactions of NO with ferryl iron (Fe<sup>IV</sup>=O) formed during catalysed reactions (catalase, peroxidase) have been documented *in vitro*. The reduction of this species, however, occurs slowly at very high (millimolar) NO concentrations and seems very unlikely to be of physiological importance. NO may react also with thiol groups, forming, S-nitrosothiols (RS-NO) (Gaston 1999). S-nitrosoglutathione, formed by the reaction of the tripeptide glutathione with NO, is considered one of the most NO releasers. NO can also be reduced to nitroxyl (NO<sup>-</sup>) to form N<sub>2</sub>O.

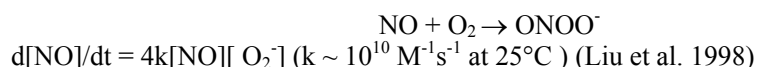
NO indirect effect are mediated by the intermediates and product of the reactions with either oxygen or with the superoxide anion (O<sub>2</sub><sup>-</sup>). The ability of nitrogen to exist in different oxidation states

may explain the numerous reactive nitrogen species, each one with its own particular reactivity. The reaction of NO with oxygen occurs with a third order kinetics:



This reaction at low (nanomolar) concentration of NO estimated *in vivo* for bioregulatory processes such as blood pressure regulation and neurotransmission is too low to have physiological relevance. NO in this condition is relatively un-reactive and should be sufficiently long-lived (100–500 s) to allow for reaction with haem proteins. The consequences of the stability of the NO molecule in solution are the diffusion of NO from the site of synthesis and its decrease in concentration with distance. Diffusion is essential for understanding the ability of NO to act as a local modulator since its action is dependent on concentration. The charge neutrality of NO facilitates the free diffusion in aqueous solution and across cell membrane. However, due to the low electric dipole moment, NO is about ~9 folds more soluble in hydrophobic compartments than in water, whereas O<sub>2</sub> is about 3 folds (Liu et al. 1998). The partitioning of NO and O<sub>2</sub> into biological membranes increases the local concentration of both gases, favouring their reaction. The increased rate of NO oxidation in lipid structures has been proposed (Shiva et al. 2001) to be the main mechanism of NO consumption in hydrophobic structures (adipose tissue, atherosclerotic plaques) and in cells and organelles rich in membranes (neurons and mitochondria). Moreover, the high NO concentration in membranes may be important in modulating NO dependent enzymatic activities in these structures (respiration) and in regulating the availability of the signalling molecule, which will increase as a function of the proximity of biological membranes. At the elevated levels of NO within membranes and produced also under certain conditions, e.g. by stimulated macrophages or pathological conditions, NO and O<sub>2</sub> reaction produces the free radical nitrogen dioxide (NO<sub>2</sub>) which rapidly reacts with a second NO molecule ( $>10^9 \text{ M}^{-1}\text{s}^{-1}$ ) to give dinitrogen trioxide (N<sub>2</sub>O<sub>3</sub>). NO<sub>2</sub> may oxidize or nitrate (adding an NO<sub>2</sub><sup>+</sup> group to) a variety of molecules, however its contribution is limited to the chemistry of endogenously generated NO because of the high reactivity. N<sub>2</sub>O<sub>3</sub>, the predominant RNS formed in biological systems, can nitrosate thiols and amine and is probably responsible for most of the nitrosative reactions *in vivo* (Wink et al. 1998). NO in fact, in the absence of transition metal, reacts too slowly with these groups to be biologically relevant.

The reaction of NO with superoxide, proceeding at near diffusion rates, produces a powerful oxidant, peroxynitrite (ONOO<sup>-</sup>):



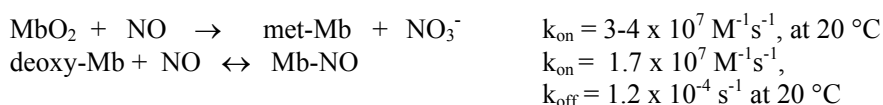
Under physiological conditions the rate of this reaction is limited by the availability of NO and superoxide (less than nanomolar under non stressed condition) which is dependent on the relative amount and on the reaction of these radicals between each other and with other biological reactants/scavengers (glutathione and oxyhemoglobin). Peroxynitrite formation is likely to occur in localized areas where NO and, more importantly, superoxide are produced, like in mitochondria and in macrophages. ONOO<sup>-</sup> can undergo a variety of chemical reactions and seems responsible for most of the deleterious effects of NO in cells and in tissue. It reacts in fact irreversibly and non-selectively with proteins, peptides, DNA, lipids and carbohydrates contributing to cytotoxic and genotoxic activities. From this scenario, it seems that the relative NO concentration and, consequently, the rate of NO breakdown in aqueous media may provide insights regarding how this reactive molecule can play important bioregulatory roles or have cytotoxic properties.

#### 1.3.4 Interaction with iron- proteins.

The reactions of NO with iron enzymes are of fundamental biological significance in bacteria as well in eukarya. Haem iron is present in the enzymes catalysing NO synthesis, the eukaryotic NO synthase and the bacterial *cd1* nitrite reductase, as well in the enzymes target for the action of NO, the best-characterized mammalian guanylate cyclase and the bacterial NO reductase. The activation of guanylate cyclase, through the binding of NO to the haem iron in the active site, is required to mediate several physiological processes including smooth muscle relaxation and neurotransmission. In these events NO acts as a paracrine modulator of cellular responses in line with its relatively stability in the



absence of metals, its solubility and diffusivity both in aqueous and hydrophobic compartments. For example, NO produced by eNOS during hypoxic-ischemic insult diffuses through the cell membranes of endothelial and smooth muscle. In the cytosol of these latter cells NO binding to the haem of soluble guanylate cyclase lead to conformational changes enabling the catalysis and the production of GMP cyclic from GTP. This second messenger mediates, through phosphorylations, the transmission and amplification of the signal that leads to vessel relaxation and increased blood flow. Bacterial nitric oxide reductase in denitrifiers contributes to keep the steady state level of free NO at nanomolar concentration by binding this molecule to the active site containing a haem and a non-haem iron (haem  $b_3$ -Fe). These organisms have developed a fine regulation of the activity expression of the enzymes involved in NO production and consumption to avoid toxic high NO concentration. The mechanism of NO reduction and N-N bond formation is still not completely understood. Given the ability of NO to bind to both  $\text{Fe}^{2+}$  and  $\text{Fe}^{3+}$ , several reaction mechanisms have been proposed. The mainly accepted concepts suggest that i) the primary product of the enzyme is a nitrosyl anion ( $\text{NO}^-$ ) which dimerizes to form hyponitrite ( $\text{HONNO}^-$ ); this intermediate is subsequently protonated yielding  $\text{N}_2\text{O}$  and water (Hendriks et al. 1998, Pinakoulaki et al. 2002); or ii) an N-N bond is established precisely in the reaction centre between two NO molecules (Kumita et al. 2004). In mammals the oxygen binding hemoprotein myoglobin has been recently suggested to be an efficient NO scavenger in the heart and skeletal muscle where provides an intracellular oxygen storage. In the myocytes of the cardiac and striated muscles, Mb facilitates  $\text{O}_2$  diffusion from the cell surface to the mitochondrion to avoid oxygen limitation to the respiratory chain under condition of high ATP demand. Moreover, it reacts with NO in both oxygenated ( $\text{MbO}_2$ ) and deoxygenated (deoxy-Mb) states, according to the following reactions:



Given the high Mb concentration (0.2 mM) and the very fast reaction of  $\text{MbO}_2$ , it has been argued that in the heart and skeletal muscle  $\text{MbO}_2$  may act as an efficient scavenger for NO (Brunori 2001). This property of Mb is important for cellular respiration, which is inhibited by NO at the mitochondrial cytochrome *c* oxidase site. The activity of this complex in fact is affected by the interaction of NO with the haem iron and copper atom constituting the active site. The reaction mechanisms and the implications of these interactions for the metabolism of NO will be discussed in the next paragraphs.

Finally, it is important to note that the NO reactivity with iron proteins is due not only to a direct action at the iron site; in particular, free radical intermediates (ribonucleotide reductase) and sulphhydryl groups (haemoglobin) may be target of NO action. The formation of cysteine S-NO haemoglobin (Hb) has been proposed to modulate the reactivity of this metalloprotein with oxygen and to take part in the control of vascular tone (Singel and Stamler 2004). SNO-Hb forms preferentially in the oxygenated R-state whereas conditions favouring T-state, such as low  $\text{pO}_2$ , favour the release of NO. Thus, in the R-state NO binds to the haem of  $\text{HbO}_2$  and its concentration in the vessels decreases causing vasoconstriction. NO is then sequestered, through formation of a S-nitrosothiol, by the cysteine  $\beta 93$ . Crystal structures and molecular models of SNO-Hb show that this residue is not accessible to the solvent in R state. When the hemoglobin conformation shifts to the T-state at the low  $\text{pO}_2$  in the peripheral tissue, both oxygen and NO are released. The SNO-cysteine becomes in fact accessible to the transnitrosation reaction with glutathione or band 3 protein, inducing NO release in vessels and thus favouring vasodilatation and oxygen distribution to the tissue.

### 1.3.5 Nitric oxide and cytochrome *c* oxidase.

Nitric oxide binds to and inhibits cytochrome *c* oxidase. This enzyme has a number of different potential targets to NO reactivity: all metal cofactors ( $\text{Cu}_A$ ,  $\text{Cu}_B$ , haem  $a$  and haem  $a_3$ ), the tyrosine residue at the oxygen active site which is thought to transiently form a radical during the catalytic cycle and a free cysteine at the surface (Cys 115 on subunit III). However, the only observed reactions of NO are those with the metals of the binuclear site, haem  $a_3$  and  $\text{Cu}_B$ , where the binding and the chemistry of oxygen occur. During the catalytic cycle,  $\text{Fea}_3$  and  $\text{Cu}_B$  undergo different oxidation state that can all potentially bind nitric oxide ( $\text{Fe}^{\text{IV}}=\text{O}$ ,  $\text{Fe}^{3+}$ ,  $\text{Cu}^{2+}$ ,  $\text{Cu}^+$ ).

In accordance with the high reactivity of NO with reduced iron, this gas was shown to react with reduced haem  $a_3$  yielding a tight, photosensible nitrosyl complex. The very fast kinetics of this

reaction ( $k = 0.4\text{--}1.0 \times 10^8 \text{ M}^{-1}\text{s}^{-1}$  at 20 °C Gibson and Greenwood 1963, Blackmore et al. 1991) is comparable to that of oxygen ( $k_{\text{on}} = 2 \times 10^8 \text{ M}^{-1}\text{s}^{-1}$  at 20 °C Gibson and Greenwood 1963, Blackmore et al. 1991). Interestingly, the dissociation rate is higher than expected for a haem protein ( $k_{\text{off}} = 0.004 \text{ s}^{-1}$  at 25°C Sarti et al. 2000) and similar to the value of guanylate cyclase. This observation raises the possibility of a role of NO in the modulation of respiration since fast dissociation allows fast recovery of CcOX activity upon removal of free NO. The reduced mammalian enzyme can bind only one molecule of NO (Stubauer et al. 1998) and consequently cannot catalyse the reduction of NO to  $\text{N}_2\text{O}$  in contrast to some bacterial oxidases (Giuffrè et al. 1999). The light sensitivity of the R-NO complex may be used in *in vitro* studies to identify the formation of this species formed in the reaction with NO during turnover.

Given that the rate constants for the binding of oxygen and NO to R are similar, the kinetics of inhibition may be difficult to rationalize. Therefore it was proposed that, in contrast to oxygen, NO can also bind to the half reduced E intermediate, either by trapping the electron on the haem (Giuffrè et al. 1996) or by forming this species via the reaction with copper (Torres et al. 1995). Computer simulation (Giuffrè et al. 1996) and later on the experimental evidence obtained by investigating the reduction kinetics of the *P. denitrificans* K354M mutant in the presence of NO (Giuffrè et al. 2002) strongly support this idea. However, data on the NO reaction with the half reduced enzyme has never been achieved due to the difficulty of obtaining a stabile E intermediate. The fully oxidized enzyme (O) can also rapidly bind to NO ( $k_{\text{on}} = 2.2 \times 10^5 \text{ M}^{-1}\text{s}^{-1}$  Torres et al. 1998, Giuffrè et al. 2000) when the enzyme is in the chloride-free state and in the fast conformation (Stubauer et al. 1998). In this reaction NO is oxidized by  $\text{Cu}_\text{B}$  to  $\text{NO}_2^+$ , probably via formation of a  $\text{Cu}_\text{B}^+-\text{NO}^+$  complex (Torres et al. 1998). The  $\text{NO}^+$  reacts with the  $\text{OH}^-$  liganded to  $\text{Cu}_\text{B}$  to form nitrite and the electron on reduced  $\text{Cu}_\text{B}$  redistributes between haem *a* and  $\text{Cu}_\text{A}$ . Similarly to O, the partially oxidized CcOX intermediates of the catalytic cycle, P and F, bind NO with a stoichiometry of 1:1 at a rate of  $10^4\text{--}10^5 \text{ s}^{-1}$ . This observation is consistent with a common reactive pathway involving the reduction of  $\text{Cu}_\text{B}$  and the NO oxidation to nitrite (Torres et al. 1998, Giuffrè et al. 2000). In conclusion, the reactions fast enough to be relevant to the enzyme turnover are those with reduced haem  $a_3$  and oxidized  $\text{Cu}_\text{B}$ .

The reactions of NO with CcOX leading to the nitrosylated enzyme or to the nitrite-copper complex on the other, were both shown to play a role in the prompt and reversible inhibition of the enzyme activity by NO. This conclusion was achieved not only with purified CcOX but also in mitochondria and cells (Mastronicola et al. 2003) making use of the different photosensitivity of the adducts (Sarti et al. 2000). It appears that the population of the different intermediates under turnover is dependent on the electron flux through the enzyme. At high electron flux (high reductant concentration) reduced species are more populated than the oxidised and accumulation of the nitrosyl complex is expected. Under condition of low electron flux through the enzyme (low reductant concentrations) the binuclear centre is more oxidized and the inhibited species displays the spectral features of the nitrite adduct. The possibility of generating the nitrosyl or the nitrite-bound has been proved by spectroscopic and amperometric experiments. In the polarographic data, the nature of the inhibited species formed after NO addition to the enzyme in turnover was identified by the different rate of recovery after inhibition of the activity, in the presence of oxy-hemoglobin to scavenge NO in the bulk. Relief from inhibition is associated to NO and nitrite release from the active site and the rate of these two processes is different: when the nitrosylated adduct prevails, the recovery of the activity is rate-limited by the NO dissociation from reduced haem  $a_3$  ( $k = 0.004 \text{ s}^{-1}$  at 25°C Sarti et al. 2000), whereas in the case of the nitrite complex the recovery of the oxidase activity is thought to occur upon intramolecular electron transfer to the active site through a charge compensation mechanism. This model of nitrite dissociation derives from the observation that the inhibited enzyme is fully active after a reduction and reoxygenation cycle (Giuffrè et al. 2000). Thus, whatever the reduction state of the other complexes of the respiratory chain, the cytochrome *c* level, which may change with the glycolytic rate, the citric acid cycle activity and energization of mitochondria, accounts for the different NO control of cytochrome *c* oxidase.

#### 1.3.6. Nitric oxide and inhibition of mitochondrial respiration.

Nitric oxide has been known for many years to bind cytochrome oxidase but the potential physiological relevance of this action became apparent after the discovery of the biological effect of NO (Ignarro et al. 1987, Palmer et al. 1987). The NO ability to inhibit cellular respiration was first evidenced while studying NO synthesis in denitrifying bacteria (Carr and Ferguson 1990), but clearly demonstrated when nanomolar concentrations of this signalling molecule were shown to rapidly,

reversibly and in competition with molecular oxygen inhibit respiration and at the cytochrome *c* oxidase site (Cleeter et al. 1994, Brown and Cooper 1994, Schweizer and Richter 1994). These findings were later confirmed in mitochondria, different cell types, isolated tissues and whole animals, showing the possible importance and the generality of the NO inhibition of the respiratory chain (reviewed in Brown 1999, Brown 2001, Cooper 2002,). The finding that the apparent  $K_m$  of purified cytochrome *c* oxidase or isolated mitochondria for oxygen is lower than that measured in whole cells by an order of magnitude, suggested that the physiological concentration of NO could regulate the mitochondrial respiration by decreasing the affinity of cytochrome oxidase for oxygen (Brown 1995). Consistently, inhibitors of NOS have been shown to enhance respiration either in cultured cells (increased mitochondrial membrane potential Sarti et al. 1999, enhanced oxygen consumption Miles et al. 1996) or in whole organisms (dog Shen et al. 1994, Trochu et al. 2000).

The physiological implications of inhibition of respiration can be distinguished in short- and long-term effects. The immediate consequences would be i) a different local concentration and availability of oxygen, ii) a change in the redox state of the cell and iii) a decrease of the mitochondrial membrane potential ( $\Delta\Psi_m$ ). The control of oxygen concentration by NO has been proposed to mediate directly or trigger important signals for physiological responses. In firefly, the transient oxygen diversion from the mitochondrion by NO makes it available for bioluminescence, essential for their reproduction (Trimmer et al. 2001), in mammalian cells inhibition of respiration during hypoxia increases oxygen concentration and diffusion gradient through adjacent cells (Clementi et al. 1999) while NO at the same time induce vasodilatation to improve tissue perfusion. On the other hand, at high NO concentrations the bio-availability of oxygen decrease dramatically, condition that has been proposed to occur during sepsis, in inflammatory or degenerative diseases and may be fundamental for some of the cytotoxic actions of macrophages (Brown et al. 1998). Another consequence of the NO interaction with cytochrome oxidase is the shift of the respiratory chain to a more reduced state, condition that enhances, at level of the other complexes, the formation of superoxide anions altering the intracellular balance between oxidant and antioxidant species. These anions are converted by superoxide dismutase to  $H_2O_2$  that has been proposed to modulate specific signaling pathways (Chandel et al. 2000, Antunes and Cadenas 2000, Brookes et al. 2002). Finally, inhibition of cytochrome *c* oxidase activity leads to a drop in the electron flux and consequently in proton extrusion which, in turn, might induce a decrease of the membrane potential ( $\Delta\Psi_m$ ) and ATP production. The consequences of this effect depend on the glycolytic capacity of the cells. The activation of glycolysis prevents ATP depletion and might explain the protective role towards apoptosis that require ATP, as well the increase of membrane potential. In contrast, in cells where ATP production is insufficient NO can induce apoptosis by decreasing the  $\Delta\Psi_m$ .

In addition to the reversible NO effects on the mitochondrial respiration, prolonged exposure to NO may develop irreversible inhibition. One of the first effects is on complex I probably due to S-nitrosation (Clementi et al. 1999), followed by inhibition of aconitase (Hausladen et al. 1994, Castro et al. 1994) under condition where peroxynitrite may be formed. Peroxynitrite can inhibit complex I (Cassina and Radi 1996), complex II (Cassina and Radi 1996, Bolanos et al. 1995) complex III (Bolanos et al. 1995, Cassina and Radi 1996) and cytochrome *c* oxidase (Sharpe and Cooper 1998, Bolanos et al. 1995). Thus several mitochondrial proteins may be damaged because of the conversion of NO to peroxynitrite. This process is a consequence of the high reduction level of the respiratory chain, the prolonged superoxide anions production and the increased local oxygen concentration favoured by the persistent inhibition of cytochrome *c* oxidase. The irreversible damage to the respiratory complex, the collapse of membrane potential and the consequent ATP depletion will lead to cell death.

In summary, the NO inhibition of mitochondrial respiration may lead to either physiological or pathological effects depending on several factors, such as NO concentration, time of exposure to this gas, intracellular redox state, cell type and metabolic regulation

## 2. AIMS

The work presented in this thesis was aimed at studying terminal oxidases, flavodiiron proteins and their interaction with nitric oxide. The main biochemical questions addressed in this thesis are related to the understanding of:

- 1) the mechanism of proton and electron transfer coupling in cytochrome *c* oxidases;
- 2) the molecular basis of the interaction of both terminal oxidases and flavodi-iron proteins with NO;
- 3) their role in the metabolism of NO and the relevance of this interaction to cell physiology and pathology.

In particular, studies have been conducted with the following specific aims:

**Aim1:** *to study the redox-linked protonation of cytochrome *c* oxidase during the reductive phase of the catalytic cycle.*

This study is relevant to the understanding of structure-function relationships in this enzyme. The uptake and the intermolecular transfer of the protons involved in the reduction of the enzyme, as well those to be translocated through the membrane for the generation of the electrochemical gradient, are intimately connected to redox chemistry according to mechanisms which are not yet fully understood at molecular level. The X-ray crystallography has led to an enormous advancement in the oxidase research; the high-resolution oxidase structures constitute useful frameworks to design and interpret experiments however do not provide sufficient information to define the mechanism and dynamics of the enzyme. There is still a controversial discussion on the number of protons coupled to the electron transfer to the redox cofactors. As predicted by the pH dependence of the metal centres redox potential, the enzyme on its reduction binds protons. A hydroxide group (OH<sup>-</sup>) is supposed to occupy physiologically the site between haem *a*<sub>3</sub> and Cu<sub>B</sub> in the oxidized enzyme and electrostatic calculation (Kannt et al. 1998) suggested that it would become protonated upon reduction of copper. When the enzyme is purified in the presence of chloride, the same coordination position may be occupied by this anion. Studies on the properties of chloride have determined that: ii) chloride binding to the oxidized CcOX in a stoichiometry of 1:1 proceeds formally with an uptake of one proton, ii) chloride dissociates from the active site of oxidized CcOX upon reduction and reoxygenation but rebinds very slowly. These observations suggest that both anions may dissociate from CcOX upon proton-linked electron transfer to the active site, perhaps in the protonated form. *To measure and model the redox linked protonation of cytochrome *c* oxidase during the reductive phase of CcOX catalytic cycle, the kinetics and the stoichiometry of proton uptake was studied in the chloride-bound and free form of the bovine enzyme.*

Another question still unresolved is the pathway used for the uptake of different protons at various stages of the catalytic cycle. Two proton transfer pathways were identified in the three-dimensional structures of different cytochrome *c* oxidases, the K and D channels, both leading from the N-side of the membrane side to the catalytic centre but possibly playing different roles during the catalytic cycle. Several studies on proton channel mutant oxidases have been addressed in view of its significance for the understanding of the proton pumping mechanism, but the involvement of the K and D pathway in the proton transfer associated to the reduction of either haem *a* or haem *a*<sub>3</sub>-Cu<sub>B</sub> has been not clarified. The protons associated to reduction of haem *a* have been proposed to be transferred through the K-pathway (Ruitenberget al. 2000), one proton being uptaken through an electrogenic process, or independently of both pathways with a not electrogenic 0.2-0.4 proton transfer (Verkhovsky et al. 1999, Verkhovsky et al. 2001). Moreover, the proton associated to the arrival of the second electron at the active site has been proposed to occur either through the D-channel (Verkhovsky et al. 1999) or K-pathway with an additional proton pumped through the D pathway (Ruitenberget al. 2002). Importantly, the number of protons bound upon reduction of bacterial or site-directed mutants has never been identified. *To answer this question and to verify the contribution of the K- and D-pathway to the redox-linked protonation, we performed a comparative study on the wild type Paracoccus denitrificans CcOX, the K354M and the D124N mutants, in which the D- and K-proton conducting pathways, respectively, are impaired.*

**Aim2:** *to gain insights into the NO inhibition of mitochondrial CcOX and relevance of intracellular NO scavenging system*

This study is relevant to the understanding of the mechanisms of interaction of the mammalian cytochrome *c* oxidase with NO and the inhibition of respiration, the role of cytochrome *c* oxidase in NO metabolism and the physiological consequences of the inhibition of respiration. The nitrite or

nitrosyl inhibited CcOX adducts can be formed in the active site following the reaction of NO with oxidized or reduced intermediates of CcOX catalytic cycle, respectively. Inhibition is relieved in both cases. The release of NO by dissociation from  $a_3^{2+}$ -NO complex has been observed under condition where the reduced intermediates are prevailing (high electron flux); thus this inhibitory pathway may extend the range of action of NO, its potential signalling properties and toxicity, the effective range of oxygen utilization. The inhibitory nitrite pathway, involving the formation of nitrite at the active site, breaks the propagation of NO: nitrite is released from the active site leading to an oxidative degradation of NO to harmless nitrite under condition where the oxidized intermediates are more populated (low electron flux). It has been recently reported (Pearce et al. 2003) that nitrite i) is the product of the reaction of NO with a solution of MbO<sub>2</sub> and CcOX in turnover and ii) is rapidly formed in cardiomyocytes after stimulation of the endogenous NO. To account for these findings, it has been proposed that also in the case of nitrosylated enzyme, NO is metabolised to nitrite by reacting with oxygen in the active site of the enzyme and that CcOX in turnover with cytochrome *c* and oxygen can efficiently compete with myoglobin for NO at the same enzyme concentration. These hypotheses suggest that under normal physiological and most pathological conditions, reaction of CcOX is the major route by which NO is removed from mitochondria rich cells. In contrast, oxymyoglobin has been proposed to be an efficient NO scavenger in the heart and skeletal muscle due to the high concentration in the cell and the fast ( $3\text{--}4 \cdot 10^7$ ) and irreversible reaction with NO (Brunori 2001). The best experimental evidence for this idea was the observation that knockout mice lacking myoglobin had an increased susceptibility to NO inhibition of cardiac function (Flogel et al. 2001). *To test experimentally the fate of NO bound to reduced CcOX and the competition between CcOX and Mb, spectrophotometric experiments have been conducted with these proteins and NO in solution.*

**Aim3:** *to investigate the interaction of bacterial terminal oxidases with NO.*

The study on bacterial terminal oxidases was aimed at understanding the molecular basis of the interaction of cytochromes *bo*<sub>3</sub> and *bd* with NO. Moreover, following the hypothesis that haem-copper oxidases are phylogenetically related to the bacterial NO reductase, the ability of these enzymes to reduce NO to N<sub>2</sub>O was also assayed; such activity, demonstrated for other prokaryotic oxidases (Giuffr  et al. 1999, Forte et al. 2001), might be relevant to the NO metabolism and detoxification. Cytochrome *bo*<sub>3</sub> and *bd*, and also the *cbb*<sub>3</sub> oxidase, which displays the higher NO reductase activity so far detected for the oxidases, are expressed in many human indigenous or pathogenic microorganism, which can adapt to or thrive under microaerophilic conditions. The ability to react with both oxygen and NO might provide additional and useful tools to cope with the antimicrobial NO produced by macrophages in response to bacterial infections as a part of the immune response. These enzymes, expressed under low oxygen tension, have an oxygen affinity definitely higher than the mammalian CcOX. This high affinity for oxygen, an important task for the bacteria that live in an oxygen-poor environment, if extended to NO, would suggest a possible reaction mechanism of NO reduction. The binding of two NO molecules to the active site may provide the molecular basis for N<sub>2</sub>O formation, as originally proposed for the *bo*<sub>3</sub> oxidase from *Escherichia coli* (Butler et al. 1997). In this hypothesis, based on spectroscopic data, two molecules of NO bind sequentially at Cu<sub>B</sub> of cytochrome *bd* with different observed dissociation constant. *To understand the mechanism of the NO reaction with cytochrome bo*<sub>3</sub>, the interaction of NO with of both oxidized and reduced enzyme purified from *Escherichia coli* as well its ability to reduce NO have been studied by amperometric and spectroscopic measurements. Since a role of the Cu<sub>B</sub> it has been proposed in the reaction of terminal oxidase with NO both in aerobic and anaerobic condition, it seemed interestingly to investigate the reaction of this gas with a peculiar terminal oxidase which does not contain copper, the cytochrome *bd* oxidase. With reference to the NO reductase activity, the chemical basis for the different ability of oxidases to reduce NO is still unknown. It may be assigned to a different affinity of the non-haem metal for NO or to the different redox-potential of the high-spin haem. The lack of Cu<sub>B</sub> makes cytochrome *bd* a useful system to test at least the importance of the presence of a non-haem metal in the NO reduction, since a non-haem iron (Fe<sub>B</sub>) and a copper (Cu<sub>B</sub>) are located, respectively, in the binuclear centre of the bacterial NO reductase and the oxidases so far detected to be able to reduce NO to N<sub>2</sub>O. Inhibition of the oxidase activity has also been proposed to occur upon interaction of Cu<sub>B</sub> with NO under condition in which the oxidized intermediates of CcOX catalytic cycle are more populated. Interestingly, it was reported that respiration of *Escherichia coli* cells expressing cytochrome *bd* is sensitive to NO (Stevanin et al. 2000). *To investigate the NO inhibition of cytochromes bd that lack Cu<sub>B</sub> and verify the presence of the NO reductase activity in both Escherichia*

*coli* and *Azotobacter vinelandii* purified enzymes, amperometric measurements were performed in both aerobic and anaerobic conditions.

**Aim 4:** to assess the role of the flavo di-iron proteins in the NO metabolism.

This question is important to the understanding of the interaction between NO and flavodiiron proteins, their ability to catabolise NO under anaerobic condition and the physiological relevance of this enzymatic activity. NO has the potential to damage a variety of biomolecules and organisms have evolved mechanisms for NO metabolism and detoxification in order to prevent the accumulation of toxic levels of this molecule. An inducible and robust NO metabolising and detoxifying activity has been reported (Gardner and Gardner 2002) in anaerobic *Escherichia coli* cells which lose this activity by knocking out the gene for the flavorubredoxin. The NO reduction system, however, has not been biochemically identified by these authors due to enzyme instability. *To verify whether the E.coli flavorubredoxin display NO reductase activity, amperometric measurements were performed on recombinant purified enzyme.* The flavorubredoxin is a member of the flavodiiron proteins widespread among strict and facultative anaerobic Archea and Bacteria.

Interestingly, recently genomic data and bioinformatics tools evidenced the presence in pathogenic protist (*Giardia intestinalis*, *Spironucleus barkhanus* and *Entamoeba histolytica*) of the genes encoding for these proteins, probably acquired by lateral gene transfer (Andersson et al. 2003). Other genes, indeed, in protists appear to have a bacterial ancestry; these acquisitions may be important in the evolution of the parasitic life style. The protist *Trichomonas vaginalis* is the causative agent of the trichomoniasis, the most widespread non-viral sexually transmitted disease, estimated to affect more than 200 million people worldwide. In infected individuals a chronic infection often rises suggesting that the parasites have evolved mechanisms to escape immune responses elicited by the host. However, these mechanisms are to date largely unknown. *To investigate the presence of a NO detoxification activity and correlate this function to the expression of an active flavodiiron protein, NO electrode measurements and immunodetection were performed on Trichomonas vaginalis intact and lysate cells.*

### 3. METHODS

#### 3.1 Isolation and purification of cytochrome *c* oxidase.

##### *Beef heart CcOX.*

Cytochrome *c* oxidase from beef heart was purified in TritonX-100, following the protocol of Soulimane and Buse (Soulimane and Buse 1995). The main steps of the purification in Triton-X 100 are:

- tissue homogenisation in 100 mM potassium phosphate, 250 mM sucrose, pH 11 at 4°C;
- separation of the mitochondrial membranes by centrifugation (13000 rpm, rotor JA 14, for 1h, at 4°C);
- first solubilization with 2.7% (p/v) TritonX-100 and 0.5 M KCl in 10 mM Tris/HCl, 250 mM sucrose, pH 7.6;
- centrifugation at 21000 rpm, JA 25.50, 4°C for 2.5 h : CcOX is in the pellet;
- second solubilization with 3% (p/v) TritonX-100 and 0.2 M KCl in 10 mM Tris/HCl, 250 mM sucrose, pH 7.6;
- centrifugation at 21000 rpm, rotor JA 25.50, 4°C, for 1h: CcOX is in the supernatant;
- anion exchange chromatography (Q-Sepharose Fast Flow) in 10 mM Tris/HCl, 0.1 % (p/v) Triton-X 100, pH 7.6: CcOX is eluted with a linear gradient of NaCl (100-500 mM);
- protein concentration by ultrafiltration.

This procedure delivers up to ~500 mg of protein from two bovine hearts. The enzyme is stored at -70°C, at a concentration of 100-150  $\mu$ M *aa*<sub>3</sub>, in 10 mM Tris/HCl, 500 mM NaCl, 0.1 % (p/v) Triton X-100, pH 7.6. Relevant to these studies, CcOX obtained with this protocol is in the *fast*, chloride bound conformation (§1.1.6).

#### 3.2 UV-visible absorption spectroscopy.

Absorption spectroscopy is a classical technique in the study of terminal oxidases since i) three of the four metal centres of the enzyme have characteristic and distinct absorption spectra (the two haems and Cu<sub>A</sub>), ii) the spectra of these chromophores are dependent on their redox state and, for haem *a*<sub>3</sub>, on the presence of ligands in the coordination sphere of the iron atom, allowing to study CcOX catalytic cycle as well its ligand binding properties, iii) the visible spectrum of the enzyme substrate cytochrome *c* has little or no overlay with the spectra of the different CcOX species (absorption maxima in the regions 520-550 and 580-607 nm, respectively). Relevant to the studies presented in these thesis, the optical contribution of haem *a* and haem *a*<sub>3</sub> to the reduced minus oxidized difference spectrum of CcOX have been deconvoluted using the method proposed by Vanneste (Vanneste 1966). According to this procedure, the contribution of haem *a* is obtained from the reduced minus oxidized spectrum of the cyanide-bound cytochrome oxidase: in the presence of this ligand haem *a*<sub>3</sub> reduction is considerably slowed down. The difference spectrum of haem *a*<sub>3</sub> is then obtained from the overall spectrum after subtracting the haem *a* contribution. In the Soret region, the two haems have very similar extinction coefficient, with the absorption maxima of haem *a* slightly red-shifted compared with that of haem *a*<sub>3</sub>; in the visible region (Fig.3.1) on the other hand, the contribution of the two chromophores are very different, with haem *a* spectrum characterized by a sharp, intense absorption peak and of haem *a*<sub>3</sub> producing a smaller and broader signal.

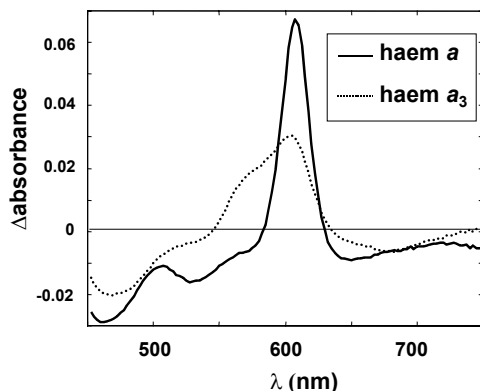


**Fig 3.1 Reduced minus oxidized absorbance spectra of haem *a* and haem *a*<sub>3</sub>.**  
Light path: 1cm

Absorption spectroscopy is a valuable experimental tool also when studying the binding and redox reactions of the oxidases with NO, since the products obtained have all distinct optical feature ( $\text{Fe}_{\text{a}_3}^{2+}\text{-NO}$  and  $\text{Fe}_{\text{a}_3}^{2+}\text{-NO}_2^-$ ). In Fig.3.2 is shown the reduced-NO bound cytochrome oxidase spectrum and the oxidized and reduced one for comparison. Static spectra were recorded with a double-beam spectrophotometer (Jasco V-550).

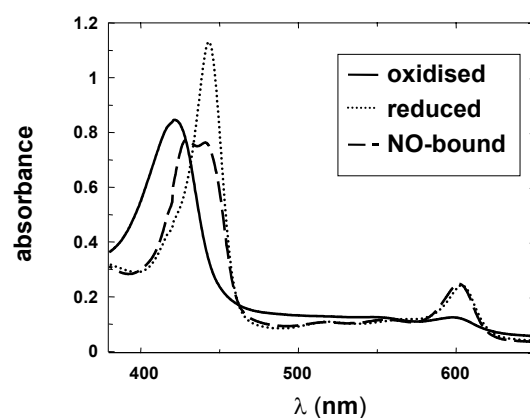


**Fig. 3.2 Oxidized, reduced and reduced NO-bound spectra of bovine cytochrome *c* oxidase.** Light path: 1cm

### 3.3 Time-resolved absorption spectroscopy.

#### 3.3.1 Apparatus.

Time-resolved absorption spectroscopy was performed in a DX.17MV Applied Photophysics stopped-flow equipped with a diode array (Leatherhead, UK). The observation chamber of this instrument has a light path of 1 cm and allows to record spectra in the range 380-650 nm, with an acquisition time of 2.5 ms. The mixing apparatus can be used in a simple and a sequential mixing mode (Fig. 3.3). In the first case, solutions A and B are mixed in equal volumes and spectra are recorded starting from 2.5 ms (dead time of the instrument). In the second case, equal volumes of solutions A and B are premixed; after a preset delay, the solution obtained from A+B is mixed with an equal volume of a third solution C and data are recorded as above. Spectra can be acquired according to a linear or a logarithmic scale. Experiments are performed under controlled temperature conditions. In the experiments presented in this thesis, the temperature was set at 20°C and the acquisition mode was according to a logarithmic scale.



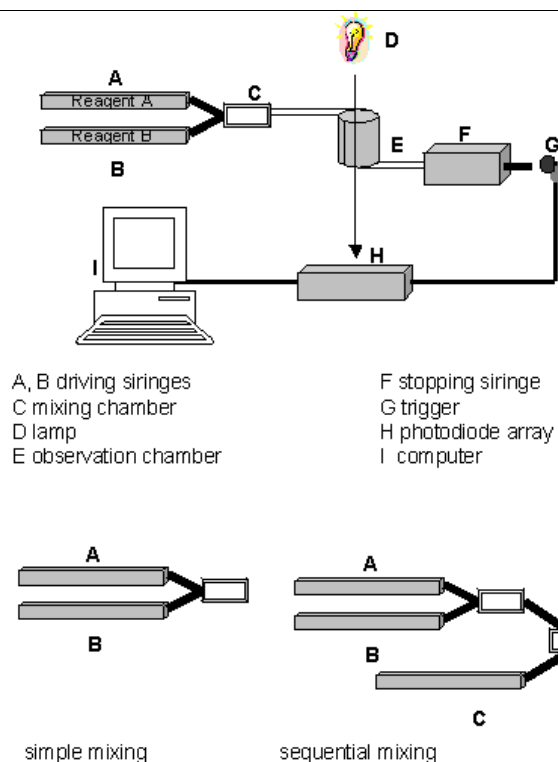


**Fig 3.3** Schematic representation of the stopped flow apparatus and of the different mixing modes.

### 3.3.2 Data analysis

Data analysis, consisting of noise filtering, spectral deconvolution and curve fitting, was carried out using the software MATLAB (The MathWorks, South Natick, MA, USA). Noise filtering was performed using the singular value decomposition (SVD) algorithm. Experimental data were expressed as difference spectra (base line: last spectrum) and matrix  $\mathbf{D}(\mathbf{w}, \mathbf{t})$   $m \times n$ , with  $m$  being the number of wavelength ( $w$ ) and  $n$  the number of spectra (each corresponding to a different point  $t$  of the time-course). Application of the SVD algorithm decomposed  $\mathbf{D}$  in the product of three orthonormal matrices:  $\mathbf{D}(\mathbf{w}, \mathbf{t}) = \mathbf{U} \mathbf{S} \mathbf{V}^T$ ; where  $\mathbf{U}$  is a matrix  $m \times n$ ,  $\mathbf{S}$  is a diagonal matrix  $n \times n$ ,  $\mathbf{V}$  is a matrix  $n \times n$  and  $\mathbf{V}^T$  is the transposed matrix of  $\mathbf{V}$ ; the elements of  $\mathbf{S}$  (*singular values*) are non negative numbers which decrease in value with increasing  $m$  (or  $n$ ) and indicate the relative weight of the corresponding columns of  $\mathbf{U}$  and  $\mathbf{V}$  in the matrix  $\mathbf{D}$ . If  $r$  is the number of strictly positive singular values which are  $> 0$ , for every  $k \leq r$ , the product  $\mathbf{U}_k \mathbf{S}_k \mathbf{V}_k^T$  is the matrix of rank  $k$  that best approximates  $\mathbf{D}$ , according to the least square minimization. The number of rows necessary to describe  $\mathbf{D}$  in good approximation defines also the number of optical components of the systems. As a consequence of the above statements, noise filtering of experimental spectra was achieved by using only the first rows of  $\mathbf{U}$ ,  $\mathbf{S}$  and  $\mathbf{V}$  to reconstruct the experimental matrix  $\mathbf{D}$ . In these studies, SVD analysis was used to assess the number of kinetic components of the reaction mixture (the rank of the matrix  $k$ ) and to obtain the time-course of the optical species ( $\mathbf{S}_k \times \mathbf{V}_k$ ) in simple reaction mixtures (one kinetic component). Spectral deconvolution, i.e. separation of the kinetic contribution of each chromophore in a complex reaction mixture (two or more optical species), was performed using the pseudoinverse algorithm. According to this method each experimental spectrum is fit to a linear combination of the spectra of the pure chromophores (reference spectra). Thus, if  $\mathbf{D}$  is the matrix of the experimental data and  $\mathbf{F}$  the matrix of the reference spectra, the time-course of each optical species  $\mathbf{C}_T$  can be obtained as

$$\mathbf{C}_T \sim \mathbf{D} \mathbf{F}$$

where the operator " $\sim$ " is the left division of MATLAB. The time courses obtained as described above were fitted to a sum of exponentials, using the algorithm

$$\mathbf{C}_T \sim \mathbf{A}(t) = \sum_i [\mathbf{A}_i^{ki(t)}]$$

where  $t$  is time,  $i$  the number of kinetic phases,  $A_i$  and  $k_i$  are the relative amplitude and kinetic constant of each phase.

### 3.3.3 The use of the pH sensitive dye phenol red.

The pH-dye phenol red was used to measure cytochrome *c* oxidase proton uptake during the reductive phase of the catalytic cycle, as described by Sarti et al (Sarti et al. 1985). This probe is particularly suitable for these studies, in fact i) it has a  $pK_a$  close to 7 ( $pK_a = 7.8$ ), ii) its visible spectrum has little overlapping with those of the two haems of CcOX (absorption maximum at 558 nm) and iii) it does not affect CcOX activity. To allow detection of pH changes in the micromolar range, all experiments were performed at pH 7.3-7.5 in an unbuffered medium (20 mM  $K_2SO_4$ , 0.2 % dodecyl- $\beta$ -maltoside, 100  $\mu$ M phenol red or 60 mM KCl, 0.2 % dodecyl- $\beta$ -maltoside, 100  $\mu$ M phenol red). The contribution of contaminant carbonates to the buffering capacity of the medium, which can be significant in these conditions, was decreased by using boiled ultrapure MilliQ water and by degassing the medium under  $N_2$ , in the presence of carbonic anhydrase (10  $\mu$ g/ml). Equilibration with  $N_2$  also decreased the concentration of oxygen, which was further scavenged by adding glucose (1-10 mM), glucose oxidase and catalase (catalytic amounts). Glucose can act as a mild reductant towards oxidase but this reaction was not observed on the time scale of our experiments. The absorbance changes of phenol red due to proton uptake by CcOX were calibrated in the stopped-flow, by monitoring the reaction of hydrolysis of  $N_\alpha$ -p-tosyl-L-arginine methyl ester (TAME) catalysed by trypsin, which is known to produce one  $H^+$ /molecule. In a typical calibration experiment, increasing concentrations of TAME (between 10 and 40  $\mu$ M) were premixed with trypsin (0.6 mg/ml); after 10 ms delay the solution obtained was mixed with oxidized CcOX (10  $\mu$ M) and spectra were collected as a function of time. Although CcOX doesn't take part to the hydrolysis reaction, it contributes to the buffering capacity of the solution during the experiments and was thus included in the reaction mixture during the calibration. The absorption spectra of phenol red were then corrected for the acidification signal obtained after diluting CcOX in the mixing chamber. This signal, in fact, was not due to the reaction studied but was small and highly reproducible when reducing the carbonates content of the medium. The corrected spectra were analysed by SVD analysis and global fitting. The total amplitude of the phenol red transition were linearly dependent on TAME concentration, although a significant variability was observed. The data were pooled and fitted by using the equation

$$y = \beta x + a_i$$

where  $i = 1, 2, \dots$  was the number of independent calibration experiments performed. From the resulting  $\beta$  value (OD at 558 nm), we reconstructed the difference spectrum of the dye corresponding to a 1  $\mu$ M change in the bulk  $H^+$  concentration. As shown fig.3.4 this procedure allowed to obtain a linear calibration curve and calculate the  $\Delta Abs$  of the phenol red transition corresponding to the release (uptake) of one  $H^+$ . To measure  $H^+$  uptake by CcOX, the enzyme was first equilibrated by dialysis against the experiment medium (~2 days, at 4°C) and then made anaerobic as described above. In a typical experiment oxidized CcOX (10  $\mu$ M) was reduced with Ru(II) hexamine (60  $\mu$ M) in the stopped-flow apparatus (simple mixing, symmetric mode) in the presence of phenol red and absorption spectra of the pH dye and of the two enzyme chromophores, haem *a* and *a*<sub>3</sub>, were recorded in the range 500-650 nm as a function of time. Ascorbate was not used to reduce the enzyme since at neutral pH this reductant exist in several protonation states and could contribute to the phenol red absorbance changes in an unbuffered medium. The contribution of the three chromophores (haem *a*, haem *a*<sub>3</sub> and phenol red) to the spectra were assessed by pseudoinverse analysis as described in § 3.3.2. The  $H^+$ /enzyme stoichiometries, expressed throughout as 90% confidence intervals, were obtained by dividing the observed redox-linked  $H^+$  concentration changes by the enzyme concentration.

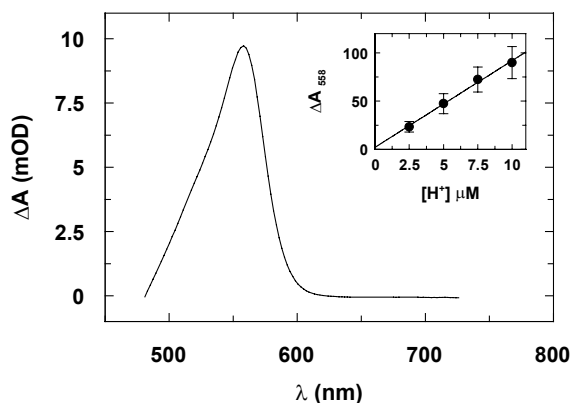


**Fig. 3.4 Absorbance spectrum of phenol red and calibration of the spectroscopic signal as a function of pH. The calibration curve was obtained as described in the text.**

### 3.4 Preparation and titration of aqueous solutions of NO.

Aqueous solutions of NO were prepared under anaerobic conditions because NO is not stable in an oxygen environment. A glass tonometer (volume: 2 litres) was washed with nitrogen to decrease the oxygen concentration, filled with pure NO gas (hours) and stored in the dark at 4°C. Aqueous solutions were prepared daily by equilibrating degassed MilliQ-pure water (15-20 ml) with the NO gas contained in the tonometer and titrated with reduced bovine cytochrome *c* oxidase under anaerobic conditions. This reaction, in fact, occurs with a known stoichiometry (1:1) and produces a distinct spectral transition (Stubauer et al. 1998). Solutions of NO prepared with this method had a typical concentration of ~2 mM.

### 3.5 Amperometric measurement of [O<sub>2</sub>] and [NO].

#### 3.5.1 General principles and experimental set-ups

O<sub>2</sub> and NO concentrations were measured polarographically with an O<sub>2</sub> and an NO Clark-type electrode respectively. In the Clark-type electrode, the probe is constituted of a platinum wire coated with Ag/AgCl, serving as reference electrode. The selectivity towards the specific gas is achieved by i) a gas-permeable hydrophobic membrane isolating the probe from the other redox-active non-gaseous species which might be present in the solution and ii) the polarization voltage applied. This is -0.67 V for O<sub>2</sub> ( $\frac{1}{2} \text{O}_2 + 2 \text{e}^- + 2 \text{H}^+ \rightarrow \text{H}_2\text{O}$ ) and +0.9 V for NO ( $\text{NO} \rightarrow \text{NO}^+ + \text{e}^-$ ); thus the two electrodes can be used in the same chamber without reciprocal interferences. In these studies different experimental set-ups have been used to measure either O<sub>2</sub> alone (Yellow Springs Instrument, model 5300, volume chamber 600 μl), NO alone (World Precision Instrument, model ISONOP, volume chamber 2 ml) and O<sub>2</sub> and NO simultaneously (Instech and World Precision Instrument respectively, volume chamber 1 ml). The oxygen electrode was calibrated by recording the signal in air-equilibrated buffer (corresponding to [O<sub>2</sub>] in the range 200-300 μM, calculated from the solubility of the gas in the buffer in the experimental conditions used) and subtracting the signal measured on addition of excess sodium dithionite ([O<sub>2</sub>] ≅ 0). The NO electrode was calibrated by recording the signal produced by adding known amount of a titrated NO solution (§ 3.4.) to nitrogen-equilibrated buffer (to minimize the NO/O<sub>2</sub> reaction).

#### 3.5.2 Stoichiometry of NO/CcOX reactions.

The stoichiometry of NO binding to terminal oxidases from was measured amperometrically with a NO electrode, according to Stubauer et al. (Stubauer et al. 1998). Experiments were performed in a gas-tight chamber, filled with nitrogen-equilibrated buffer to minimize the effects of the NO/O<sub>2</sub> reaction on the [NO]. In a typical experiment, the electrode was calibrated with two to four additions of a titrated solution of NO (1-10 μM); subsequent addition of the oxidase to the chamber caused a decrease in [NO], due to NO binding to the enzyme; the NO consumed was normalized to the enzyme concentration to calculate the stoichiometry of NO binding. With reduced enzymes, the experiment was performed in the presence of

ascorbate (10 mM) and TMPD (0.1mM) and with or without oxygen scavengers (ascorbic oxidase/ascorbate or glucose/glucose oxidase and catalase), to avoid CcOX oxidation by even contaminant amount of oxygen during the measurement. NO binding data were plotted as NO function and the observed dissociation constants were calculated using a non-linear regression analysis.

### 3.5.3 NO reductase activity

The presence of NO reductase activity in enzymes, in lysate and intact cell was tested amperometrically with a NO-electrode in the same anaerobic conditions and oxygen scavengers of §3.5.2, varying NO concentration from 1 to 20  $\mu$ M NO. To sustain the enzymatic activity enzyme-specific reductants were added. An initial drift in the NO concentration was assigned to the reaction of NO with the reductant and contaminant O<sub>2</sub>. Catalytic activities were calculated from the initial rate of NO consumption and corrected for the non-enzymatic NO consumption determined before the enzyme addition. *Trichomonas vaginalis* cells were always tested for viability in terms of mobility and trypan blue exclusion before the experiments. The functional assays were performed at pH 7.3 in phosphate-buffered saline (PBS) containing 5 mM maltose and 20  $\mu$ M ethylenediamine-tetracetic-acid sodium salt (EDTA). Before the assay, *T. vaginalis* cells were washed twice in PBS containing 5 mM maltose. Cell lysis was achieved by three cycles of freezing and thawing in the presence of 1 mM N-tosyl-L-lysine chloromethyl ketone protease inhibitor and the protease inhibitor cocktail for mammalian cell extracts.

### 3.5.4 NO inhibition measurement.

The cytochrome *bd* oxidase activity inhibition was tested after NO addition to the enzyme in turnover and the recovery of the function was measured in the presence and in the absence of oxy-hemoglobin to scavenge NO in the bulk. Mb in the oxygenated state (MbO<sub>2</sub>) was prepared by dithionite-reduction of met-Mb, followed by removal of excess dithionite by chromatography on a G25 column and subsequent oxygenation; MbO<sub>2</sub> concentration was determined spectrophotometrically ( $\epsilon_{580}=14.4 \text{ mM}^{-1} \text{ cm}^{-1}$  and  $\epsilon_{542}=13.9 \text{ mM}^{-1} \text{ cm}^{-1}$ ) and is expressed on the heme basis. The apparent inhibition constant  $K_i$  for NO inhibition was estimated by processing the amperometric traces using the software MATLAB. The extent of the enzyme inhibition was assessed by first derivative analysis of O<sub>2</sub> traces and plotted as a function of the NO concentration measured in parallel.

## 3.6 Immunoblotting.

Lysates prepared from *T. vaginalis* cultured cells were separated by SDS-PAGE electrophoresis, blotted onto a nitrocellulose membrane and blocked using standard protocols. Blots were incubated with rat polyclonal antibodies raised against *E. coli* FIRd, followed by incubation with the anti-rat IgG-alkaline phosphatase conjugate and detected with 4-nitroblue-tetrazolium chloride and 5-bromo-4-chloro-3-indolylphosphate.

## 4. RESULTS AND DISCUSSION

### 4.1 The redox-linked protonation of cytochrome *c* oxidase during the reductive phase of the catalytic cycle (paper I)

#### 4.1.1 Effect on chloride bound to the active site on beef heart cytochrome oxidase.

To study the redox-linked protonation of cytochrome oxidase (CcOX), the effect of chloride bound to the active site of beef heart CcOX during the reductive phase of the catalytic cycle was measured by multiwavelength stopped-flow spectroscopy, under anaerobic conditions and in the presence of the pH dye phenol red (§3.3.3). Upon anaerobic reduction of oxidized CcOX with ruthenium (II) hexamine, a non  $H^+$ -releasing electron donor, either in the chloride-bound or in the chloride free state, a different alkalization of the two reaction mixtures was observed. The raw data collected in the presence of ruthenium (II) hexamine at different point during the time course (shown in fig 4.1 top panels, as difference spectra with reference to the end point spectrum) were corrected for the aspecific acidification signal (inset) observed by performing the experiment in the absence of

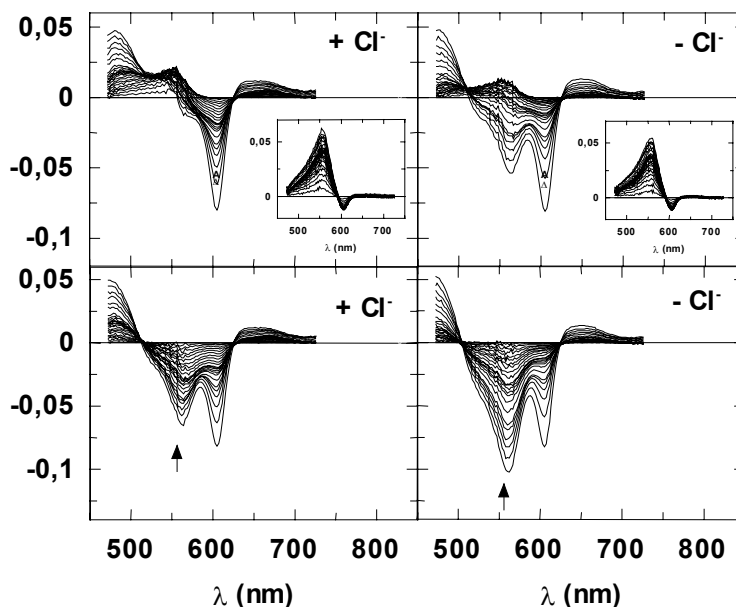


**Fig. 4.1 Effect of chloride on proton uptake during the reduction of CcOX: absorption spectra.** The effect of chloride on the apparent proton uptake is evidenced by the height of the phenol red peak at 560nm. Experimental conditions: [CcOX] = 5.5  $\mu$ M aa<sub>3</sub>, [Ru(II) hexamine] = 30  $\mu$ M, [phenol red] = 100  $\mu$ M. Buffer: 20mM K<sub>2</sub>SO<sub>4</sub>, 0.2% dodecyl- $\beta$ -D-maltoside.

the reductant over the same time range. The resulting corrected spectra are reported in Fig. 4.1, bottom panels. The amplitude of the absorption peak of the phenol red dye (absorbance changes at  $\sim$ 560 nm) evidences that in the chloride-bound enzyme the apparent stoichiometry of proton uptake, coupled to the reduction of CcOX (peak at 605 nm), is lower than that observed in the chloride-free one. To assess the effect of chloride on the reduction kinetics of the three chromophores (haem *a*, haem *a*<sub>3</sub>, and phenol red), their optical contribution was separated by pseudoinverse algorithm, involving a linear combination of the reduced-*minus*-oxidized spectra of haem *a* and haem *a*<sub>3</sub> and the alkaline-*minus*-acid spectrum of phenol red. The result of the analysis (fig. 4.2) shows that chloride did not affect the reduction of haem *a*, proceeding at  $\sim$ 35 s<sup>-1</sup>, but had some effect on the rate of haem *a*<sub>3</sub> reduction, the two rate constants of the biphasic kinetics being 7.3 s<sup>-1</sup> and 0.33 s<sup>-1</sup> in the chloride free enzyme and 3.2 s<sup>-1</sup> and 0.39 s<sup>-1</sup> in the chloride-bound form (relative amplitudes of the fast phase:  $\sim$ 60% and 35% respectively).

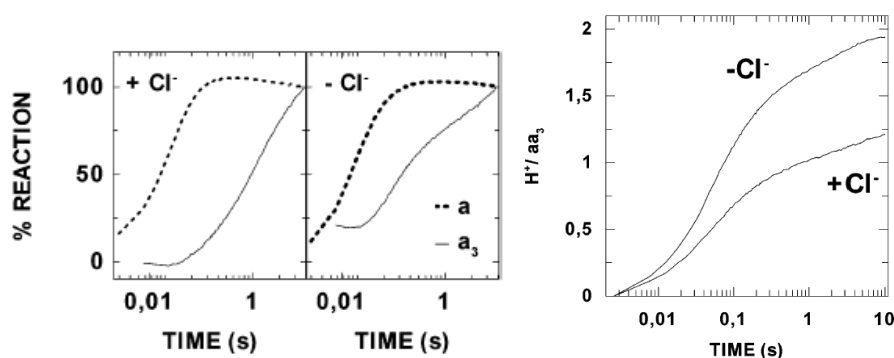


**Fig.4.2 Effect of chloride on proton uptake during the reduction of CcOX: kinetic analysis.** Right: Time courses of haem *a* and *a*<sub>3</sub>. Cl<sup>-</sup> does not affect haem *a* reduction while having some effect on haem *a*<sub>3</sub> reduction. Left: Time course of H<sup>+</sup> uptake, obtained by normalizing phenol red absorbance changes to the enzyme concentration.

It is worth noticing that the most important effect of chloride was on the extent of proton uptake that is smaller in the chloride bound enzyme, as revealed by the amplitude of the phenol red spectral transition normalized to the enzyme concentration. To estimate the apparent stoichiometries of protonation, the described experiments were repeated at different ionic strength and reductant concentration: we observed  $1.40 \pm 0.21$  H<sup>+</sup>/aa<sub>3</sub> for the chloride-bound CcOX (16 independent measurements) and  $2.28 \pm 0.36$  H<sup>+</sup>/aa<sub>3</sub> for the chloride-free enzyme (15 independent measurements). The time course of the phenol red deprotonation observed in a subset of experiments performed in the same condition of fig. 4.1 was best fitted by three different kinetics phases: the first phase was almost associated to haem *a* reduction, while the second and the third phase were reasonably synchronous to the biphasic reduction of haem *a*<sub>3</sub>. The result of this kinetic analysis, reported in table I, confirms that the absence of chloride increases the apparent stoichiometry by 0.8-0.9 H<sup>+</sup>/aa<sub>3</sub>.

Table I

Kinetic analysis of proton uptake coupled to CcOX reduction			
		Cl <sup>-</sup> -free	Cl <sup>-</sup> -bound
First phase	k (s <sup>-1</sup> )	25 ± 4 (39±8)*	32± 6 (34± 2) *
	H <sup>+</sup> /aa <sub>3</sub>	1.19 ± 0.25	0.57 ± 0.02
Second phase	k (s <sup>-1</sup> )	5.2± 1.1 (8.7± 2.0)§	7.1± 2.7 (3.6± 0.7)§
	H <sup>+</sup> /aa <sub>3</sub>	0.61± 0.03	0.54± 0.18
Third phase	k (s <sup>-1</sup> )	0.39± 0.07 (0.43±0.11)§	0.44± 0.22 (0.42± 0.03)§
	H <sup>+</sup> /aa <sub>3</sub>	0.42± 0.16	0.27 ± 0.04
Total	H <sup>+</sup> /aa <sub>3</sub>	2.22 ± 0.32 (n=5)°	1.38 ± 0.15 (n=3)°

\* rate constant of haem *a* reduction

§ rate constant for haem *a*<sub>3</sub> reduction

° number of experiments

Importantly, by comparison of these kinetic data, it appears that most of this extra proton is taken up during a process synchronous with haem *a* reduction and faster than that of haem *a*<sub>3</sub>; thus, the 0.8-0.9 proton could be associated to the reduction of either haem *a* or Cu<sub>B</sub>, but the chosen experimental conditions do not allow to assign unequivocally this extra proton since a concomitant reduction of haem *a* and Cu<sub>B</sub> is expected. In fact, in the presence of the detergent dodecyl-β-D-maltoside at pH 7 and at the low concentration of the reductant ruthenium II hexamine (30 μM) used, the rate of reduction of haem *a* and haem *a*<sub>3</sub>-Cu<sub>B</sub> site are quite similar ( $k' = 35$  s<sup>-1</sup> vs 25-85 s<sup>-1</sup> Brunori 1997, Verkhovsky et al. 1995). Reduction of Cu<sub>B</sub> cannot be monitored by optical spectroscopy and, to distinguish the relative contribution, these experiments were repeated at different reductant concentration after replacing dodecyl-β-D-maltoside with Triton X-100, a detergent known to slow

down the electron transfer between haem *a* and haem  $a_3$ -Cu<sub>B</sub> site (Malatesta et al. 1990). Under these conditions the reduction kinetics of both Cu<sub>B</sub> and haem *a* are resolved.

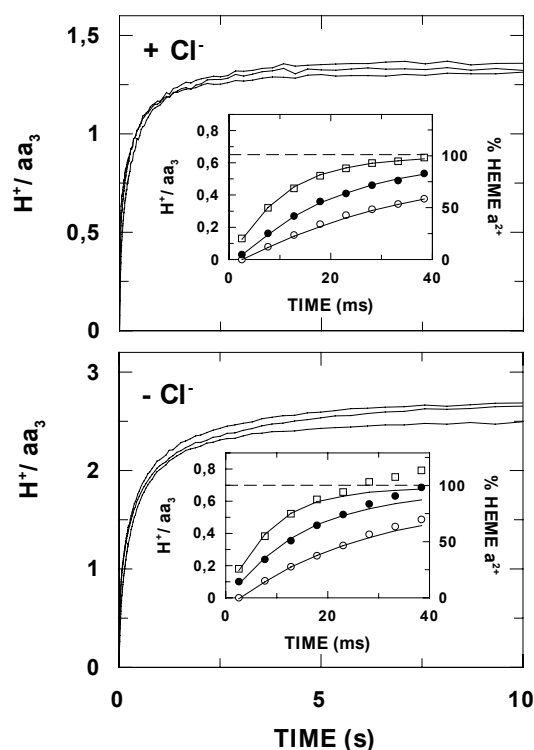


**Fig.4.3. Effect of chloride on H<sup>+</sup> uptake during haem reduction.** The experiment described in fig. 4.1 was repeated at different Ru (II) hexamine concentration, replacing dodecyl-β-D-maltoside with Triton X-100. In these conditions haem *a*-Cu<sub>B</sub> reduction is slowed down and does not interfere with haem *a* reduction, occurring in the few tens of ms. Top and bottom: overall stoichiometry of H<sup>+</sup> uptake: chloride decreases the apparent as H<sup>+</sup>/aa<sub>3</sub> as shown in fig.4.1. Insets: Time courses of haem *a* reduction at 30(○), 60 (●) and 125 μM(□) Ru (II) hexamine chloride has no effect on the H<sup>+</sup>/aa<sub>3</sub> whose asymptotic value is ~0.6-0.7

The proton uptake timecourses, obtained analysing of the experiments in Triton X-100, show (fig. 4.3) that i) the effect of chloride on the overall apparent proton uptake is the same observed in the experiments conducted in the presence of dodecyl-β-D-maltoside; ii), the reduction of haem *a*, over the first 40 ms of the reaction, occurs at a rate proportional to the concentration of the reductant, iii) is always associated to same amount of protons ( $0.59 \pm 0.06$  H<sup>+</sup>/aa<sub>3</sub>, n=11) and iv), interestingly, is not dependent on the presence of chloride at the active site. Based on these observations, the uptake of these  $0.59 \pm 0.06$  protons was associated to haem *a* reduction of both chloride-bound and chloride free CcOX, whereas the extra proton uptake ( $\sim 0.9$  H<sup>+</sup>) measured in the chloride-free enzyme to Cu<sub>B</sub> reduction.

**Final remarks:** the apparent stoichiometry of proton uptake in the presence of chloride is  $1.40 \pm 0.21$  H<sup>+</sup>/aa<sub>3</sub>, ( $\sim 0.6$  H<sup>+</sup> and  $\sim 0.8$  H<sup>+</sup> taken upon haem *a* and haem  $a_3$ -Cu<sub>B</sub> reduction, respectively), and in its absence  $2.28 \pm 0.36$  H<sup>+</sup>/aa<sub>3</sub>. ( $\sim 0.6$  H<sup>+</sup> and  $\sim 1.7$  taken upon haem *a* and haem  $a_3$ -Cu<sub>B</sub> reduction, respectively). The analysis of protonation/reduction kinetics in the two ligand states and in different experimental conditions shows that the uptake of the extra proton observed in the chloride-free enzyme ( $\sim 0.9$  H<sup>+</sup>/aa<sub>3</sub>) is coupled to the reduction of Cu<sub>B</sub>.

#### 4.1.2 Implications for the proton uptake coupled to CcOX reduction.

The study of biological proton-transfer is complex since, in contrast to redox reactions, protonation reactions are generally not associated with spectral changes and it is often difficult to define the properties (e.g. pK<sub>a</sub> values) of the donor-acceptor pair. A skillful protocol which make use of time resolved spectroscopy and the pH-indicator dye phenol red was developed to measure the stoichiometry and the kinetics of redox-linked protonation upon soluble beef heart CcOX reduction. Protonation of the hydroxide anions (OH<sup>-</sup>), formed in the active site during the oxidative phase of CcOX catalytic cycle, has been proposed to occur during the successive reductive phase, ensuring a tight coupling between proton and electron transfer in the enzyme through a mechanism of charges compensation; the following H<sub>2</sub>O dissociation has been tentatively proposed to be synchronous to Cu<sub>B</sub> reduction, but never demonstrated (Michel 1999, Zaslavsky and Gennis 2000, Wikstrom et al. 2000). The comparative study on chloride-bound and chloride-free beef heart CcOX has proved to be a good method to evidence the proton-electron transfer processes occurring upon enzyme reduction since i)

the sensitivity of the assay is high, HCl is a strong acid and changes in  $H^+/aa_3$  stoichiometry are associated quantitatively to the dissociation of the anion, in contrast to  $H_2O$ ; ii) the chloride bound form can be easily obtained by purifying the enzyme in the presence of chloride; iii) the chloride free-form can be generated by extensive dialysis against a chloride-free buffer or with a reduction/reoxygenation cycle, followed by a chromatographic step to remove chloride and excess of reductant; iv) the presence or absence of chloride at the active site can be easily demonstrated making use of their different properties (optical spectroscopic features and reactivity towards NO).

The results of this study show that the overall reduction of CcOX in the presence chloride is associated to an apparent stoichiometry of proton uptake of  $1.40 \pm 0.21 H^+/aa_3$ , which is lower than that measured in its absence ( $2.28 \pm 0.36 H^+/aa_3$ ). The kinetic analysis showed that the extra  $\sim 0.9 H^+/aa_3$  proton observed in the chloride-free enzyme is coupled to the reduction of  $Cu_B$ . Based on these data, a model of proton-electron coupling at the  $Cu_B$  site has been hypothesised (fig. 4.4). In the fully oxidized chloride-bound CcOX  $Cu_B$  has as a fourth ligand chloride, never assessed crystallographically, but inferred from its effect on the reactivity of this metal with external ligands and confirmed by EXAFS data. When the first electron is transferred to the active site,  $Cu_B$  is reduced, this metal being preferentially reduced in the single electron reduced binuclear site, and concomitantly, chloride, charge-neutralized by protonation, diffuses as an electroneutral molecule (HCl) from the protein. Once released in the bulk, HCl dissociates releasing one proton back in the medium. The complete dissociation of chloride explains the lower apparent proton uptake in the bound chloride CcOX. With the assumption that other ligands behave as chloride, we could extend this reaction scheme to the dissociation other anions, such as hydroxide, present in the catalytically competent CcOX, and nitrite, formed in the active site upon NO binding to CcOX oxidized catalytic intermediates.

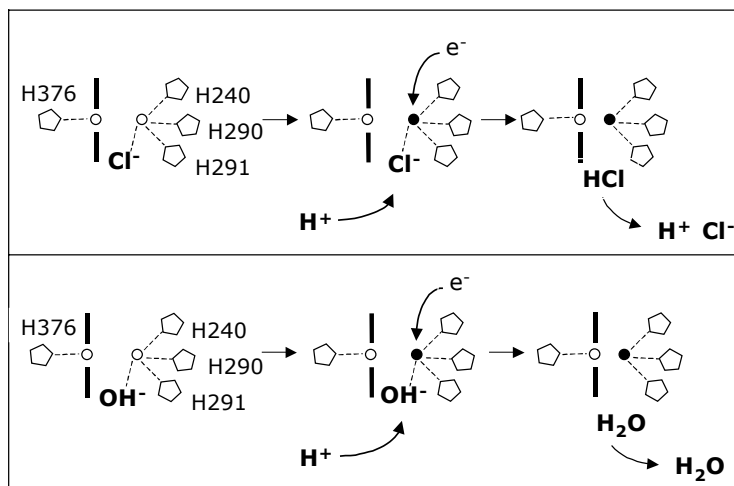


**Fig. 4.4. Possible model of proton-electron coupling at the  $Cu_B$  site.** Haem  $a_3$  and  $Cu_B$  are depicted with their crystallographically determined histidine ligands.

The application of this model to hydroxide is supported by several structural and functional studies: i) EXAFS and ENDOR spectroscopic data, showing an hydroxide as a ligand of  $Cu_B$  (Fann et al. 1995), ii) modelling of the X-ray crystallographic data of the oxidized *Paracoccus denitrificans* CcOX, proposing a water plus an hydroxide between haem  $a_3$  and  $Cu_B$ , iii) electrostatic calculation (Kannt et al. 1998), reporting the stabilization function of the hydroxide liganded to  $Cu_B$  (by lowering the level the electrostatic repulsion between the two metals in the active site), iv) kinetics data, suggesting the dissociation and protonation of the hydroxide upon transfer of the first electron to the active site coupled to uptake of a proton coming either from the K pathway (Kannt et al. 1998), or a nearby water molecule liganded to haem  $a_3$  (Wikstrom et al. 2000), v) the X-ray structure of the reduced cytochrome c oxidases (Yoshikawa, et al. 1998), (Harrenga and Michel 1999) showing the lack of continuous electron density between haem  $a_3$  and  $Cu_B$  (observed in the oxidised enzyme



structures); this observation is consistent with water dissociation from the active site during the reductive phase of the catalytic phase, whatever the detailed molecular mechanism.

It is worth noticing that the hydroxyl protonation and dissociation from  $\text{Cu}_B$  may have an essential role in the enzymatic function. The change in the coordination state of  $\text{Cu}_B$  from tetragonal to trigonal after reduction of the active site and/or the protonation required in the dissociation mechanism might increase the energy associated to the electron transfer process, accounting for the rate-limiting electron transfer between haem *a* and the binuclear centre. In addition, the dissociation of a water molecule formed in the active site could diffuse through the protein matrix restoring the proton connectivity with the D-pathway required for the mechanism of proton pumping (Backgren et al. 2000), (Wikstrom et al. 2003). Finally, the free energy associated with electron transfer to the binuclear centre and protonation of the hydroxide anion upon reduction of the oxidized enzyme provides the driving force for the pumping of one proton (Branden et al. 2003). *The results reported in this study, indeed, represent the experimental support for the water formation mechanism on  $\text{Cu}_B$  reduction hypothesized in the past, but never proven.*

The information available in the literature on the structure and dissociation mechanism of hydroxide reveals that this anion behaves similarly to chloride and for analogy the proposed model may apply also to nitrite. Although there are not data on the structure of the nitrite adduct, this anion formation upon reaction of NO with  $\text{Cu}_B$  strongly supports the binding of this anion to the active site and the nitrite dissociation upon reduction of the binuclear centre suggests that this anion behaves as chloride and hydroxide.

## 4.2 The role of the K and D proton conducting pathways during the reductive phase of cytochrome oxidase catalytic cycle (paper II)

### 4.2.1 Effect of the K354M and D124M mutations on proton-electron transfer coupled to *Paracoccus denitrificans* cytochrome c oxidase reduction.

To assess the role of the crystallographically identified K and D proton conducting pathways during the reductive phase of the catalytic cycle, the redox-linked protonation upon reduction of *Paracoccus denitrificans* CcOX was investigated in the wild type, K354M and D124N mutant of the subunit I by using the spectrophotometric and quantitative protocol set up working on the mechanism of chloride dissociation from beef heart CcOX. Calibration of phenol red dye signals (§3.3.3) was performed in the presence of *P.denitrificans* CcOX to account for the contribution the enzyme to the overall buffer power and corrected for the unspecific non-redox-linked acidification signal invariably observed upon when the oxidase is mixed with buffer (also noticed with the beef heart enzyme). Comparison of the calibrations obtained with the bovine and *Paracoccus* enzyme under identical conditions shows that the power buffer of the bacterial enzyme is ~ 20% greater than that of the mammalian enzyme. It was assumed that the power buffer of the D124N and K354M mutants was identical to the wild-type enzyme. Upon mixing oxidized *P.denitrificans* CcOX, either the wild-type or the mutants, with ruthenium II hexamine, an absorption increase of the phenol red dye (560 nm), corresponding to an alkalization of the buffer, was observed (fig. 4.5). The raw data were expressed as difference spectra and corrected by subtracting the aspecific non redox-linked acidification. This acidification, not observed in the absence of the enzyme and significantly smaller in the K354M mutant, seems to be due to a slow proton release from the protein through the K-pathway. The effect of the mutation in the K channel on the apparent proton uptake coupled to the reduction of the haems (peak at 605 nm) is evidenced by the small amplitude of the absorption peak of the phenol red dye (560 nm) compared to that of the wild-type and the D124N mutant, which, instead, are similar.

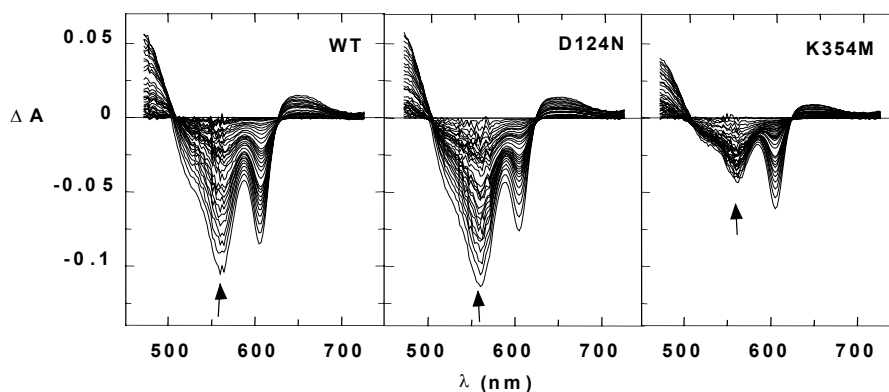


**Fig.4.5 Effect of mutations in the K and D channels on proton uptake during the reduction of CcOX: absorption spectra.** The effect of mutations on the apparent proton uptake and the partial reduction of the haems in the K354M mutant are evidenced by the height of peaks of phenol red at 560nm (arrows) and of the reduced haems at 605nm. Experimental conditions as in Fig.4.1

To study the effect of the mutations on the proton-linked reduction kinetics of the chromophores (haem *a* haem *a*<sub>3</sub> and phenol red) the corrected spectra were separated by pseudoinverse analysis. Both mutations did not affect the reduction of haem *a* (fig. 4.6 top and left panel), proceeding a little faster in the mutants ( $32 \pm 6 \text{ s}^{-1}$  and  $3.5 \pm 1.3 \text{ s}^{-1}$ , relative amplitude 75 and 25%) than in the wild-type enzyme ( $23 \pm 3 \text{ s}^{-1}$  and  $2.3 \pm 0.5 \text{ s}^{-1}$ , relative amplitude 70 and 30%). The biphasicity observed in haem *a* reduction may be explained by: i) the low excess of ruthenium II hexammine relative to the enzyme (30 and 5  $\mu\text{M}$ ) and ii) the faster equilibration of the electrons within the metal centre respect to the reductant oxidation. Interestingly, the main effect of the mutation in the K channel was on the kinetics of reduction of haem *a*<sub>3</sub> that is severely retarded (fig 4.6 op and right panel).

Consistently, the stoichiometry of proton uptake in the K354M, in which electron transfer to the active site is impaired, is significantly smaller (Fig. 4.6 bottom panel) than in the wild-type and in the D124N mutant, both completely reduced over the same time scale (wild-type  $6.7 \pm 1.4 \text{ s}^{-1}$  and  $0.3 \pm 0.16 \text{ s}^{-1}$  relative amplitude 70 and 30%, D124N  $6.9 \pm 0.7 \text{ s}^{-1}$  and  $0.3 \pm 0.02 \text{ s}^{-1}$  relative amplitude 60 and 40%). To quantify the effect of the mutations on the stoichiometry of protonation several experiments were performed and the estimation was  $3.3 \pm 0.6 \text{ H}^+$  (n=12) for the wild type enzyme,  $3.2 \pm 0.5 \text{ H}^+$  (n=8) for the D124N mutant and

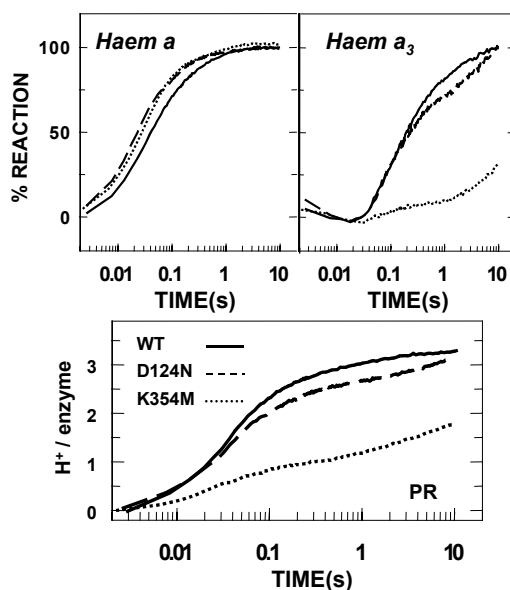


**Fig.4.6 Effect of proton pathways mutations on proton uptake during the reduction of CcOX: kinetic analysis.** Top: Time courses of haem *a* and *a*<sub>3</sub>. Mutations in the D and K channels do not affect haem *a* reduction while having an effect on haem *a*<sub>3</sub> reduction, slight in the D124N and strong in the K354M. Bottom: Time course of  $\text{H}^+$  uptake, obtained by normalizing phenol red absorbance changes to the enzyme concentration. K354M mutation decreases the apparent stoichiometry of  $\text{H}^+$  uptake.

$1.7 \pm 0.3 \text{ H}^+$  ( $n=6$ ) for the K354M mutant. Thus, the D124N mutation does not affect the number of protons uptaken by *P. denitrificans* CcOX. Comparison of the reduction and protonation kinetics shows that  $\sim 2.2 \text{ H}^+$  in the wild type and  $\sim 1.7 \text{ H}^+$  in the D124N are associated to haem *a* (and presumably  $\text{Cu}_B$ ) reduction and the additional protons (1.1 and 1.5 in the wild type and in the D124N mutant respectively) with the reduction of haem  $a_3$ . In the K354M mutant only  $0.8 \pm 0.1 \text{ H}^+$  is taken up synchronously to haem *a* reduction, followed by a slow binding of  $0.7\text{--}0.9 \text{ H}^+$ , compatible with the partial and retarded reduction of the active site. The extra protons seen in the D124N and in the wild type are not associated to the reduction of haem *a*, in fact only  $\sim 0.8 \text{ H}^+$  is bound upon reduction of this site in the K354M mutant. Since in the wild type enzyme the reduction kinetics of haem *a* and haem  $a_3\text{--Cu}_B$  are partially overlapping and the reduction of  $\text{Cu}_B$  cannot be monitored by optical spectroscopy, this conclusion has been drawn from the following observations on the K354M mutant: i) the reduction of haem  $a_3$  is much slower than that of haem *a* (reduction of haem *a* and haem  $a_3$  kinetically resolved), ii) electron transfer to  $\text{Cu}_B$  is strongly retarded probably occurring (Verkhovsky et al. 2001) over a few hundreds of milliseconds ( $\text{Cu}_B$  reduction should not contribute to the measured  $0.8 \text{ H}^+$  upon haem *a* reduction).

**Final remarks:** The stoichiometry of proton uptake associated to the reduction of the *P. denitrificans* oxidase is  $3.3 \pm 0.6 \text{ H}^+$  for the wild type, out of which  $0.8 \pm 0.1 \text{ H}^+$  upon reduction of haem *a* and by subtraction,  $2.5 \pm 0.7 \text{ H}^+$  upon reduction of the binuclear site,  $3.2 \pm 0.5 \text{ H}^+$  for the D124N mutant and  $1.7 \pm 0.3 \text{ H}^+$  for the K354M.

#### 4.2.2 Role of the K and D proton pathways during enzyme reduction

Functional and structural studies on haem copper oxidases have provided informations on the temporal and energetic coupling between the electron and the proton transfer associated to the oxygen reduction. The K- and D-channels, identified on the basis of results from studies on mutant oxidases and the analysis of the X-ray crystal structures, are the pathways known to transfer protons to the catalytic side as well to a proton-accepting group in the exit pathway (chemical and pumped protons respectively). To distinguish the role of both these channels in the redox-linked protonation during the reductive phase of the catalytic cycle, reduction and protonation kinetics of the wild type and the K and D channel mutant oxidases of *P. denitrificans* were studied.

Interestingly, upon complete reduction, the wild type *P. denitrificans* oxidase binds about one proton in excess compared to the bovine enzyme ( $\sim 3.3$  vs  $2.3\text{--}2.5 \text{ H}^+$ ). This finding may be consistent with the proton pumping mechanism model (Yoshikawa et al. 1998), based on the comparison of the three-dimensional structures of the fully reduced and fully oxidized bovine CcOX, in which D51 would be deprotonated upon enzyme reduction. The lack of this residue, not conserved in the bacterial oxidase, might be an explanation of the extra proton observed upon reduction of this enzyme. In addition, it is worth noticing that CcOX is a redox-linked pump and the  $\text{pK}_a$  of different ionisable residues depends on the redox/ligation state of the metal centres; these groups indeed are at the heart of the proton-electron coupling. Thus, the different proton uptake observed in the bacterial and mitochondrial enzyme may be due to i) different redox-linked ionisable residues or ii) different redox-linked  $\Delta\text{pK}_a$ 's of the same residues. Consistently, the oxidized *P. denitrificans* CcOX showed a pH buffer power  $\sim 20\%$  larger than that of the oxidised bovine enzyme, indicating that the two proteins have a different number of ionisable groups.

The stoichiometry of proton uptake upon reduction of the D124N mutant ( $\sim 3.2 \text{ H}^+$ ) is not significantly different from that of the wild type, but decreases in the K354M mutant ( $\sim 1.7 \text{ H}^+$ ). When the wild type *P. denitrificans* oxidase is completely reduced,  $3.3 \pm 0.6 \text{ H}^+$  are taken up, of which  $0.8 \pm 0.1 \text{ H}^+$  upon reduction of haem *a* and by subtraction,  $2.5 \pm 0.7 \text{ H}^+$  upon reduction of the binuclear site. As the  $\text{H}^+/\text{e}^-$  ratio is bigger than the expected ( $1.25 \pm 0.35$  vs 1), it has been assumed that part of the extra proton may be bound in response to redox-coupled conformational changes ('Bohr protons'). Electrostatic calculation, based on the structure of the two subunits *P. denitrificans* CcOX resolved at  $2.7\text{\AA}$  (Kannt et al. 1998), predicted that  $0.7\text{--}1.1 \text{ H}^+$  should be coupled to haem *a* reduction and  $1.8 \text{ H}^+$  for the active site reduction. The importance of the differences of the measured and predicted overall protonation ( $3.2$  vs  $2.5\text{--}2.9 \text{ H}^+$ ), at the present available resolution of the structure, has to be stated. Importantly, the estimate of the protons bound by *P. denitrificans* CcOX upon reduction of haem *a* is in agreement with the value found with the beef CcOX (experiments in Triton X-100 (paper I) and working with the mixed valence-CO enzyme (Capitanio et al. 1997)). Thus, the extra proton observed in the bacterial enzyme respect to the bovine is linked to the reduction of the haem  $a_3\text{--Cu}_B$  and cannot

be justified by the absence of the D51, as the conformational changes of the D51 in the bovine enzyme were proposed to be associated to the haem *a* reduction (Okuno et al. 2003).

Relevant to the role of the proton channels, since *the stoichiometry of proton uptake coupled to haem a reduction is not affected by blocking either the K- or the D-pathway, these channels are not involved in this process*. This assumption is supported by other studies conducted on CcOX mutants in residues buried in the channels (Wikstrom et al. 2000, Vygodina et al. 1998, Giuffrè et al. 2000), and located at the entrance of the K pathway (E78 of the *Rhodobacter sphaeroides* oxidase Tomson et al. 2003). Thus, the residue(s) involved in haem *a* redox-coupled reduction are not part of the protonic channels, but could be on the surface of the protein or in the membrane matrix whereby protonation would affect the electrogenicity of the haem *a* reduction; in this latter case a role of haem *a* in the mechanism of proton pumping may be hypothesized.

The participation of the D pathway in the proton uptake coupled to reduction of the haem  $a_3$ -Cu<sub>B</sub> is not clear in the literature. The small effect observed on the reduction kinetics in the D124N analogous mutant of *R. sphaeroides*, suggesting that the D pathway is not involved in proton transfer upon enzyme reduction (Vygodina et al. 1998), is in contrast to the very slow rate (minutes) of haem  $a_3$  reduction in *P. denitrificans* D124N mutant (Wikstrom et al. 2000) which lead to hypothesize that at least one proton is transferred through the D pathway. Our data show that *at least part of the ~ 2.5 protons involved in haem  $a_3$ -Cu<sub>B</sub> reduction are transferred through the K pathway*. The D124N is fully reduced within 10 seconds and, as expected, binds approximately the same numbers of protons as the wild-type. The only slight effect observed with this mutant is a delay in the kinetics of binding of ~ 0.5 protons, suggesting a slower proton transfer in the D124N mutant respect to the wild-type enzyme, but leaving unchanged the overall stoichiometry over the same time scale. In conclusion, *the comparative study on the K and D channel mutants support a major role of the K pathway in the protonation coupled to the binuclear site reduction and exclude an involvement of either the K- or the D-pathway in the redox-linked protonation synchronous to haem a reduction*.

### 4.3 The reaction of nitrosylated cytochrome c oxidase with oxygen and the competition between MbO<sub>2</sub> and cytochrome c oxidase.

#### 4.3.1 The reaction of reduced nitrosylated cytochrome c oxidase with oxygen.

The reaction of reduced nitrosylated CcOX with oxygen has been studied by time resolved spectroscopy in order to discriminate between nitrite and NO as reaction products. MbO<sub>2</sub> was used as a probe for NO as i) MbO<sub>2</sub> is oxidized by NO to met-Mb very rapidly (microseconds to milliseconds) and stoichiometrically, and ii) micromolar nitrite does not react with MbO<sub>2</sub> over hundreds of seconds. Upon mixing in the diode-array stopped-flow instrument CcOX-NO with an air-equilibrated solution containing excess MbO<sub>2</sub>, an absorption decrease at 602 nm of CcOX and at the  $\alpha$  and  $\beta$  bands of MbO<sub>2</sub> is observed (fig 4.7), indicating that NO dissociates from haem  $a_3$ , CcOX is oxidized by O<sub>2</sub> and, concomitantly, MbO<sub>2</sub> is oxidized to met-Mb. The slow rate of formation of met-Mb corresponds to the rate of NO dissociation from reduced heme  $a_3$ . Thus, NO is released from CcOX-NO as such and very quickly scavenged by MbO<sub>2</sub>. Obviously, when MbO<sub>2</sub> was mixed with reduced CcOX in the absence of NO, no optical changes at the level of Mb bands were observed.

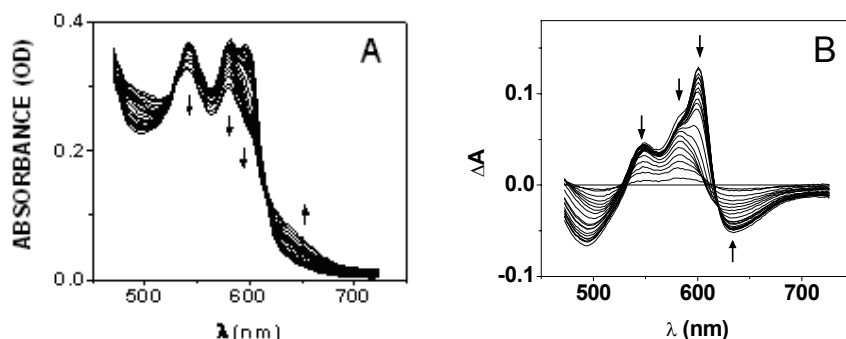


**Fig. 4.7 MbO<sub>2</sub> is oxidized by the product of the reaction of nitrosylated CcOX with oxygen.** Absorption spectra collected over 200 s after mixing reduced nitrosylated CcOX with an air-equilibrated solution of MbO<sub>2</sub> (A); data are shown as difference spectra (B) with reference to the final spectrum. It may be seen that MbO<sub>2</sub> is partly (~ 50 %) oxidized concomitantly with the dissociation of NO from CcOX and the subsequent oxidation of

the enzyme. Nitrosylated CcOX was prepared by anaerobic incubation with 2 mM ascorbate and 50 nM Ru-hexamine, followed by addition of stoichiometric amounts of NO immediately before the experiment. Concentrations after mixing: [CcOX] = 8.5  $\mu$ M aa<sub>3</sub>; [MbO<sub>2</sub>] = 17.4  $\mu$ M. T = 20 °C.

The optical contributions of the two proteins was separated by analysis of the absorption changes at 599 and 577 nm; these wavelengths were found to be virtually isosbestic for MbO<sub>2</sub> and CcOX-NO oxidation, respectively: the corresponding time courses of oxidation of the two proteins are shown in Fig. 4.8. Met-Mb accumulates to an extent that nicely corresponds to the amount of NO initially bound to CcOX and at a rate compatible with NO dissociation from reduced haem a<sub>3</sub> (Fig. 4.8 A, CcOX-NO). MbO<sub>2</sub> was mixed with a large excess of nitrite or nitrate, but no significant met-Mb accumulation is observed (Fig. 4.8 A). *These data support the hypothesis that, in the presence of excess O<sub>2</sub>, NO dissociates from reduced haem a<sub>3</sub> and is released as NO into the bulk, where it reacts with MbO<sub>2</sub>, ruling out the possibility that nitrite putatively produced in the reaction of CcOX-NO with O<sub>2</sub> is responsible for the oxidation of MbO<sub>2</sub>.*

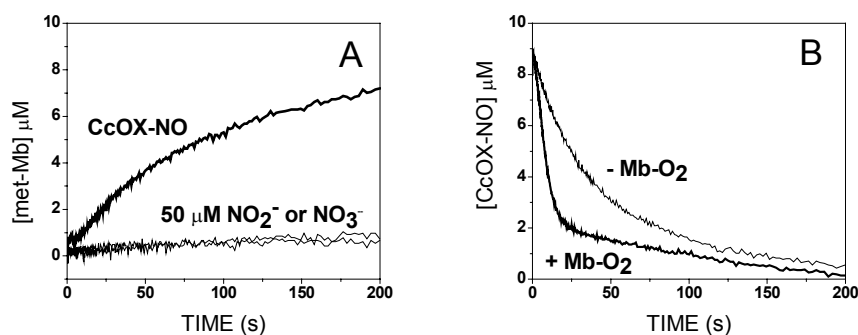


**Fig 4.8. The reaction product is neither nitrite nor nitrate.** The traces depict the time courses of oxidation of MbO<sub>2</sub> (A) and of CcOX-NO (B), respectively obtained by analysis of the absorption changes at 577 nm and 599 nm from the data set in Fig. 4.1 A) Oxidation of MbO<sub>2</sub> proceeds at  $k' = 0.012 \text{ s}^{-1}$  and the amount of accumulated met-Mb matches the concentration of nitrosylated CcOX which becomes oxidized upon reaction with O<sub>2</sub>. Over the same time range, no significant oxidation of MbO<sub>2</sub> is observed upon exposure to either nitrite or nitrate.

**B)** Oxidation of CcOX is biphasic and faster in the presence of MbO<sub>2</sub> than in its absence.

Consistently, the presence of MbO<sub>2</sub> or flavohemoglobin and NADH, that act as scavengers of free NO, accelerates the apparent oxidation of CcOX-NO (Fig. 4.8B): under these conditions, NO recombination to reduced CcOX, which would occur in the absence of MbO<sub>2</sub>, is prevented. The oxidation of CcOX observed in the presence of MbO<sub>2</sub>, at a wavelength (599 nm) isosbestic for the MbO<sub>2</sub> → met-Mb transition, is biphasic with a fast component accounting for approximately 80 % of the reaction amplitude, assigned to the oxidation of haem a, followed by the slower oxidation of haem a<sub>3</sub>, whose rate matches the oxidation of MbO<sub>2</sub>. The oxidation of haem a that follows NO dissociation from reduced CcOX is apparently faster than the rate of met-Mb accumulation; this phenomenon was already observed with the CO derivative of the enzyme (Antonini et al. 1987). In these experiments no effects were observed upon addition of superoxide dismutase.

**Final remark:** NO is released in the reaction of nitrosylated CcOX with oxygen.

#### 4.3.2 NO dissociation from nitrosylated COX in anaerobiosis.

To consolidate the hypothesis that the concomitant oxidation of CcOX-NO and oxymyoglobin is actually due to NO dissociation from reduced haem  $a_3$ , the kinetics of NO transfer from CcOX to Mb has been investigated under strict anaerobic conditions. CcOX was mixed with a two-fold excess of deoxy-Mb and a synchronous transfer of NO from reduced haem  $a_3$  to deoxy-Mb was observed (fig.4.9A). Analysis of the data showed that the NO transfer to Mb is essentially

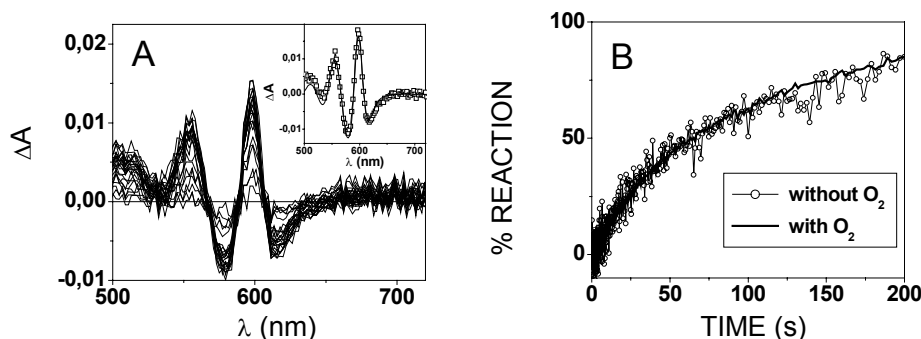


**Fig.4.9 NO is transferred from reduced CcOX to deoxy-Mb.**

A) Absorption changes collected over 200 s after anaerobically mixing nitrosylated CcOX with deoxy-Mb. Baseline: final spectrum. Nitrosylated CcOX was prepared by anaerobic incubation with 2 mM ascorbate and 1  $\mu$ M Ru-hexamine, while MbO<sub>2</sub> was deoxygenated by anaerobic incubation with 2 mM ascorbate + 90 ng/ml ascorbic oxidase. Concentrations after mixing: [CcOX]  $\sim$  7.0  $\mu$ M  $aa_3$ ; [deoxy-Mb]  $\sim$  15  $\mu$ M. T = 20 °C. Inset: optical species as obtained by SVD analysis of the difference spectra in A (open squares), which corresponds to at least 6.0  $\mu$ M NO being transferred from reduced CcOX to deoxy-Mb (solid spectrum). B) Time course of NO transfer from nitrosylated CcOX to either deoxy-Mb (open circles, as obtained by SVD analysis of the spectra in A) or MbO<sub>2</sub> (solid curve, from the data in Fig.4.8B after normalization to 100%).

quantitative (inset). The presence or absence of O<sub>2</sub> makes no difference on the rate and extent of NO transfer arising from dissociation from CcOX. *The time course of NO binding to Mb under anaerobic conditions is identical to that of met-Mb formation measured under aerobic conditions by exposing CcOX-NO to O<sub>2</sub>* (fig.4.9B). NO dissociation from reduced haem  $a_3$  proceeded at  $k' = 0.012$  s<sup>-1</sup>, a value significantly faster than the intrinsic NO off-rate from CcOX in the dark ( $k = 4 \times 10^{-3}$  s<sup>-1</sup> Sarti et al. 2000). However, in these experiments, the incident white-light beam intensity was intentionally kept high to accelerate NO dissociation from reduced haem  $a_3$ . To demonstrate that the effect of light is to enhance the rate of NO dissociation without affecting the chemistry, we confirmed that met-Mb accumulation, when followed at single wavelengths (i.e., at the very low intensity of the monochromatic incident light), proceeds at a rate ( $k' = 2-3 \times 10^{-3}$  s<sup>-1</sup>) consistent with the intrinsic NO off-rate from CcOX in the dark.

**Final remark:** *The time course of NO transfer from nitrosylated CcOX to either deoxy-Mb or MbO<sub>2</sub> is identical.*

#### 4.3.3 On the competition between MbO<sub>2</sub> and CcOX in turnover.

To assess whether CcOX in turnover can compete with oxymyoglobin as recently proposed by Pearce et al. (Pearce et al. 2003), the stopped flow apparatus was used in a sequential mixing mode. This set-up was chosen as allows i) a tight control of the experimental timing in the millisecond time scale, ii) a safe control of the concentrations of the gaseous components (NO and oxygen), iii) reduced CcOX to begin turnover before mixing with NO. In the first mixing CcOX, pre-reduced by anaerobic incubation with excess reductant (ascorbate and Ru-hexamine), is mixed with an air-equilibrated solution containing MbO<sub>2</sub> and after a delay time of 10 s, the mixture of MbO<sub>2</sub> and CcOX in turnover is further mixed with an anaerobic NO solution. The concentrations of reactants were chosen in order to have in the final reaction mixture (i.e., after the second mixing) equimolar concentration (1.2  $\mu$ M) of MbO<sub>2</sub> and CcOX in turnover in the presence of 1  $\mu$ M NO. The absorption changes

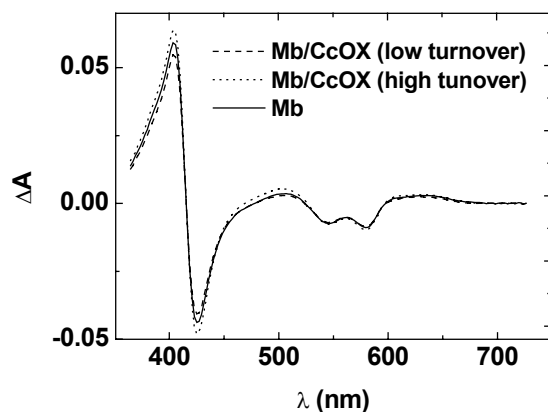


**Fig 4.10 MbO<sub>2</sub> outcompetes CcOX in turnover for NO.** Absorption changes occurring within 200 ms after exposing to NO a solution containing equimolar MbO<sub>2</sub> and CcOX in turnover, the steady-state of CcOX being sustained by 2.5 mM ascorbate and either 5 (dotted spectrum) or 125  $\mu$ M (dashed spectrum) Ru-hexamine. T = 20 °C. The observed absorption changes correspond solely to the oxidation of Mb to met-Mb. An identical signal is observed by omitting CcOX in the experiment (solid spectrum).

collected immediately after the rapid mixing of these proteins with NO, shown in fig.4.10, correspond solely and quantitatively to MbO<sub>2</sub>  $\rightarrow$  met-Mb transition. No reaction with CcOX is observed; consistently, identical absorption changes are observed in a control experiment where CcOX has been omitted. Thus, under the explored experimental conditions, all NO present in solution does not react with CcOX in turnover but is trapped by MbO<sub>2</sub> leading to formation of met-Mb and NO<sub>3</sub><sup>-</sup>. It is worth noticing that identical data are obtained at two different (low and high) concentrations of Ru-hexamine, ruling out that this result is dependent of the turnover rate of CcOX.

**Final remark:** *MbO<sub>2</sub> outcompetes CcOX in turnover for NO.*

#### 4.3.4 Physiological relevance of NO dissociation from nitrosylated CcOX and the competition between oxyMb and CcOX in turnover.

Under condition of high electron flux, the inhibition of CcOX by NO occurs through formation of the nitrosyl complex Fea<sub>3</sub>-NO, as evidenced by spectroscopic and amperometric studies. To gain insight into the mechanism of reversal of the inhibition in this reaction pathway, as it was still controversial whether this involves either a simple displacement of bound NO by O<sub>2</sub> or a chemical reaction between the two ligands at the active site (oxidation of NO to nitrite), spectrophotometric measurements of the reaction between reduced CcOX in solution and NO were performed in presence of MbO<sub>2</sub>. The data obtained in both aerobic and anaerobic conditions clearly demonstrated that NO is released as such (not as nitrite) and reacts with MbO<sub>2</sub> leading to formation of stoichiometric amounts of met-Mb. The possibility that, in the presence of O<sub>2</sub> peroxynitrite may be formed at the active site and released in the bulk, where it oxidizes MbO<sub>2</sub> it is not excluded, but all the results makes it really unlikely. *This pathway of NO inhibition may contribute, therefore, to slow NO recycling and persistency* that, depending on the NO concentrations, may result in physiological or pathological responses. At low NO concentration the reversible COX inhibition may allow the modulation of the respiration and the oxygen availability, and there are different signalling pathways that use NO dependent variation in oxygen concentration as triggering signals of physiological responses. A prolonged inhibition of respiration would mean: i) an increased local oxygen concentration, ii) a reduction of the electron transport chain which favour the formation of superoxide anions (OH<sup>-</sup>); iii) a collapse of  $\Delta\Psi$  which has been shown to play a role in apoptosis, iv) the formation, due to the intracellular redox conditions, of peroxynitrite (ONOO<sup>-</sup>) from the reaction between superoxide anions and NO, resulting in macromolecular damage and cell death.

The proposal that CcOX might be the enzyme responsible for the catabolism of NO in the cell (Pearce et al. 2003) came from the experiments carried out both i) *in vitro*, where nitrite has been determined by the Griess method as the product of NO reaction with purified CcOX and MbO<sub>2</sub> in solution in the presence of high cytochrome *c* concentrations, and ii) in cardiomyocytes, where nitrite (and not nitrate) has been detected by single cell microelectrode measurements after the stimulation of endogenous NO synthesis. In addition, electron paramagnetic resonance spectroscopic data, showed

no evidence for Met-Mb formation in heart tissue. Considering that inert nitrate, and not nitrite, is formed quickly and irreversibly in the reaction of MbO<sub>2</sub> with NO (MbO<sub>2</sub> + NO → met-Mb + NO<sub>3</sub><sup>-</sup> k<sub>on</sub> = 3-4 × 10<sup>7</sup> M<sup>-1</sup>s<sup>-1</sup>) Pearce et al. (Pearce et al. 2003) excluded that, MbO<sub>2</sub>, besides facilitating O<sub>2</sub> diffusion, might be involved in NO scavenging and protecting CcOX from NO present in the red muscles (Brunori 2001). They proposed a role of CcOX in cellular NO breakdown and postulated a mechanism of NO oxidation to nitrite through formation of peroxynitrite in the active site. However, if we consider the kinetics of NO binding to MbO<sub>2</sub> and CcOX, the expected reaction would be the oxidation of MbO<sub>2</sub> to Met-Mb by NO. This prediction is based on the fact that, among all the CcOX intermediates, only the fully reduced species (R) was shown to bind NO as rapidly (~10<sup>8</sup>) as MbO<sub>2</sub>; its occupancy, however, is almost negligible at steady-state, while the intermediates O, P, F, which react with NO much more slowly than MbO<sub>2</sub> (k ≈ 10<sup>4</sup> – 10<sup>5</sup> M<sup>-1</sup> s<sup>-1</sup> Torres et al. 1998, Giuffrè et al. 1998 Giuffrè et al. 2000) vs 3-4 × 10<sup>7</sup> M<sup>-1</sup> s<sup>-1</sup> (Eich et al. 1996, Herold et al. 2001), are predominantly populated. Our kinetic data showed, as expected, that at equimolar concentration of CcOX and MbO<sub>2</sub>, and regardless of the turnover rate of CcOX, the added NO is solely and quantitatively scavenged by MbO<sub>2</sub> with formation of met-Mb (stoichiometric with NO). *This finding rules out the possibility that in vitro purified CcOX, in turnover with reductants and O<sub>2</sub>, can compete with MbO<sub>2</sub> for NO, even when the two proteins are at comparable concentration.* Considering that in a myocyte the Mb/CcOX concentration ratio can be estimated in orders of magnitude (mM vs μM), and given the kinetic constants of the reactions of Mb and CcOX with NO, it might be postulated that in these cells Mb would trap bulk NO impeding the diffusion through the cytoplasm to reach CcOX in the mitochondrion. Consistently, Flögel et al (Flogel et al. 2001) showed met-Mb formation in the heart upon pulses of NO exposure. However, if we consider that the production of NO in the mitochondrion by the mtNOS (Haynes et al. 2004) may account for the local (and nearby CcOX!) NO release within a compartment inaccessible to Mb, the discrepancy of the data could be only apparent. In this view, the mitochondrial production of NO may be fully compatible with the observed accumulation of nitrite that follows the stimulation of endogenous NO production in cardiomyocytes. Nitrite formation has also been shown in cultured neuroblastoma cells (Mastronicola et al. 2003). The formation of nitrite-bound or nitrosylated CcOX has been shown to depend on the electron flux efficiency at the CcOX site (Sarti et al. 2000). Consistently, it has been noticed that, upon increasing the concentration of reduced cytochrome *c*, the mechanism of NO inhibition involving CcOX nitrosylation prevailed in neuroblastoma cells (Mastronicola, 2003); only under this latter conditions, recovery of CcOX activity has been proposed to be associated to straight NO dissociation in the bulk. *From all above observations, it seems that in the mitochondria of cultured cells CcOX can either contribute to both NO persistency in the environment or to NO oxidative degradation.*

#### 4.4 Nitric oxide and the bacterial *bo*<sub>3</sub> oxidase (paper III).

##### 4.4.1. The reaction of NO with fast oxidized and reduced cytochrome *bo*<sub>3</sub> purified from *Escherichia coli*.

NO binding and turnover of cytochrome *bo*<sub>3</sub> has been studied using amperometric methods. When cytochrome pre-reduced *bo*<sub>3</sub> is added to the NO electrode chamber containing an excess of reductants, an immediate decrease in the NO concentration, corresponding to the NO binding of the oxidase, is observed (Fig. 4.11). Interestingly, this binding is followed by a slow, but significant NO consumption. The estimate of the rate of NO degradation, after subtraction of the initial rate observed before addition of the enzyme, is ~ 0.3 mol NO mol *bo*<sub>3</sub><sup>-1</sup> min<sup>-1</sup>. To test the enzymatic nature of this activity, controls have been carried out by repeating the experiment described above i) in the absence of reductants, ii) after cytochrome *bo*<sub>3</sub> denaturation by boiling for 10 minutes in the presence of 0.1% SDS and iii) upon addition of cyanide which blocks the active site of the enzyme. In all these cases NO decay was absent. Thus, this enzyme can reduce NO to N<sub>2</sub>O.



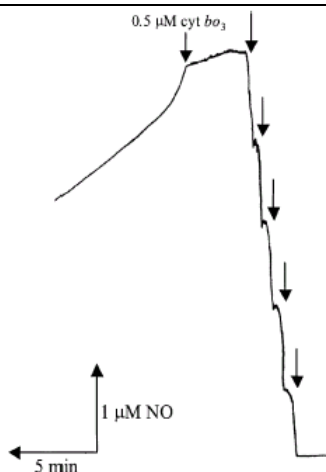


Fig. 4.11 **NO consumption by  $b_0_3$  oxidase.** Cytochrome  $b_0_3$  was prereduced with ascorbate (10mM) and TMPD (0.1 mM). NO was added (arrows) to deoxygenated buffer containing 50mM phosphate, pH 7.2 containing; EDTA (20  $\mu$ M), octyl  $\beta$ -D-glucopyranoside (0.2% w/v), glucose (3 mM), glucose oxidase (4 U/ml), catalase (130 U/ml), ascorbate (10 mM), and TMPD (N,N,N',N'-tetramethyl-p-phenylenediamine). (0.1 mM). Chamber volume: 2 ml,  $T = 20^\circ\text{C}$ .

To better understand the reaction of cytochrome  $b_0_3$  with NO, the stoichiometry of the binding of this molecule to both oxidized and reduced oxidase was determined at the NO electrode in the range of NO concentrations ranging from 1 to 14  $\mu$ M. In order to avoid any reaction between oxygen and NO both the buffer and the solution of the enzyme were made anaerobic by adding glucose, glucose oxidase and catalase. As shown in Fig. 4.12, the stoichiometry NO:reduced cytochrome  $b_0_3$  was 1:1 in all concentrations tested, demonstrating the very high affinity of this ligand to the reduced active site of the enzyme. The pulsed and the fast oxidized cytochrome  $b_0_3$  bind NO with the same stoichiometry which only at the highest NO concentration (15  $\mu$ M) is 1:1, in contrast to the oxidized bovine CcOX which binds one molecule of NO already at the lowest NO concentration tested (\* in the Fig. 4.12). From the plot of NO binding per enzyme unit as a function of NO an observed dissociation constant of  $K_d = 5.6 \pm 0.6 \mu\text{M}$  was determined. Since chloride affects the binding of NO not only in the mammalian CcOX, but also in the cytochrome  $b_0_3$ , allowing the binding of just one molecule, we investigated whether chloride inhibits the low or the high affinity ( $K_d \sim 33 \mu\text{M}$ ) binding sites. The decrease of the stoichiometry NO:enzyme from 1:1 to 0.5:1 at low NO concentrations (Fig. 4.12) clearly demonstrates that the presence of chloride controls the reactivity of the high affinity sites towards NO.

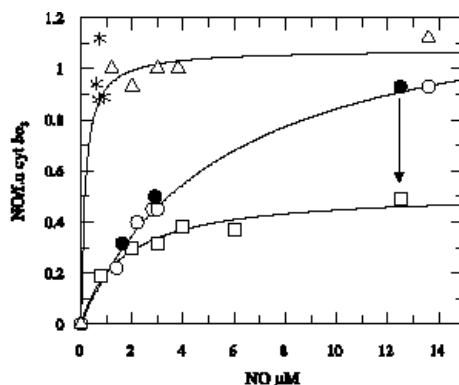
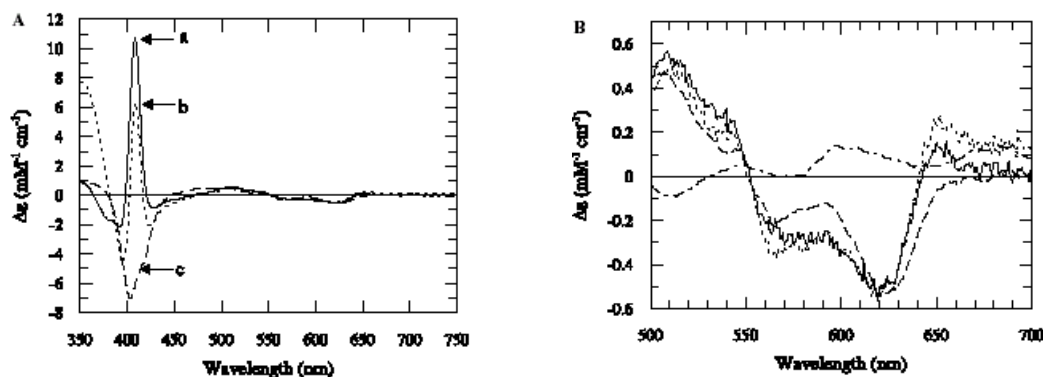


Fig. 4.12 **Stoichiometry of NO binding to fast, pulsed, and chloride-bound cyt  $b_0_3$ .** NO binding per enzyme unit as a function of NO concentration.

( $\Delta$ ) reduced cyt  $b_0_3$ , ( $\circ$ ) oxidised fast cyt  $b_0_3$ , ( $\bullet$ ) pulsed cyt  $b_0_3$  and ( $\square$ ) pulsed cyt  $b_0_3$  plus  $\text{Cl}^-$ . Each point represents the mean of three determinations from two different batches of cyt  $b_0_3$ . The arrow indicates the maximum inhibitory effect of  $\text{Cl}^-$  on NO binding. (\*) shows the high affinity binding of NO to oxidised CcOX

To assess if nitrite is the product of the reaction of the oxidized cytochrome  $b_0_3$  with NO, spectral changes were monitored after mixing this enzyme with both nitrite and NO. Since the affinity of CcOX for nitrite is low, relatively high concentrations of nitrite (10 mM) were required to induce spectral changes of measurable amplitude. Complete nitrite binding occurred over 30 minutes. The raw spectra observed upon binding of nitrite or NO to the oxidase were corrected by subtraction of the free nitrite and NO spectrum, respectively, and expressed as difference spectra (Fig 4.13). The spectral

changes induced by nitrite binding to the oxidase show a decrease in intensity at 408 nm. The same hypochromic effect is caused by the addition to cytochrome  $bo_3$  of i) high potassium chloride concentrations (Moody et al. 1998), and, ii) more interestingly, NO in a 10 fold excess over the cytochrome  $bo_3$  (trace b, Fig. 4.13). In this latter condition, the increase at 350 nm after addition of 70  $\mu\text{M}$  NO may be explained by the release of nitrite into the bulk. In the visible region (Fig. 4.13 B), the spectral changes induced by both NO and nitrite are nearly identical (a peak at 510 nm, and the troughs at 565 and 620 nm). The similarity of the difference spectra induced by the binding of NO and nitrite suggests that the product of the reaction of cytochrome  $bo_3$  with NO is nitrite that binds to the active site. Since chloride has been proposed to control ligand binding to the active site, the effect of chloride on nitrite binding was also investigated. As expected (Fig. 4.13 B), the presence of chloride inhibits nitrite binding to the enzyme, confirming that nitrite binds to the haem  $a_3$ -Cu<sub>B</sub> site and chloride prevents ligand binding to the binuclear centre.



**Fig. 4.13** Changes in the electron absorption spectra of fast cyt  $bo_3$  following the reaction with NO and nitrite. Concentration of cyt  $bo_3$  was 7  $\mu\text{M}$  in all experiments. A. Spectra of: (a) cyt  $bo_3$  plus NO (9  $\mu\text{M}$ ) (—); (b) cyt  $bo_3$  plus NO (70  $\mu\text{M}$ ) (....); and (c) cyt  $bo_3$  plus  $\text{NO}_2^-$  (10mM) (- -). B. Visible region of the difference spectra of cyt  $bo_3$  plus NO (9  $\mu\text{M}$ ) (—); cyt  $bo_3$  plus NO (70  $\mu\text{M}$ ) (....); and cyt  $bo_3$  (7  $\mu\text{M}$ ) plus  $\text{NO}_2^-$  (10mM) (- - -), and Cl<sup>-</sup> bound cyt  $bo_3$  plus  $\text{NO}_2^-$  (-.-.).

**Final remarks:** i) cytochrome  $bo_3$  degrades NO anaerobically, ii) the binding of NO and nitrite to the oxidised enzyme induce very similar spectral changes, iii) both fast and pulsed oxidised cyt  $bo_3$  bind NO with a stoichiometry of 1:1 with a  $K_d = 5.6 \pm 0.6 \mu\text{M}$ , iv) NO binding is inhibited by the presence of chloride.

#### 4.4.2 Implications for the interaction of NO with cytochrome $bo_3$ .

Despite the high degree of similarity with the structure of the bovine haem-copper oxidases around the binuclear active site, the cytochrome  $bo_3$  displays distinct functional properties. Contrary to the bovine enzyme that has been demonstrated by optical and amperometric experiments to not contribute to a reductive degradation of NO (Stubauer et al. 1998), a slow NO reductase activity has been detected in cytochrome  $bo_3$ . This is the first quinol oxidase known to display such activity, although other terminal oxidases, the  $cbb_3$  from *Pseudomonas stutzeri* (Forte et al. 2001) and the  $caa_3$  and the  $ba_3$  from *Thermus thermophilus* (Giuffrè et al. 1999), are able to catalyse NO reduction. Amperometric measurements showed that NO binds to the *fast/pulsed* oxidized enzyme with a stoichiometry of 1:1 only at NO concentration (15  $\mu\text{M}$ ) higher than that observed with the reduced cytochrome  $bo_3$  and the oxidized bovine enzyme. The plot of NO binding per enzyme unit gave an observed dissociation constant of  $K_d \sim 5 \mu\text{M}$ , in agreement with the high affinity NO binding site determined by EPR; the sensitivity of the NO electrode did not allow the measurement of the second low (EPR detected) affinity site ( $K_d \sim 33 \mu\text{M}$ ). Chloride, which has been suggested to be a Cu<sub>B</sub> ligand, affects NO binding to this high affinity site, in agreement with the measurements on the bovine enzyme in which chloride inhibits the binding of the single NO molecule.

From the observation reported above, it appears that the redox chemistry of NO binding to Cu<sub>B</sub> could be of particular importance for the observed properties of quinol cytochrome  $bo_3$ . The reaction of the oxidized mammalian enzyme with NO has been proposed to occur by binding of one NO molecule to Cu<sup>II</sup><sub>B</sub>, leading to nitrite formation in the active site (Torres et al. 1998). The spectra observed after NO and nitrite binding to cytochrome  $bo_3$  are quite similar, suggesting that nitrite is

also produced in the active site of this oxidase after reaction with NO. The mechanism of reaction of NO with both oxidized CcOX and cytochrome *bo*<sub>3</sub> seems to demand i) the formation of a nitrosonium complex ( $\text{Cu}^{\text{I}}_{\text{B}}\text{-NO}^+$ ), ii) the reaction of  $\text{NO}^+$  with the  $\text{OH}^-$  liganded to  $\text{Cu}_{\text{B}}$  to form nitrite. However, the electron on reduced  $\text{Cu}_{\text{B}}$ , ejected from the binuclear site to the haem *a* and  $\text{Cu}_{\text{A}}$  in the mammalian enzyme, is not redox equilibrated in cytochrome *bo*<sub>3</sub>. Reverse electron transfer is not favoured in the bacterial enzyme probably due to the much lower ( $\sim 200\text{mV}$ ) redox potential of the low-spin haem *b* compared to the low-spin haem *a* in CcOX. Based on the above data and the observation that  $\text{Cu}^{\text{I}}_{\text{B}}$  loses the coordination of one histidine imidazole ligand, a plausible model of the reaction of the quinol oxidase with NO has been hypothesized (fig 4.14). When the high affinity NO binds to  $\text{Cu}^{\text{II}}_{\text{B}}$ , the nitrosonium complex may form (B). Then, the  $\text{NO}^+$  will react with the hydroxyl forming  $\text{HNO}_2$  that can bind to the binuclear site or diffuse from the protein (C). The reduction of  $\text{Cu}_{\text{B}}$  may facilitate the loss of an imidazole ligand. Since it has been shown that chloride can bind  $\text{Cu}_{\text{B}}$  (Ralle, et al. 1999), this free coordination site can accommodate another exogenous ligand, and perhaps another molecule of NO (C). The binding of this second NO molecule is consistent with the spectroscopic data showing a second low affinity site at high NO concentrations and would result in the formation of the observed EPR silent species  $\text{Fe}^{\text{III}}\text{-X-Cu}^{\text{I}}_{\text{B}}\text{-NO}$  (Butler et al. 1997). Can this model explain the reduction of NO to  $\text{N}_2\text{O}$ ? The binding of the second NO molecule may favour, under reducing condition, the formation of a dinitrosyl adduct,

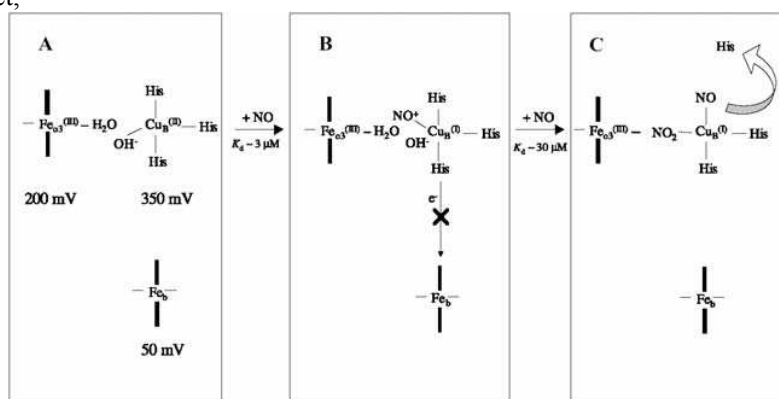


**Fig.4.14 Model showing the possible reaction of fast cyt *bo*<sub>3</sub> with NO.**  $\text{Cu}^{\text{II}}_{\text{B}}$  four coordinate with three histidine and one hydroxyl ligands.

and, then, the reduction of NO to  $\text{N}_2\text{O}$ . Since other member of the haem-copper oxidases are able to reduce NO, it would be interesting to know if the ligand changes at  $\text{Cu}_{\text{B}}$  upon reduction are a prerequisite for the NO metabolism. Whatever the mechanism, *the NO reductase activity detected in cytochrome bo<sub>3</sub> is very low suggesting that cytochrome bo<sub>3</sub> cannot play a physiological role in NO detoxification.* It is worth mentioning that in *E.coli* cells the flavorubredoxin, a member of the flavodiiron proteins, has been recently reported to be important in NO catabolism under anaerobic conditions. It is probable that this novel type of soluble nitric oxide reductase plays in *E.coli* the main role in NO detoxification rather than cytochrome *bo*<sub>3</sub>.

#### 4.5 NO and the bacterial *bd*-type quinol oxidases (paper IV).

##### 4.5.1 The reaction of NO with *bd* oxidases purified from the bacteria *Escherichia coli* and *Azotobacter vinelandii*.

Reduced cytochrome *bd* binds NO. To avoid the use of dithionite that rapidly reacts with NO, ascorbate and TMPD (N,N,N',N'-tetramethyl-p-phenylenediamine) was used as reductants for the oxidase. Fig. 4.15 shows the absolute absorption spectra of the fully reduced unliganded and the NO-bound cytochrome *bd* from *E. coli* after addition of micromolar concentrations of NO to the reduced sample. A shift of the ferrous haem *d* peak from 629 nm to 641 nm is observed and evidenced (inset) by the difference symmetric-shaped spectrum (baseline = fully reduced enzyme). Very similar NO-induced absorption changes are observed with cytochrome *bd* from *A. vinelandii*. Such a *red* shift might originate from peculiar surroundings of haem *d* in *bd*-type oxidases, since NO binding to a reduced high spin haem (*a*<sub>3</sub>, *o*<sub>3</sub>, or *b*<sub>3</sub>) in all haem-copper terminal oxidases induces a *blue* shift, as it does upon binding to ferrous haem *d*<sub>1</sub> in cytochrome *cd*<sub>1</sub> nitrite reductase. This result suggests that reduced haem *d* is a high-affinity binding site for NO, yielding a  $\text{Fe}^{2+}\text{-NO}$  nitrosyl-adduct.

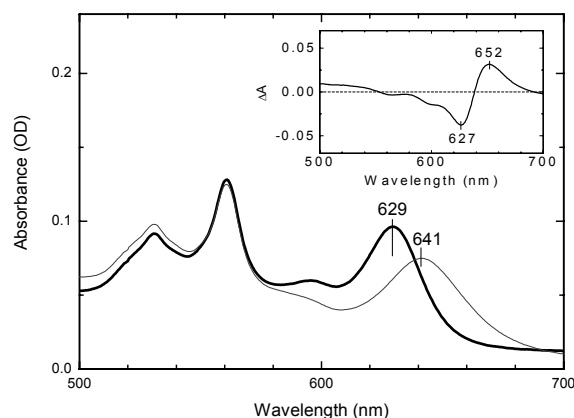


**Fig 4.15 NO binding to reduced cytochrome bd.** Absorption spectra of the fully reduced (thick line) and NO-bound (thin line) *E. coli* enzyme. The enzyme (3.1  $\mu\text{M}$ ) was made anaerobic by  $\text{N}_2$ -equilibration and addition of glucose (5 mM), glucose oxidase (8 units/mL) and catalase (260 units/mL), prior to addition of ascorbate (4 mM) plus TMPD (40  $\mu\text{M}$ ). After complete reduction, 6  $\mu\text{M}$  NO was added. Inset: difference spectrum, NO-bound minus fully reduced enzyme.

To test the ability of cytochrome *bd* oxidases from both *E. coli* and *A. vinelandii* to reduce NO under anaerobic conditions, amperometric experiments were performed at NO concentration ranging from 3 to 30  $\mu\text{M}$ . Either dithiothreitol (DTT)/ coenzyme  $\text{Q}_1$  or ascorbate/TMPD were used as reductants and ascorbate and ascorbate oxidase were added to scavenge residual oxygen. Addition of cytochrome *bd* (Fig 4.16), either pre-reduced or as isolated, in the NO electrode chamber in the presence of excess of reductants, although associated to a small decrease in NO concentration (partly due to NO binding to the enzyme), did not change significantly the rate of NO degradation. Neither in *E. coli* nor in the *A. vinelandii* cytochrome *bd* oxidases NO reductase activity was detected.

The inhibition of cytochrome *bd* oxidase activity by NO was also tested in an apparatus that records oxygen and NO traces in parallel.  $\text{O}_2$ -reductase activity of cytochrome *bd* from *E. coli*, sustained by an excess of reductants (DTT and  $\text{Q}_1$ ), is rapidly inhibited by the addition of some  $\mu\text{M}$  NO (Fig. 4.17). This gas in air-equilibrated solution spontaneously degrades by reacting with  $\text{O}_2$ . When NO concentration decays below 200 nM, cytochrome *bd* gradually recovers the activity

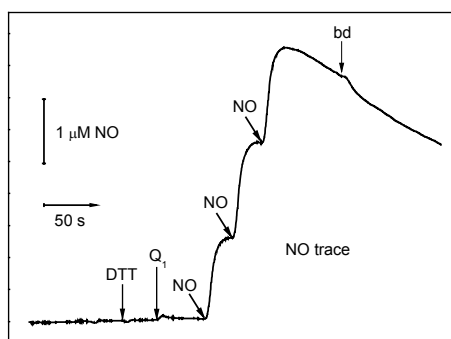


**Fig.4.16 Absence of NO reductase activity.** Three aliquots of 1.5  $\mu\text{M}$  NO were successively added to degassed buffer containing 4 mM DTT, 0.25 mM  $\text{Q}_1$ , as well as 5 mM ascorbate and 5 units/mL ascorbate oxidase to scavenge residual  $\text{O}_2$ . Addition of 70 nM *E. coli* cytochrome *bd*, did not change the rate of NO consumption.

measured before the NO addition and the inhibition fully reverts. Interestingly, under similar experimental condition, the addition of 100nM NO to the enzyme results in 50-60% of the inhibition of the oxidase activity. To quantify the sensitivity to NO inhibition of cytochrome *bd* from *E. coli*, analysis of the NO and  $\text{O}_2$  experimental traces recorded in parallel has been performed and yielded an apparent inhibition constant ( $K_i$ ) for NO of  $100 \pm 34$  nM, at oxygen concentration of  $\sim 70\mu\text{M}$ . Similar results were obtained for the *A. vinelandii* enzyme. The apparent inhibition constant for these enzymes

measured at higher oxygen concentration ( $\sim 1$  mM) increased to  $\sim 230$  nM. The higher value of the  $K_i$  obtained in this condition suggest a competition between NO and oxygen for the quinol oxidase active site. To study the kinetics of activity recovery oxy-hemoglobin was used to promptly scavenge bulk NO. As shown in Fig 4.17 B upon addition of oxy-hemoglobin, a very fast and complete recovery of the oxygen reductase activity of cytochrome *bd* from *E. coli* is observed. Similar traces were recorded when using the enzyme purified from *A. vinelandii*.

**Final remarks:** cytochrome *bd* i) does not reduce NO, ii) is rapidly inhibited by NO. This inhibition is reversible, potent and occurs in competition with  $O_2$ .

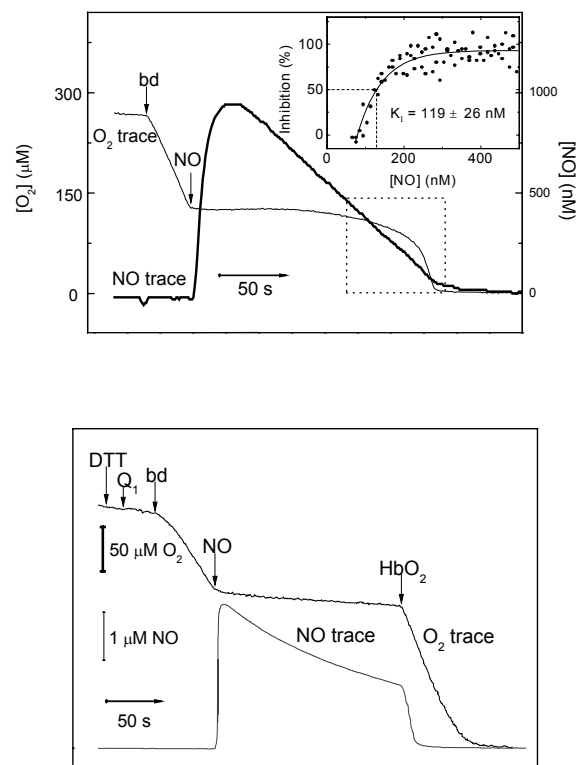


**Fig.4.17 NO inhibition of cytochrome *bd* oxidase activity.** Top. Cytochrome *bd* (17 nM) sustained by 4 mM DTT and 0.25 mM  $Q_1$  is rapidly inhibited by addition of 1  $\mu$ M NO, to be fully recovered at low NO concentrations (dotted box). Inset: extent of cytochrome *bd* inhibition at low NO concentration. Bottom: a fast and complete recovery of the enzyme activity after addition of 15  $\mu$ M Hb- $O_2$  to promptly scavenge bulk NO.

#### 4.5.2 Considerations on the interaction of NO with the *bd*-type quinol oxidases.

The ability of some terminal oxidases to catalyse the reduction of NO has been related to the similarities between NO and oxygen and to the close phylogenetic relationship between haem-copper oxidases and bacterial NO reductases (NOR), implicating that some structural feature of the active site may favour the binding and catalysis of NO reduction. Both enzymes have a binuclear ligand active site, consisting of a haem-iron and a second metal, which is iron in NOR and copper in haem-copper oxidases. Whether the catalytic activity depends on the properties of the high spin haem or the non-haem metal has not been clarified. The incapacity of quinol cytochrome *bd*, which does not contain  $Cu_B$  in the active site, to catabolise NO under anaerobic condition, differently from other bacterial haem-copper oxidases ( $<0.1$  mol NO mol *bd*<sup>-1</sup> min<sup>-1</sup> to be compared to  $\sim 100$  mol NO mol enzyme<sup>-1</sup> min<sup>-1</sup> as measured for *cbb*<sub>3</sub> oxidase from *P. stutzeri*), suggests that  $Cu_B$  is important in this reaction. Since the mitochondrial beef heart cytochrome *c* oxidase (Stubauer et al. 1998) and the “nitric oxide reductase homolog” from *Roseobacter denitrificans* (Matsuda et al. 2004), both containing a copper ion in the binuclear active site, do not catalyse NO reduction, it is likely that the NO reductase activity observed in some members of haem-copper oxidase family require not only the presence of a non haem metal, but specific structural feature around the active site which can modulate the affinity of  $Cu_B^+$  for NO. Interestingly, a peculiar high affinity of  $Cu_B^+$  for CO was observed in

those oxidases endowed with NO-reductase activity (Woodruff 1993) (Stavrakis et al. 2002). Thus, the reported low affinity for CO and NO for ferrous haem  $b_{595}$ , proposed to replace  $Cu_B$  in *bd* oxidases, may explain the absence of NO-reductase activity in this enzyme. In contrast, the presence of  $Cu_B$  seems not a prerequisite for the inhibitory action of NO on terminal oxidases in the presence of an excess of reductants, as cytochrome *bd* has been shown to be promptly and efficiently inhibited by this gas. This result is in agreement with the observation that *E.coli* cells expressing this quinol oxidase are sensitive to NO (Stevanin et al. 2000). The NO inhibition is fully reversible as demonstrated for the mitochondrial enzyme. However, the rate of activity recovery after NO scavenging by oxy-hemoglobin seems to be faster than in CcOx. It has been postulated that under high electron flux NO binds to CcOx forming a nitrosyl adduct and that the recovery of the activity is rate-limited by the NO dissociation from ferrous haem  $a_3$ . Since under this condition a similar  $Fe^{2+}$ -NO adduct is observed in the absorption spectrum of fully reduced NO-bound cytochrome *bd*, the faster activity recovery should correlate with a faster NO dissociation from ferrous heme *d*. The estimated  $K_i$  value ( $100 \pm 34$  nM at  $70 \mu M O_2$ ) of cytochrome *bd* is not very different from that of cytochrome *c* oxidase ( $\sim 60$  nM at  $30 \mu M O_2$  Brown and Cooper 1994) and, more interestingly, is dependent on oxygen concentration. If NO competes with oxygen for the active site of cytochrome *bd*, at low oxygen concentration NO inhibition should be more potent. As *in vivo* oxygen concentration are quite low and NO is produced during bacterial infection by macrophages, this inhibition might be patho-physiologically relevant. Cytochrome *bd*, in fact, has been recently proposed to play a key role in the survival of pathogenic anaerobic bacteria (Endley et al. 2001) (Baughn and Malamy 2004) at nanomolar oxygen concentration by scavenging this gas and, on the other hand, cannot contribute to NO detoxification mechanisms being not able to reduce NO.

#### 4.6 Nitric oxide and *Escherichia coli* flavorubredoxin (paper V).

##### 4.6.1 NO reductase activity of *Escherichia coli* flavorubredoxin

The ability of *Escherichia coli* flavorubredoxin to metabolise NO was tested at the NO electrode under anaerobic condition in the presence glucose, glucose oxidase and catalase to remove contaminant oxygen. The physiological partner, the flavorubredoxin reductase, and NADH were used as electron donors to sustain the enzymatic activity. As shown in the fig.4.18, following the addition of 22.5 nM

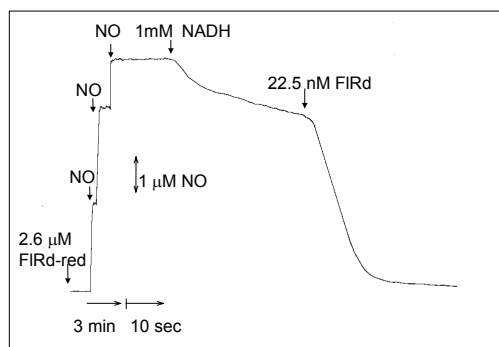


**Fig.4.18. NO consumption by *E.coli* flavorubredoxin.** Typical NO trace showing the high flavorubredoxin NO reductase activity sustained by its physiological reductase and NADH. The enzyme has been added at about  $4.7 \mu M$  NO. Buffer: 50mM Tris-HCl pH 7.6, EDTA  $20 \mu M$ .

flavorubredoxin to a NO solution of about  $4.7 \mu M$  NO, a fast NO consumption is observed whose time-course followed a zero-order kinetics. The rate, estimated by averaging 26 independent experiments performed at different FIRd reductase concentrations and at saturating NADH concentration (from 0.2 to 2 mM), was  $14.9 \pm 6.7$  mol of NO mol FIRd $^{-1}$  s $^{-1}$ . To verify that the observed NO

degradation was an enzymatic activity mediated by the flavorubredoxin, the following controls were carried out: i) the absence of the activity after enzyme denaturation by boiling the protein for 10 minutes in the presence of 10% SDS (thus excluding that the organic contaminants were responsible for the observed NO consumption), ii) the lower NO degradation mediated by the reducing agents (the flavorubredoxin reductase and NADH) in the absence of the flavorubredoxin, iii) the linear dependence of the activity on flavorubredoxin concentration. Interestingly, the activity is independent on the NO concentration ranging from 1 (the physiological level) to 10  $\mu\text{M}$ , demonstrating that the protein has a very high affinity for NO ( $K_m < 1$ ). All these results demonstrate that *E.coli* flavorubredoxin is an efficient NO reductase with turnover numbers comparable to that determined for the heme  $b_3\text{-Fe}_B$  containing nitric oxide reductases expressed in denitrifying bacteria (e.g.  $\sim 10 - 50 \text{ mol NO} \cdot \text{mol enzyme}^{-1} \cdot \text{s}^{-1}$  for the *Paracoccus denitrificans* enzyme (Zumft, 1997). Since flavorubredoxin contain two metal centres integrated in different domains (the rubredoxin centre in a rubredoxin-like fold and the diiron centre), to establish the site responsible for the NO reductase activity, experiments has been performed with a truncated form of the protein, consisting only of the rubredoxin domain. This centre, although efficiently reduced by the reductase/NADH couple, cannot reduce NO. Thus, the di-iron centre of flavorubredoxin is the site in which the NO chemistry occurs.

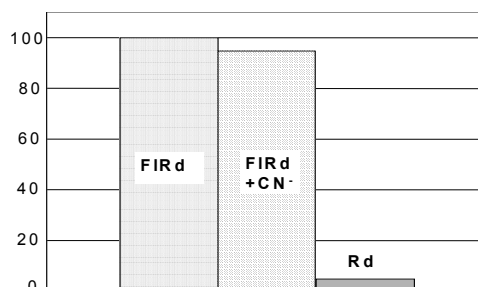


**Fig. 4.19 The di-iron cluster is the active site.** NO reductase activity quantification of FIRD (flavorubredoxin), FIRD + cyanide and the isolated rubredoxin domain (Rd). NO reductase activity (% , vertical axis) is not inhibited by cyanide and the rubredoxin domain is unable to process the NO.

Consistently with the low affinity for cyanide of this centre, long cyanide incubations (1 day at 3mM cyanide at 4 °C or at room temperature) did not decrease the NO reductase activity. Since an involvement in the oxygen metabolism has been proposed not only for the *E.coli* flavorubredoxin (Gomes, 2000) but also for *Desulfovibrio gigas* and cyanobacterial flavodiiron proteins (Helman et al. 2003), the oxygen reductase activity has also been probed in the recombinant *E.coli* flavorubredoxin. This enzyme consumes oxygen but much slower than NO; in addition, oxygen reduction does not proceeds with a zero-order kinetics, the rate of this process beginning to slow down at 200 $\mu\text{M}$  oxygen concentration. This observation suggests that the affinity of the *E.coli* enzyme for oxygen is lower compared to the high value measured for NO.

**Final remarks:** recombinant *E.coli* flavorubredoxin can reduce NO, the diiron centre is the site where the NO chemistry occurs.

#### 4.6.2 Implications for the NO reductase activity of *Escherichia coli* flavorubredoxin.

Nitric oxide may be a poison, and organisms employ diverse systems to protect against its harmful effects. In *Escherichia coli* flavohemoglobin has been proposed to catalyse NO dioxygenation converting NO to  $\text{NO}_3^-$  in the presence of oxygen (Gardner et al 1998), although controversial (Bonamore et al. 2003). Under anaerobic condition, although the list of proteins displaying a low NO reductase activity *in vitro* with potential for function in *E. coli* is long (includes terminal respiratory oxidases, flavohemoglobin, cytochrome *c* or *c'*, multi-haem nitrite reductase, copper-nitrite reductase, bacterioferritin, ribonucleotide reductase, Cu,Zn-superoxide dismutase), only the flavorubredoxin has been proposed (Gardner, 2002) to have a role in NO reduction function in cells since i) its activity is induced in *E.coli* by NO incubation and ii) deletion of the genes encoding for either flavorubredoxin or its the reductase impairs the inducible anaerobic NO metabolism. This biochemical study shows that the purified recombinant *E.coli* flavorubredoxin under anaerobic conditions degrades nitric oxide with a high turnover number, comparable to that of canonical bacterial haem  $b_3\text{-Fe}_B$  NO reductase.

*Escherichia coli* flavorubredoxin is a member of the family of the flavodiiron proteins, which are built by two core domains: a metallo- $\beta$ -lactamase like domain at the N-terminal region, harbouring a non-haem di-iron site, and a flavodoxin-like domain, containing one FMN moiety. The enzyme from *E. coli* has an extra module at the C-terminus, the rubredoxin-like centre containing an iron. Reduction of NO is proposed to occur at the di-iron centre because of the absence of activity of the isolated rubredoxin domain. For turnover, the NADH-dependent flavorubredoxin reductase, encoded in the same gene locus of flavorubredoxin, would supply two electrons to the di-ferric centre via the rubredoxin domain and the proximal FMN. Two possible NO reduction catalytic mechanisms has been hypothesized: i) one imply the binding to the di-ferrous centre ( $\text{Fe}^{2+}\text{--O--Fe}^{2+}$ ) of two NO molecules, their reduction to form a di-ferric centre and two nitroxyl anions which combine to form  $\text{N}_2\text{O}$  and water (as suggested for the cytochrome *bc*-type NO reductase Dermastia et al. 1991, Zumft 1997); ii) the other one the binding of only one NO molecule to the di-ferrous centre and NO reduction by two electrons to produce a diferric nitrite intermediate ( $\text{Fe}^{3+}\text{--O--Fe}^{3+}\text{--NO}^{2-}(\text{H}^+)$ ) that reacts with the second NO molecule to form  $\text{N}_2\text{O}$  (as proposed for cytochrome P450nor Shiro et al. 1995).

The elevated NO reductase activity measured in *Escherichia coli* flavorubredoxin has led us to propose the existence of a novel family of NO reducing enzymes, with a non-haem di-iron site as the catalytic centre. The high similarity in amino acid sequence among most members of the flavodiiron protein, especially the conservation of the residues near the di-iron site, suggest that the NO reductase activity is a property of this family. Consistently the homologue of flavorubredoxin, FprA, purified from *Moorella thermoacetica* has been later shown (Silaghi-Dumitrescu et al. 2003) to endow with anaerobic NO consumption activity. Expression of this protein in an *Escherichia coli* strain deficient in NO reductase activity restored the anaerobic growth phenotype of cultures exposed to otherwise toxic levels of exogenous NO. Thus, *Moorella thermoacetica* FprA is fully capable of functioning in nitrosative stress protection as proposed for flavorubredoxin in *E. coli* (Gomes et al. 2000). Interestingly, these enzymes have been proposed to display both oxygen and NO reductase (NADH dependent) activities. NO reductase activity, however, is significantly more efficient due to a lower  $K_m$  for NO. The same bifunctional activity has been observed also in the haem-copper oxygen and bacterial NO reductases, strongly suggesting the versatility of the bacterial response to different environmental conditions. In this context it is worth mentioning that the genomic organization of the flavoproteins is quite diversified and only in enterobacteria the gene for the flavorubredoxin is adjacent the gene encoding for its reductase (Gomes, 2000), both close to a plausible NO regulator (Gardner et al 2002). In some organisms (for example *Moorella thermoacetica* Silaghi-Dumitrescu et al 2003) the genes encoding for these enzymes are in clusters containing genes coding for proteins expressed during the oxidative stress (such as superoxide dismutases, superoxide reductases and alkyl hydroperoxide reductase). Although there is not direct link between the localization of genes and the regulation of their expression and activities, this peculiar genomic organization support a physiological correlation between the oxygen and NO metabolisms. In addition, while in *Rhodobacter capsulatus* and in *Desulfovibrio gigas* the flavodiiron protein are expressed under nitrogen-fixing and in sulphate reducing growth conditions respectively, the *E. coli* FIRd, which has been shown to display NO reductase activity, is induced by exposure to NO. Thus, this enzyme seems to be important for the resistance of *E. coli* cells to NO present in various niches and produced by the immune system. Importantly, genes encoding for flavodiiron proteins are also found in genomes of pathogenic bacteria, such as *Salmonella typhimurium* and *Klebsiella pneumoniae*. In conclusion, the purified *E. coli* flavorubredoxin has been shown to endow with a high NO reductase activity, comparable to the canonical bacterial NO reductase; it is likely that the newly identified NO-scavenging activity may play a critical role in the detoxification of NO and bacterial survival in the anaerobic and microaerobic environments encountered by *E. coli* and other microorganisms.

#### 4.7 NO and *Trichomonas vaginalis* (paper VI).

##### 4.7.1 *Trichomonas vaginalis* degrades NO.

To verify the ability of the protist pathogen *Trichomonas vaginalis* to degrade NO, measurement were carried out under anaerobic conditions. As shown in Fig. 4.20 (top panel) following the addition of *Trichomonas vaginalis* cells to the NO electrode chamber containing NO and ascorbate/ascorbic oxidase to scavenge oxygen, a rapid NO consumption was observed. After NO exhaustion, further additions of NO were followed by reactivation of the NO degradative function, suggesting that the NO consumption is an enzymatic activity and is not due to a non-specific and



saturable NO-binding process. Consistently, the rate of NO consumption was linearly dependent on cells density and did not change after addition of the medium to the chamber, demonstrating that the extracellular components were not responsible for the observed phenomenon. At NO concentration ranging from 0.6 to 3  $\mu\text{M}$  the rate of NO degradation was  $130 \pm 33 \text{ nmol NO } 10^8 \text{ cells}^{-1} \text{ min}^{-1}$  ( $n = 6$  independent experiments). Cyanide incubation for 1h at 37° C did not effect the NO scavenging function in both intact and lysate cells. Interestingly, addition of the lysate to NO in solution caused only a partial NO disappearance; catalytic activity was observed only after addition of 1mM NADH that restored the enzymatic activity up to the 50% of that measured in intact cells (Fig.4.20 bottom).

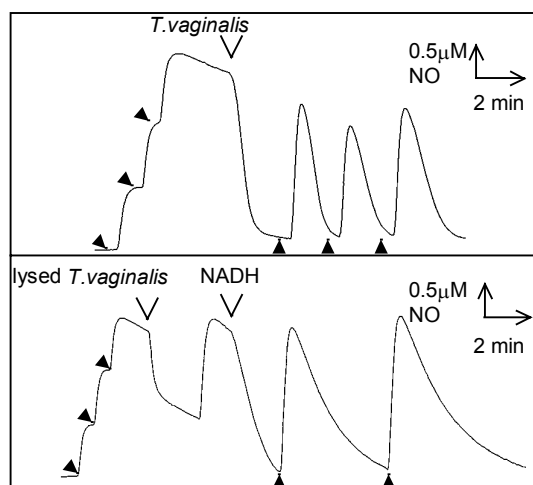


**Fig. 4.20 NO degradation by *T.vaginalis*.** Typical NO electrode traces showing the NO consumption following the addition of intact *T.vaginalis* cells (bottom panel) or lysate in the presence of 1 mM NADH, both at about 3  $\mu\text{M}$  NO concentration. Number of intact or lysed cells:  $3 \times 10^6$ . Reaction medium: PBS pH 7.3, 20 mM EDTA, 5 mM maltose, 10 mM ascorbate, 0.13 mg/ml ascorbic oxidase. V= 1ml, T= 20°C. Black arrows: NO additions.

To investigate the range of NO concentration where *Trichomonas vaginalis* mediated NO consumption was maximal we performed experiments ranging from 0.6 to  $\sim 15 \mu\text{M}$  NO. At the highest NO concentrations, the rate of NO degradation decreased to  $\sim 30 \%$ , suggesting an inhibitory role of NO at relatively high concentration. The drop in activity might be due to i) a direct NO inhibition of the enzyme responsible for the observed NO consumption or to ii) an indirect effect on a different target which made NO degradation less efficiently. Also oxygen inhibited NO consumption. The addition of oxygen to the NO electrode chamber containing NO metabolising *Trichomonas vaginalis* cells (Fig. 4.21) rapidly caused a significant decrease of the NO activity (about 70%). The inhibition of the NO activity was also seen after addition of a further aliquot of NO, however, the function was fully recovered by complete deoxygenation mediated by the addition of ascorbic oxidase in the presence of an excess of ascorbate. The results obtained from several experiments conducted at different oxygen concentration showed that few micromolar oxygen concentrations induce significant inhibition of the NO consumption activity (Fig.14.21B). Since NO consumption catalysed by *E.coli* flavorubredoxin has been shown to be: i) NADH dependent, ii) cyanide insensitive, iii) oxygen sensitive (Gardner et al. 2002) and iv) genomic data reported the presence genes encoding for flavodiiron proteins in pathogenic protists (Andersson et al. 2003), cell extracts of this microorganism were tested for the presence of these enzymes by immunoblotting (Fig. 4.22). The polyclonal antibodies against the *E.coli* recombinant FIRd protein detected an immunoreactive protein with an apparent molecular weight ( $\sim 60 \text{ Kda}$ ) similar to that of *E.coli* flavorubredoxin. Finally, a BLAST search of the incomplete genome of *Trichomonas vaginalis* showed the presence of three genes encoding for flavodiiron proteins, all containing the key residue for the catalytic activity.

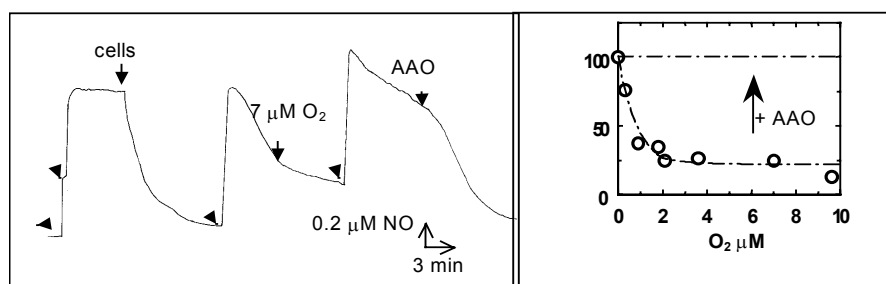


**Fig. 4.21 Oxygen dependence of the NO degradative activity.** Right: the NO consumption is promptly inhibited by low oxygen concentration and is restored by ascorbic oxidase (AAO) mediated oxygen depletion. Experimental condition as in fig. 4.19 with the following exceptions: i) ascorbic oxidase was not added at the beginning of the reaction, ii)  $V = 2$  ml. Oxygen stock solution obtained by equilibrating water with this pure gas at 1 atm, was 1.3 mM. Left: NO consumption rates were measured varying oxygen concentration and normalized to the value of the activity under anaerobic conditions, taken as 100%. Data are the average of three independent experiments

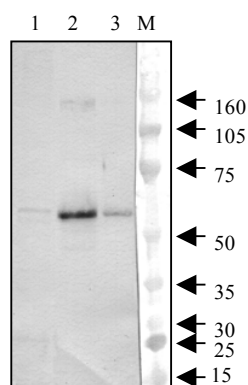


**Fig.4.22 Immunoblot of *T.vaginalis* cell lysate.** Lane 1:  $4.4 \times 10^5$  cells, lane2 and 3: *E.coli* flavorubredoxin 2 and 10 ng. M= molecular weight marker.

**Final remarks:** *Trichomonas vaginalis* degrades NO under anaerobic condition; this activity is cyanide insensitive and dependent on both NO and oxygen concentrations. A cell lysate immunoblot shows a band similar to the *E.coli* flavorubredoxin

#### 4.7.2 Relevance of the NO reductase activity detected in *Trichomonas vaginalis*.

Nitric oxide plays an important role in the immune response in humans and, generated in large amount by the inducible NO synthase in macrophages, controls and restricts the growth of several pathogens, including protists. The antimicrobial effect seems to be partly due to the production of peroxynitrite produced upon reaction of NO with superoxide anion (Beckman and Koppenol 1996) and to the NO mediated activation of natural killer cells to respond to interleukins (Bogdan 2001). The extracellular killing of cultured *Trichomonas vaginalis* by activated mouse peritoneal macrophages has been proposed (Park et al. 1997) to be mediated by NO, as inhibitors of NO synthase block the cytotoxicity towards the parasite; on the other hand, arginine, a NO synthase substrate, competitively restores the macrophages capacity to kill. In the microaerobic and NO enriched host environments, however, *Trichomonas vaginalis* often survives and chronic infections are observed. Thus, the parasite may have evolved the ability to evade the immune system and to cope with the NO produced, although the mechanism by which *Trichomonas vaginalis* survives is unknown. The finding of a NO reductase

activity in this pathogen is of intense patho-physiological importance and might explain the ability of this protist to survive in oxygen poor environments. The observed oxygen sensitivity, NADH dependence and cyanide insensitivity of the NO consumption measured under anaerobic conditions, are properties typical of the flavodiiron protein family, widely distributed in prokaryotes. In addition, the immunodetection in the *Trichomonas vaginalis* lysate, using polyclonal antibodies raised against *E.coli* flavorubredoxin, of a protein band with a molecular weight compatible with the presence of a flavodiiron protein, strongly supports the hypothesis that the NO metabolising activity measured is due to the expression in the parasite of an enzyme belonging to this family. In agreement with the results obtained with the recombinant *E.coli* flavorubredoxin, *Trichomonas vaginalis* degrades NO more efficiently at low and physiological NO concentrations. Interestingly, the flavorubredoxin expression is enhanced by submicromolar NO concentrations (Gardner and Gardner 2002). All above observations are consistent with the BLAST analysis of the incomplete *Trichomonas vaginalis* genome that has been shown to contain three different genes encoding for flavodiiron proteins, probably laterally transferred from prokaryotes to the protists during the evolution. Lateral gene transfer may be especially important in the evolution of a parasitic life style, as infection related factors could be transmitted and many of these factors would presumably confer an immediate advantage. The nature of the genes involved may have affected the adaptation of *Trichomonas vaginalis* to parasitisms. Interestingly, a genomic analysis (Andersson et al. 2003) has shown that other protists, *Giardia intestinalis*, *Spironucleus barkhanus* and *Entamoeba histolytica*, have genes encoding for flavodiiron proteins and, considering the similarity in the aminoacid sequences, it may be hypothesized that the NO reductase activity would be also present in the three pathogens. Although the flavodiiron proteins expression has never been tested in these other protists, the presence of the respective genes supports the hypothesis that the flavoprotein gene transfer from a bacterium to these eukaryotes represented an important factor in the evolution of the parasitism, allowing the microorganisms to catabolise the toxic NO. *In conclusion, the finding of a NO reductase activity in Trichomonas vaginalis and the assignment of this function to a flavodiiron protein, extended to the other protists, would be important to both evolutionary biology and human pathology. These protists may take benefit from such an enzymatic activity to counteract cytotoxic NO production by the host immune system.* In this context, understanding the complex role of NO reductase and their regulators in NO detoxification and microbial pathogenesis may be essential to the development of novel therapies.

## 5. CONCLUSIONS

In this thesis new findings on terminal oxidases, flavodiiron proteins and their interaction with nitric oxide are presented. A kinetic approach has allowed us to gain insight to the understanding of the proton-electron coupling upon cytochrome *c* oxidase reduction and on the inhibition mechanisms of this mammalian enzyme by NO at the molecular level. Functional studies have been useful to investigate the interaction of NO with both bacterial terminal oxidases *bd* and *bo<sub>3</sub>* and the flavodiiron proteins purified from *E.coli* and present in the pathogenic protist *Trichomonas vaginalis*.

The study on the redox-linked protonation coupled to the reduction of soluble CcOX (paper I) provides the experimental basis for a reaction mechanism hypothesis during the reductive phase of the catalytic cycle. The enzyme upon reduction binds  $\sim 2.5 \text{ H}^+/\text{aa}_3$  out of which  $\sim 0.6 \text{ H}^+/\text{aa}_3$  are associated to haem *a* reduction. Comparison of the reduction and protonation kinetics of the chloride-bound and chloride-free enzyme allowed the modelling of the mechanism of proton-electron coupling upon arrival of the first electron on the active site. According to this proposal, following Cu<sub>B</sub> reduction, a proton is taken up and the anion (OH<sup>-</sup> or Cl<sup>-</sup>), bound to the oxidized active site, is released in the protonated form (H<sub>2</sub>O or HCl). Dissociation of the acidic form of chloride in the bulk, explains the lower protonation stoichiometry coupled to the reduction of the chloride-bound enzyme. As the electron and proton transfer are tightly coupled in CcOX, the role of K and D proton conducting channels during the reductive phase of the catalytic cycle has been investigated making use of the *Paracoccus denitrificans* inactive K354M and D124N mutant oxidases (paper II). The mutation of key residues of the two main proton pathways within the enzyme causes a delay in the intramolecular electron transfer and in the reduction of the active site, which is minor in the D124N mutant and severe in the K354M mutant. The results presented in paper II show that  $0.8 \text{ H}^+$  is bound to the enzyme upon haem *a* reduction in wild type enzyme and in both mutants, while the  $\sim 2.5 \text{ H}^+$  linked to the reduction of the wild type and D124N haem *a*<sub>3</sub>-Cu<sub>B</sub> are only partially up-taken in the K354M mutant. According to these data, a major role of the K channel in the proton uptake associated to the reduction of the active site is proposed, while the involvement of both the D and K channel in the proton uptake coupled to haem *a* reduction is excluded. The different proton uptake observed in the bacterial and mitochondrial enzyme ( $3.3$  vs  $2.4 \text{ H}^+/\text{aa}_3$ ) may be explained by either the presence of different redox-linked ionisable residues or different redox-linked  $\Delta\text{pK}_a$ 's of the same residues.

Concerning the reversible inhibition of cytochrome *c* oxidase by nitric oxide, the mechanisms of recovery of the oxidase activity in the nitrosylated adduct have been inspected. Previous studies on the interaction of NO with cytochrome *c* oxidase (reviewed in (Sarti et al. 2003)) evidenced the existence of two alternative reaction pathways, leading to formation of either a nitrosyl (Fe-*a*<sub>3</sub><sup>2+</sup>-NO) or a nitrite-bound (Fe-*a*<sub>3</sub><sup>3+</sup>-NO<sub>2</sub><sup>-</sup>) active site which become inhibited under conditions where the reduced or the oxidized catalytic intermediates are more populated, respectively. The predominance of one mechanism over the other appears to depend on the rate of electron flux through the enzyme. At high electron flux, when the binuclear centre is more reduced, the formation of Fe-*a*<sub>3</sub><sup>2+</sup>-NO is favoured. In this pathway, inhibition is clearly oxygen-dependent. Two mechanisms of NO inhibition relief have been proposed, one involving displacement of bound NO by oxygen (Sarti et al. 2000), the other one a chemical reaction between the two ligands in the active site and leading to NO oxidation to nitrite (Pearce et al. 2003). This latter model, as nitrite is a non-toxic compound, would also account for NO detoxification. The kinetic study on this topic, which employed time-resolved absorption spectroscopic techniques, provides clear evidence that NO and not nitrite is released from the fully nitrosylated CcOX upon exposition to oxygen. In these experiments, oxymyoglobin was used as a probe for NO since it is oxidized to met-myoglobin quickly and stoichiometrically by NO, whereas nitrite does not react with the probe over hundreds of seconds. The concomitant oxidation of CcOX and oxymyoglobin occurring at a rate consistent with NO dissociation from haem *a*<sub>3</sub> suggested that NO dissociates as such from the active site. This conclusion was further confirmed in the experiments conducted in anaerobiosis where oxymyoglobin oxidation occurred at the same rate of NO dissociation measured in air. Thus, when the nitrosylated adduct forms, CcOx appears not to contribute to NO degradation.

Regarding the competition between CcOx in turnover and oxymyoglobin in solution, sequential mixing stopped flow experiments showed that, when the two proteins are at the same concentration, oxymyoglobin out-competes the oxidase for NO, metabolising this molecule to nitrate independently of the CcOX turnover rate. In this context, the cellular compartmentalization of NO production acquires particular significance; the NO released by mitochondrial NO synthase, not

accessible to Mb, may bind CcOX in the cell. In conclusion, CcOx may contribute both to NO degradation by nitrite formation and dissociation upon reduction of the active site and to NO persistency which could trigger, depending on its concentration, physiological and pathological responses.

The ability of terminal oxidases to degrade NO has been measured also in the *bo<sub>3</sub>* (paper III) and *bd* (paper IV) bacterial terminal oxidases purified from *E.coli*. Previous studies reported the ability of some bacterial oxidases to reduce NO to N<sub>2</sub>O under anaerobic conditions. As NO is produced in the immune response to combat the infections and responses to NO in pathogenic bacteria likely occur, the reported NO degradation activity may have biological relevance. Furthermore, the study on the oxidases purified from an enteric bacterium may have general significance, since this organism lives in an environment where NO is present. The reported binding with different affinity of two NO molecules to Cu<sub>B</sub> in the active site of cytochrome *bo<sub>3</sub>* (Butler et al. 1997) suggested that this enzyme might display NO reductase activity. The experimental evidences of this hypothesis and a possible reaction mechanism are presented in paper III. According to this model, when the first NO molecule binds to Cu<sub>B</sub>, a change in the coordination of this metal occurs, enabling the binding of a second NO molecule; the dinitrosyl adduct formed allows the reduction of NO to N<sub>2</sub>O. A different scenario is proposed under aerobic conditions where the reduction and change in the coordination of Cu<sub>B</sub> upon NO binding results in the formation of the nitrosonium (NO<sup>+</sup>) adduct, followed by *in situ* nitrite formation. This hypothesis is supported by the spectrophotometric observation that both nitrite and NO binding to cytochrome *bo<sub>3</sub>* oxidase induce the same spectral changes, evidencing that nitrite is produced in the reaction of the oxidized cytochrome *bo<sub>3</sub>* with NO. The slow rate of NO reduction measured under anaerobic conditions with *E.coli* quinol oxidase as well as the existence of other NO-degrading enzymes in this bacterium exclude, however, a physiological role of the cytochrome *bo<sub>3</sub>* in NO detoxification.

Thus, based on the *bo<sub>3</sub>* oxidase experiment, it looks like that Cu<sub>B</sub> plays an important role in the interaction of NO with terminal oxidases. This hypothesis has been further experimentally tested on cytochrome *bd*, a terminal oxidase that lacks Cu<sub>B</sub> in the active site. The work presented in paper IV, showing the absence of a NO reductase activity in this peculiar enzyme, evidences that the presence of this metal is indeed a prerequisite for the NO reduction. Moreover, since mammalian haem-copper oxidase containing Cu<sub>B</sub> in the binuclear active site is not able to degrade NO under anaerobic conditions, then one may conclude that the structural features in the surroundings of this metal contribute to the modulation of the NO reductase activity. On the contrary, Cu<sub>B</sub> appear not to be essential to NO inhibition of reduced terminal oxidases, as low physiological concentrations of NO were able to reversibly inhibit cytochrome *bd* lacking Cu<sub>B</sub>. Moreover, inhibition occurs in competition with oxygen, thus, at the low oxygen concentration encountered *in vivo*, the NO inhibition of respiration will be more potent, a reaction that may become relevant to the defence mechanisms against pathogens. Consistently, recent molecular genetic data showed that the deletion of genes encoding for cytochrome *bd* decreases the infectivity of two mammalian pathogens, *Brucella abortus* and *Bacteroides fragilis* (Endley et al. 2001) (Baughn and Malamy 2004). The survival and pathogenicity of these strictly anaerobic microorganisms at nanomolar oxygen concentration has been proposed to be due to the oxidase oxygen consuming and preventing the build-up of oxidative free radicals. In light of these new findings, the mechanism of NO inhibition, which may lead to an increase in oxygen concentration, may acquire special relevance to the relief from some bacterial infections.

A number of mechanisms have been postulated to protect microorganisms from NO toxicity, including the NO reductase activity of the bacterial terminal oxidases. NO reductases and NO dioxygenases likely contribute to the resistance of microbes to the immune system and the NO released in various niches. In *E.coli*, flavohemoglobin (Gardner et al. 2000) has been hypothesized to have a role in NO metabolism and detoxification under aerobic conditions. Recently, by deletion of the corresponding gene, a novel NO-inducible and O<sub>2</sub>-sensitive NO reductase activity has been assigned to a flavodiiron protein, the *E.coli* flavorubredoxin, containing a diiron center, a tightly bound FMN, and mononuclear iron in the rubredoxin domain. This newly discovered anaerobic NO degrading activity is of special interest because the known NO reductases, the *bc*- and P450-type, have not homologs in *E. coli*. The biochemical study presented in paper V proves that the *E.coli* flavorubredoxin reduces NO efficiently and that this reaction occurs in the di-iron centre, since the activity is lost by deleting the corresponding domain. In accordance with the low affinity of the di-iron centre for cyanide, the flavorubredoxin NO reductase activity is insensitive to this poison.

Interestingly, the *E.coli* flavorubredoxin was proposed to take part both in oxygen and NO reduction. The flavodiiron proteins have been hypothesized to be crucial in oxygen detoxification and oxidative stress protection in anaerobes. Their NO reduction function, however, appears more likely at least based on of the high affinity of the di-iron centre for NO; in addition *E.coli* lacks an identifiable NO reductase, but clearly expresses oxygen-reducing respiratory chains. The high turnover number measured for NO degradation and the conservation of the residues near the di-iron site among most members of the flavodiiron protein suggest the existence of a novel family of NO reducing enzymes. This study proposes that the flavodiiron proteins might play a critical role in the NO metabolism and detoxification in the anaerobic and microaerobic environments encountered by *E.coli* and other microorganisms. Consistently, recent genomic analyses have shown the existence of gene coding for proteins belonging to the flavodiiron proteins in three eukaryotes, all pathogenic protists (Andersson et al. 2003).

Greater knowledge of NO metabolism may be particularly important to understand the pathogenesis and persistence of infective organisms. The study presented in paper VI provides new insights in this direction, by showing the ability of *Trichomonas vaginalis* to efficiently degrade NO. *Trichomonas vaginalis* is a pathogenic protist able to severely and chronically infect women. Specifically, the NO reductase activity was tested under anaerobic condition mimicking the vaginal oxygen poor and NO rich environment where these parasites live. This study has provided the experimental evidence for the expression of a flavodiiron protein in *Trichomonas vaginalis*. The NO degradation function observed is oxygen sensitive, cyanide insensitive, dependent on NADH and an immunoblot run on this cellular lysate displays a band compatible with a flavodiiron protein.

The expression of this enzyme is of great evolutionary interest, supporting a lateral gene transfer between bacteria and eukaryotes. The presence of three genes encoding for this enzyme has been found in the genome of *Trichomonas vaginalis*. More importantly, the NO reductase activity could be crucial for the observed chronic infectivity and survival of the parasites and a better characterization of this novel family of NO reductases may be at the basis of the development of new and possibly less toxic strategies to combat the protist infections.

## 6. REFERENCES

- Abramson, J., S. Riistama, et al. (2000). "The structure of the ubiquinol oxidase from Escherichia coli and its ubiquinone binding site." Nat Struct Biol **7**(10): 910-7.
- Adak, S., K. S. Aulak, et al. (2002). "Direct evidence for nitric oxide production by a nitric-oxide synthase-like protein from Bacillus subtilis." J Biol Chem **277**(18): 16167-71.
- Alderton, W. K., C. E. Cooper, et al. (2001). "Nitric oxide synthases: structure, function and inhibition." Biochem J **357**(Pt 3): 593-615.
- Andersson, J. O., A. M. Sjogren, et al. (2003). "Phylogenetic analyses of diplomonad genes reveal frequent lateral gene transfers affecting eukaryotes." Curr Biol **13**(2): 94-104.
- Antonini, E., M. Brunori, et al. (1977). "Oxygen "pulsed" cytochrome c oxidase: functional properties and catalytic relevance." Proc Natl Acad Sci U S A **74**(8): 3128-32.
- Antonini, G., M. Brunori, et al. (1985). "Pulsed cytochrome c oxidase." J Inorg Biochem **23**(3-4): 289-93.
- Antonini, G., M. Brunori, et al. (1987). "Reconstitution of monomeric cytochrome c oxidase into phospholipid vesicles yields functionally interacting cytochrome aa3 units." J Biol Chem **262**(21): 10077-9.
- Antunes, F. and E. Cadenas (2000). "Estimation of H<sub>2</sub>O<sub>2</sub> gradients across biomembranes." FEBS Lett **475**(2): 121-6.
- Backgren, C., G. Hummer, et al. (2000). "Proton translocation by cytochrome c oxidase can take place without the conserved glutamic acid in subunit I." Biochemistry **39**(27): 7863-7.
- Baughn, A. D. and M. H. Malamy (2004). "The strict anaerobe Bacteroides fragilis grows in and benefits from nanomolar concentrations of oxygen." Nature **427**(6973): 441-4.
- Beckman, J. S. and W. H. Koppenol (1996). "Nitric oxide, superoxide, and peroxynitrite: the good, the bad, and ugly." Am J Physiol **271**(5 Pt 1): C1424-37.
- Blackmore, R. S., C. Greenwood, et al. (1991). "Studies of the primary oxygen intermediate in the reaction of fully reduced cytochrome oxidase." J Biol Chem **266**(29): 19245-9.
- Bloch, D., I. Belevich, et al. (2004). "The catalytic cycle of cytochrome c oxidase is not the sum of its two halves." Proc Natl Acad Sci U S A **101**(2): 529-33.
- Bogdan, C. (2001). "Nitric oxide and the immune response." Nat Immunol **2**(10): 907-16.
- Bolanos, J. P., S. J. Heales, et al. (1995). "Effect of peroxynitrite on the mitochondrial respiratory chain: differential susceptibility of neurones and astrocytes in primary culture." J Neurochem **64**(5): 1965-72.
- Bonamore, A., P. Gentili, et al. (2003). "Escherichia coli flavohemoglobin is an efficient alkylhydroperoxide reductase." J Biol Chem **278**(25): 22272-7.
- Branden, M., A. Namslauer, et al. (2003). "Water-hydroxide exchange reactions at the catalytic site of heme-copper oxidases." Biochemistry **42**(45): 13178-84.
- Brookes, P. S., A. L. Levonen, et al. (2002). "Mitochondria: regulators of signal transduction by reactive oxygen and nitrogen species." Free Radic Biol Med **33**(6): 755-64.
- Brown, G. C. (1995). "Nitric oxide regulates mitochondrial respiration and cell functions by inhibiting cytochrome oxidase." FEBS Lett **369**(2-3): 136-9.
- Brown, G. C. (1999). "Nitric oxide and mitochondrial respiration." Biochim Biophys Acta **1411**(2-3): 351-69.
- Brown, G. C. (2001). "Regulation of mitochondrial respiration by nitric oxide inhibition of cytochrome c oxidase." Biochim Biophys Acta **1504**(1): 46-57.
- Brown, G. C. and V. Borutaite (2001). "Nitric oxide, mitochondria, and cell death." IUBMB Life **52**(3-5): 189-95.
- Brown, G. C. and C. E. Cooper (1994). "Nanomolar concentrations of nitric oxide reversibly inhibit synaptosomal respiration by competing with oxygen at cytochrome oxidase." FEBS Lett **356**(2-3): 295-8.
- Brown, G. C., N. Foxwell, et al. (1998). "Transcellular regulation of cell respiration by nitric oxide generated by activated macrophages." FEBS Lett **439**(3): 321-4.
- Brunori, M. (2001). "Nitric oxide, cytochrome-c oxidase and myoglobin." Trends Biochem Sci **26**(1): 21-3.
- Brunori, M., A. Giuffre, et al. (1997). "Internal electron transfer in Cu-heme oxidases. Thermodynamic or kinetic control?" J Biol Chem **272**(32): 19870-4.

- Buse, G., T. Soulimane, et al. (1999). "Evidence for a copper-coordinated histidine-tyrosine cross-link in the active site of cytochrome oxidase." *Protein Sci* **8**(5): 985-90.
- Butler, C. S., M. R. Cheesman, et al. (1997). "Fast cytochrome bo from *Escherichia coli* reacts with azide and nitric oxide to form a complex analogous to that formed by cytochrome c oxidase." *Biochem Soc Trans* **25**(3): 392S.
- Carr, G. J. and S. J. Ferguson (1990). "Nitric oxide formed by nitrite reductase of *Paracoccus denitrificans* is sufficiently stable to inhibit cytochrome oxidase activity and is reduced by its reductase under aerobic conditions." *Biochim Biophys Acta* **1017**(1): 57-62.
- Cassina, A. and R. Radi (1996). "Differential inhibitory action of nitric oxide and peroxynitrite on mitochondrial electron transport." *Arch Biochem Biophys* **328**(2): 309-16.
- Castro, L., M. Rodriguez, et al. (1994). "Aconitase is readily inactivated by peroxynitrite, but not by its precursor, nitric oxide." *J Biol Chem* **269**(47): 29409-15.
- Chandel, N. S., D. S. McClintock, et al. (2000). "Reactive oxygen species generated at mitochondrial complex III stabilize hypoxia-inducible factor-1 $\alpha$  during hypoxia: a mechanism of O<sub>2</sub> sensing." *J Biol Chem* **275**(33): 25130-8.
- Chen, Y. and J. P. Rosazza (1994). "A bacterial nitric oxide synthase from a *Nocardia* species." *Biochem Biophys Res Commun* **203**(2): 1251-8.
- Cleeter, M. W., J. M. Cooper, et al. (1994). "Reversible inhibition of cytochrome c oxidase, the terminal enzyme of the mitochondrial respiratory chain, by nitric oxide. Implications for neurodegenerative diseases." *FEBS Lett* **345**(1): 50-4.
- Clementi, E., G. C. Brown, et al. (1999). "On the mechanism by which vascular endothelial cells regulate their oxygen consumption." *Proc Natl Acad Sci U S A* **96**(4): 1559-62.
- Cooper, C. E. (1999). "Nitric oxide and iron proteins." *Biochim Biophys Acta* **1411**(2-3): 290-309.
- Cooper, C. E. (2002). "Nitric oxide and cytochrome oxidase: substrate, inhibitor or effector?" *Trends Biochem Sci* **27**(1): 33-9.
- Corker, H. and R. K. Poole (2003). "Nitric oxide formation by *Escherichia coli*. Dependence on nitrite reductase, the NO-sensing regulator Fnr, and flavohemoglobin Hmp." *J Biol Chem* **278**(34): 31584-92.
- Cutruzzola, F. (1999). "Bacterial nitric oxide synthesis." *Biochim Biophys Acta* **1411**(2-3): 231-49.
- da Costa, P. N., M. Teixeira, et al. (2003). "Regulation of the flavorubredoxin nitric oxide reductase gene in *Escherichia coli*: nitrate repression, nitrite induction, and possible post-transcription control." *FEMS Microbiol Lett* **218**(2): 385-93.
- Das, A., E. D. Coulter, et al. (2001). "Five-gene cluster in *Clostridium thermoaceticum* consisting of two divergent operons encoding rubredoxin oxidoreductase- rubredoxin and rubrerythrin-type A flavoprotein- high-molecular-weight rubredoxin." *J Bacteriol* **183**(5): 1560-7.
- Dermastia, M., T. Turk, et al. (1991). "Nitric oxide reductase. Purification from *Paracoccus denitrificans* with use of a single column and some characteristics." *J Biol Chem* **266**(17): 10899-905.
- Eich, R. F., T. Li, et al. (1996). "Mechanism of NO-induced oxidation of myoglobin and hemoglobin." *Biochemistry* **35**(22): 6976-83.
- Einarsdottir, O., K. E. Georgiadis, et al. (1995). "Intramolecular electron transfer and conformational changes in cytochrome c oxidase." *Biochemistry* **34**(2): 496-508.
- Endley, S., D. McMurray, et al. (2001). "Interruption of the *cydB* locus in *Brucella abortus* attenuates intracellular survival and virulence in the mouse model of infection." *J Bacteriol* **183**(8): 2454-62.
- Fabian, M. and G. Palmer (1998). "Hydrogen peroxide is not released following reaction of cyanide with several catalytically important derivatives of cytochrome c oxidase." *FEBS Lett* **422**(1): 1-4.
- Fann, Y. C., I. Ahmed, et al. (1995). "Structure of Cu<sub>B</sub> in the binuclear heme-copper center of the cytochrome aa<sub>3</sub>-type quinol oxidase from *Bacillus subtilis*: an ENDOR and EXAFS study." *Biochemistry* **34**(32): 10245-55.
- Flogel, U., M. W. Merx, et al. (2001). "Myoglobin: A scavenger of bioactive NO." *Proc Natl Acad Sci U S A* **98**(2): 735-40.
- Ford, P. C., D. A. Wink, et al. (1993). "Autoxidation kinetics of aqueous nitric oxide." *FEBS Lett* **326**(1-3): 1-3.
- Forte, E., A. Urbani, et al. (2001). "The cytochrome cbb3 from *Pseudomonas stutzeri* displays nitric oxide reductase activity." *Eur J Biochem* **268**(24): 6486-91.



## References

- Frazao, C., G. Silva, et al. (2000). "Structure of a dioxygen reduction enzyme from *Desulfovibrio gigas*." *Nat Struct Biol* **7**(11): 1041-5.
- Gardner, A. M. and P. R. Gardner (2002). "Flavohemoglobin detoxifies nitric oxide in aerobic, but not anaerobic, *Escherichia coli*. Evidence for a novel inducible anaerobic nitric oxide-scavenging activity." *J Biol Chem* **277**(10): 8166-71.
- Gardner, A. M., C. R. Gessner, et al. (2003). "Regulation of the nitric oxide reduction operon (norRVW) in *Escherichia coli*. Role of NorR and sigma54 in the nitric oxide stress response." *J Biol Chem* **278**(12): 10081-6.
- Gardner, A. M., R. A. Helmick, et al. (2002). "Flavorubredoxin, an inducible catalyst for nitric oxide reduction and detoxification in *Escherichia coli*." *J Biol Chem* **277**(10): 8172-7.
- Gardner, A. M., L. A. Martin, et al. (2000). "Steady-state and transient kinetics of *Escherichia coli* nitric-oxide dioxygenase (flavohemoglobin). The B10 tyrosine hydroxyl is essential for dioxygen binding and catalysis." *J Biol Chem* **275**(17): 12581-9.
- Gaston, B. (1999). "Nitric oxide and thiol groups." *Biochim Biophys Acta* **1411**(2-3): 323-33.
- Gibson, Q. H. and C. Greenwood (1963). "Reactions of cytochrome oxidase with oxygen and carbon monoxide." *Biochem J* **86**: 541-54.
- Giuffre, A., M. C. Barone, et al. (2002). "Nitric oxide reacts with the single-electron reduced active site of cytochrome c oxidase." *J Biol Chem* **277**(25): 22402-6.
- Giuffre, A., M. C. Barone, et al. (2000). "Reaction of nitric oxide with the turnover intermediates of cytochrome c oxidase: reaction pathway and functional effects." *Biochemistry* **39**(50): 15446-53.
- Giuffre, A., P. Sarti, et al. (1996). "On the mechanism of inhibition of cytochrome c oxidase by nitric oxide." *J Biol Chem* **271**(52): 33404-8.
- Giuffre, A., G. Stubauer, et al. (1998). "Chloride bound to oxidized cytochrome c oxidase controls the reaction with nitric oxide." *J Biol Chem* **273**(49): 32475-8.
- Giuffre, A., G. Stubauer, et al. (1999). "The heme-copper oxidases of *Thermus thermophilus* catalyze the reduction of nitric oxide: evolutionary implications." *Proc Natl Acad Sci U S A* **96**(26): 14718-23.
- Gomes, C. M., J. B. Vicente, et al. (2000). "Spectroscopic studies and characterization of a novel electron-transfer chain from *Escherichia coli* involving a flavorubredoxin and its flavoprotein reductase partner." *Biochemistry* **39**(51): 16230-7.
- Harrenga, A. and H. Michel (1999). "The cytochrome c oxidase from *Paracoccus denitrificans* does not change the metal center ligation upon reduction." *J Biol Chem* **274**(47): 33296-9.
- Hausladen, A. and I. Fridovich (1994). "Superoxide and peroxynitrite inactivate aconitases, but nitric oxide does not." *J Biol Chem* **269**(47): 29405-8.
- Haynes, V., S. Elfering, et al. (2004). "Mitochondrial nitric-oxide synthase: enzyme expression, characterization, and regulation." *J Bioenerg Biomembr* **36**(4): 341-6.
- Helman, Y., D. Tchernov, et al. (2003). "Genes encoding A-type flavoproteins are essential for photoreduction of O<sub>2</sub> in cyanobacteria." *Curr Biol* **13**(3): 230-5.
- Hendriks, J., A. Warne, et al. (1998). "The active site of the bacterial nitric oxide reductase is a dinuclear iron center." *Biochemistry* **37**(38): 13102-9.
- Herold, S., M. Exner, et al. (2001). "Kinetic and mechanistic studies of the NO\*-mediated oxidation of oxymyoglobin and oxyhemoglobin." *Biochemistry* **40**(11): 3385-95.
- Hill, B. C. (1994). "Modeling the sequence of electron transfer reactions in the single turnover of reduced, mammalian cytochrome c oxidase with oxygen." *J Biol Chem* **269**(4): 2419-25.
- Hong, I. S., Y. K. Kim, et al. (2003). "Purification and characterization of nitric oxide synthase from *Staphylococcus aureus*." *FEMS Microbiol Lett* **222**(2): 177-82.
- Ignarro, L. J., G. M. Buga, et al. (1987). "Endothelium-derived relaxing factor produced and released from artery and vein is nitric oxide." *Proc Natl Acad Sci U S A* **84**(24): 9265-9.
- Ignarro, L. J., C. Napoli, et al. (2002). "Nitric oxide donors and cardiovascular agents modulating the bioactivity of nitric oxide: an overview." *Circ Res* **90**(1): 21-8.
- Iwata, S., C. Ostermeier, et al. (1995). "Structure at 2.8 Å resolution of cytochrome c oxidase from *Paracoccus denitrificans*." *Nature* **376**(6542): 660-9.
- Junemann, S. (1997). "Cytochrome bd terminal oxidase." *Biochim Biophys Acta* **1321**(2): 107-27.
- Kannt, A., C. R. Lancaster, et al. (1998). "The coupling of electron transfer and proton translocation: electrostatic calculations on *Paracoccus denitrificans* cytochrome c oxidase." *Biophys J* **74**(2 Pt 1): 708-21.

- Kharitonov, V. G., M. Russwurm, et al. (1997). "Dissociation of nitric oxide from soluble guanylate cyclase." *Biochem Biophys Res Commun* **239**(1): 284-6.
- Kumita, H., K. Matsuura, et al. (2004). "NO reduction by nitric oxide reductase from denitrifying bacterium *Pseudomonas aeruginosa*: Characterization of reaction intermediates that appear in the single-turnover cycle." *J Biol Chem*.
- Lee, H. M., T. K. Das, et al. (2000). "Mutations in the putative H-channel in the cytochrome c oxidase from *Rhodobacter sphaeroides* show that this channel is not important for proton conduction but reveal modulation of the properties of heme a." *Biochemistry* **39**(11): 2989-96.
- Lepoivre, M., F. Fieschi, et al. (1991). "Inactivation of ribonucleotide reductase by nitric oxide." *Biochem Biophys Res Commun* **179**(1): 442-8.
- Liu, X., M. J. Miller, et al. (1998). "Accelerated reaction of nitric oxide with O<sub>2</sub> within the hydrophobic interior of biological membranes." *Proc Natl Acad Sci U S A* **95**(5): 2175-9.
- Malatesta, F., P. Sarti, et al. (1990). "Electron transfer to the binuclear center in cytochrome oxidase: catalytic significance and evidence for an additional intermediate." *Proc Natl Acad Sci U S A* **87**(19): 7410-3.
- Mastronicola, D., M. L. Genova, et al. (2003). "Control of respiration by nitric oxide in Keilin-Hartree particles, mitochondria and SH-SY5Y neuroblastoma cells." *Cell Mol Life Sci* **60**(8): 1752-9.
- Matsuda, Y., T. Uchida, et al. (2004). "Structural characterization of a binuclear center of a Cu-containing NO reductase homologue from *Roseobacter denitrificans*: EPR and resonance Raman studies." *Biochim Biophys Acta* **1656**(1): 37-45.
- Michel, H. (1999). "Cytochrome c oxidase: catalytic cycle and mechanisms of proton pumping--a discussion." *Biochemistry* **38**(46): 15129-40.
- Miles, P. R., L. Bowman, et al. (1996). "Nitric oxide alters metabolism in isolated alveolar type II cells." *Am J Physiol* **271**(1 Pt 1): L23-30.
- Moncada, S. and J. D. Erusalimsky (2002). "Does nitric oxide modulate mitochondrial energy generation and apoptosis?" *Nat Rev Mol Cell Biol* **3**(3): 214-20.
- Moody, A. J., C. S. Butler, et al. (1998). "The reaction of halides with pulsed cytochrome bo from *Escherichia coli*." *Biochem J* **331** ( Pt 2): 459-64.
- Nicholls, P., K. J. van Buuren, et al. (1972). "Biochemical and biophysical studies on cytochrome aa<sub>3</sub>. 8. Effect of cyanide on the catalytic activity." *Biochim Biophys Acta* **275**(3): 279-87.
- Okuno, D., T. Iwase, et al. (2003). "FTIR detection of protonation/deprotonation of key carboxyl side chains caused by redox change of the Cu(A)-heme a moiety and ligand dissociation from the heme a<sub>3</sub>-Cu(B) center of bovine heart cytochrome c oxidase." *J Am Chem Soc* **125**(24): 7209-18.
- Ostermeier, C., A. Harrenga, et al. (1997). "Structure at 2.7 Å resolution of the *Paracoccus denitrificans* two-subunit cytochrome c oxidase complexed with an antibody FV fragment." *Proc Natl Acad Sci U S A* **94**(20): 10547-53.
- Palmer, R. M., A. G. Ferrige, et al. (1987). "Nitric oxide release accounts for the biological activity of endothelium-derived relaxing factor." *Nature* **327**(6122): 524-6.
- Park, G. C., J. S. Ryu, et al. (1997). "The role of nitric oxide as an effector of macrophage-mediated cytotoxicity against *Trichomonas vaginalis*." *Korean J Parasitol* **35**(3): 189-95.
- Pearce, L. L., E. L. Bominaar, et al. (2003). "Reversal of cyanide inhibition of cytochrome c oxidase by the auxiliary substrate nitric oxide: an endogenous antidote to cyanide poisoning?" *J Biol Chem* **278**(52): 52139-45.
- Pfützner, U., A. Odenwald, et al. (1998). "Cytochrome c oxidase (heme aa<sub>3</sub>) from *Paracoccus denitrificans*: analysis of mutations in putative proton channels of subunit I." *J Bioenerg Biomembr* **30**(1): 89-97.
- Pinakoulaki, E., S. Gemeinhardt, et al. (2002). "Nitric-oxide reductase. Structure and properties of the catalytic site from resonance Raman scattering." *J Biol Chem* **277**(26): 23407-13.
- Proshlyakov, D. A., M. A. Pressler, et al. (1998). "Dioxygen activation and bond cleavage by mixed-valence cytochrome c oxidase." *Proc Natl Acad Sci U S A* **95**(14): 8020-5.
- Puustinen, A. and M. Wikström (1999). "Proton exit from the heme-copper oxidase of *Escherichia coli*." *Proc Natl Acad Sci U S A* **96**(1): 35-7.
- Ralle, M., M. L. Verkhovskaya, et al. (1999). "Coordination of Cu<sub>B</sub> in reduced and CO-liganded states of cytochrome bo<sub>3</sub> from *Escherichia coli*. Is chloride ion a cofactor?" *Biochemistry* **38**(22): 7185-94.

## References

- Renner, E. D. and G. E. Becker (1970). "Production of nitric oxide and nitrous oxide during denitrification by *Corynebacterium nephridii*." *J Bacteriol* **101**(3): 821-6.
- Rochelle, L. G., S. J. Morana, et al. (1995). "Interactions between hydroxocobalamin and nitric oxide (NO): evidence for a redox reaction between NO and reduced cobalamin and reversible NO binding to oxidized cobalamin." *J Pharmacol Exp Ther* **275**(1): 48-52.
- Ruitenbergh, M., A. Kannt, et al. (2002). "Reduction of cytochrome c oxidase by a second electron leads to proton translocation." *Nature* **417**(6884): 99-102.
- Ruitenbergh, M., A. Kannt, et al. (2000). "Single-electron reduction of the oxidized state is coupled to proton uptake via the K pathway in *Paracoccus denitrificans* cytochrome c oxidase." *Proc Natl Acad Sci U S A* **97**(9): 4632-6.
- Saraste, M. and J. Castresana (1994). "Cytochrome oxidase evolved by tinkering with denitrification enzymes." *FEBS Lett* **341**(1): 1-4.
- Sarti, P., A. Colosimo, et al. (1983). "Kinetic studies on cytochrome c oxidase inserted into liposomal vesicles. Effect of ionophores." *Biochem J* **209**(1): 81-9.
- Sarti, P., A. Giuffrè, et al. (2003). "Nitric oxide and cytochrome oxidase: reaction mechanisms from the enzyme to the cell." *Free Radic Biol Med* **34**(5): 509-20.
- Sarti, P., A. Giuffrè, et al. (2000). "Nitric oxide and cytochrome c oxidase: mechanisms of inhibition and NO degradation." *Biochem Biophys Res Commun* **274**(1): 183-7.
- Sarti, P., M. G. Jones, et al. (1985). "Kinetics of redox-linked proton pumping activity of native and subunit III-depleted cytochrome c oxidase: a stopped-flow investigation." *Proc Natl Acad Sci U S A* **82**(15): 4876-80.
- Sarti, P., E. Lendaro, et al. (1999). "Modulation of mitochondrial respiration by nitric oxide: investigation by single cell fluorescence microscopy." *Faseb J* **13**(1): 191-7.
- Schweizer, M. and C. Richter (1994). "Nitric oxide potentially and reversibly deenergizes mitochondria at low oxygen tension." *Biochem Biophys Res Commun* **204**(1): 169-75.
- Scott, R. A., P. M. Li, et al. (1988). "The binuclear site of cytochrome c oxidase. Structural evidence from iron X-ray absorption spectroscopy." *Ann N Y Acad Sci* **550**: 53-8.
- Sharma, V. S. and H. M. Ranney (1978). "The dissociation of NO from nitrosylhemoglobin." *J Biol Chem* **253**(18): 6467-72.
- Shen, W., X. Xu, et al. (1994). "Role of nitric oxide in the regulation of oxygen consumption in conscious dogs." *Circ Res* **75**(6): 1086-95.
- Shiro, Y., M. Fujii, et al. (1995). "Spectroscopic and kinetic studies on reaction of cytochrome P450<sub>nor</sub> with nitric oxide. Implication for its nitric oxide reduction mechanism." *J Biol Chem* **270**(4): 1617-23.
- Shiva, S., P. S. Brookes, et al. (2001). "Nitric oxide partitioning into mitochondrial membranes and the control of respiration at cytochrome c oxidase." *Proc Natl Acad Sci U S A* **98**(13): 7212-7.
- Silaghi-Dumitrescu, R., E. D. Coulter, et al. (2003). "A flavodiiron protein and high molecular weight rubredoxin from *Moorella thermoacetica* with nitric oxide reductase activity." *Biochemistry* **42**(10): 2806-15.
- Singel, D. J. and J. S. Stamler (2004). "Chemical Physiology of Blood Flow Regulation by Red Blood Cells: Role of Nitric Oxide and S-Nitrosohemoglobin." *Annu Rev Physiol*.
- Soulimane, T. and G. Buse (1995). "Integral cytochrome-c oxidase. Preparation and progress towards a three-dimensional crystallization." *Eur J Biochem* **227**(1-2): 588-95.
- Stavakis, S., K. Koutsoumpakis, et al. (2002). "Decay of the transient Cu(B)-CO complex is accompanied by formation of the heme Fe-CO complex of cytochrome cbb(3)-CO at ambient temperature: evidence from time-resolved Fourier transform infrared spectroscopy." *J Am Chem Soc* **124**(15): 3814-5.
- Stevanin, T. M., N. Ioannidis, et al. (2000). "Flavohemoglobin Hmp affords inducible protection for *Escherichia coli* respiration, catalyzed by cytochromes bo' or bd, from nitric oxide." *J Biol Chem* **275**(46): 35868-75.
- Stubauer, G., A. Giuffrè, et al. (1998). "Cytochrome c oxidase does not catalyze the anaerobic reduction of NO." *Biochem Biophys Res Commun* **245**(2): 459-65.
- Svensson-Ek, M., J. Abramson, et al. (2002). "The X-ray crystal structures of wild-type and EQ(I-286) mutant cytochrome c oxidases from *Rhodobacter sphaeroides*." *J Mol Biol* **321**(2): 329-39.
- Tomson, F. L., J. E. Morgan, et al. (2003). "Substitutions for glutamate 101 in subunit II of cytochrome c oxidase from *Rhodobacter sphaeroides* result in blocking the proton-conducting K-channel." *Biochemistry* **42**(6): 1711-7.

- Torreilles, J. (2001). "Nitric oxide: one of the more conserved and widespread signaling molecules." *Front Biosci* **6**: D1161-72.
- Torres, J., C. E. Cooper, et al. (1998). "A common mechanism for the interaction of nitric oxide with the oxidized binuclear centre and oxygen intermediates of cytochrome c oxidase." *J Biol Chem* **273**(15): 8756-66.
- Torres, J., V. Darley-USmar, et al. (1995). "Inhibition of cytochrome c oxidase in turnover by nitric oxide: mechanism and implications for control of respiration." *Biochem J* **312** ( Pt 1): 169-73.
- Torres, J. and M. T. Wilson (1999). "The reactions of copper proteins with nitric oxide." *Biochim Biophys Acta* **1411**(2-3): 310-22.
- Trimmer, B. A., J. R. Aprille, et al. (2001). "Nitric oxide and the control of firefly flashing." *Science* **292**(5526): 2486-8.
- Trochu, J. N., J. B. Bouhour, et al. (2000). "Role of endothelium-derived nitric oxide in the regulation of cardiac oxygen metabolism: implications in health and disease." *Circ Res* **87**(12): 1108-17.
- Tsukihara, T., H. Aoyama, et al. (1995). "Structures of metal sites of oxidized bovine heart cytochrome c oxidase at 2.8 Å." *Science* **269**(5227): 1069-74.
- Tsukihara, T., H. Aoyama, et al. (1996). "The whole structure of the 13-subunit oxidized cytochrome c oxidase at 2.8 Å." *Science* **272**(5265): 1136-44.
- Vanneste, W. H. (1966). "The stoichiometry and absorption spectra of components a and a-3 in cytochrome c oxidase." *Biochemistry* **5**(3): 838-48.
- Verkhovsky, M. I., N. Belevich, et al. (1999). "Proton linkage of cytochrome a oxidoreduction in carbon monoxide-treated cytochrome c oxidase." *Biochim Biophys Acta* **1412**(2): 184-9.
- Verkhovsky, M. I., A. Jasaitis, et al. (1999). "Proton translocation by cytochrome c oxidase." *Nature* **400**(6743): 480-3.
- Verkhovsky, M. I., J. E. Morgan, et al. (1995). "Control of electron delivery to the oxygen reduction site of cytochrome c oxidase: a role for protons." *Biochemistry* **34**(22): 7483-91.
- Verkhovsky, M. I., A. Tuukkanen, et al. (2001). "Charge translocation coupled to electron injection into oxidized cytochrome c oxidase from *Paracoccus denitrificans*." *Biochemistry* **40**(24): 7077-83.
- Vicente, J. B., C. M. Gomes, et al. (2002). "Module fusion in an A-type flavoprotein from the cyanobacterium *Synechocystis* condenses a multiple-component pathway in a single polypeptide chain." *Biochem Biophys Res Commun* **294**(1): 82-7.
- Vygodina, T. V., C. Pecoraro, et al. (1998). "Mechanism of inhibition of electron transfer by amino acid replacement K362M in a proton channel of *Rhodobacter sphaeroides* cytochrome c oxidase." *Biochemistry* **37**(9): 3053-61.
- Wasserfallen, A., S. Ragetti, et al. (1998). "A family of flavoproteins in the domains Archaea and Bacteria." *Eur J Biochem* **254**(2): 325-32.
- Wikstrom, M. (1989). "Identification of the electron transfers in cytochrome oxidase that are coupled to proton-pumping." *Nature* **338**(6218): 776-8.
- Wikstrom, M., A. Jasaitis, et al. (2000). "The role of the D- and K-pathways of proton transfer in the function of the haem-copper oxidases." *Biochim Biophys Acta* **1459**(2-3): 514-20.
- Wikstrom, M., M. I. Verkhovsky, et al. (2003). "Water-gated mechanism of proton translocation by cytochrome c oxidase." *Biochim Biophys Acta* **1604**(2): 61-5.
- Wink, D. A., I. Hanbauer, et al. (1996). "Chemical biology of nitric oxide: regulation and protective and toxic mechanisms." *Curr Top Cell Regul* **34**: 159-87.
- Wink, D. A., I. Hanbauer, et al. (1994). "Nitric oxide protects against the cytotoxic effects of reactive oxygen species." *Ann N Y Acad Sci* **738**: 265-78.
- Wink, D. A., Y. Vodovotz, et al. (1998). "The role of nitric oxide chemistry in cancer treatment." *Biochemistry (Mosc)* **63**(7): 802-9.
- Woodruff, W. H. (1993). "Coordination dynamics of heme-copper oxidases. The ligand shuttle and the control and coupling of electron transfer and proton translocation." *J Bioenerg Biomembr* **25**(2): 177-88.
- Yonetani, T. (1961). "Studies on cytochrome oxidase. III. Improved preparation and some properties." *J Biol Chem* **236**: 1680-8.
- Yoshikawa, S., K. Shinzawa-Itoh, et al. (1998). "Crystal structure of bovine heart cytochrome c oxidase at 2.8 Å resolution." *J Bioenerg Biomembr* **30**(1): 7-14.
- Zaslavsky, D. and R. B. Gennis (2000). "Proton pumping by cytochrome oxidase: progress, problems and postulates." *Biochim Biophys Acta* **1458**(1): 164-79.

### *References*

---

- Zumft, W. G. (1997). "Cell biology and molecular basis of denitrification." Microbiol Mol Biol Rev **61**(4): 533-616.
- Zweier, J. L., A. Samouilov, et al. (1999). "Non-enzymatic nitric oxide synthesis in biological systems." Biochim Biophys Acta **1411**(2-3): 250-62.